STUDY OF T-JOINT SUBSTRUCTURE IN BUS BODY BY MEANS OF BENDING TEST

SAGPICHEST SARINYAVAJN

A THESIS REPORT SUBMITTED IN PARTIAL FULFILLMENT
OF THE REQUIREMENTS FOR THE DEGREE OF
MASTER OF ENGINEERING IN AUTOMOTIVE ENGINEERING
INTERNATIONAL COLLEGE
KING MONGKUT'S INSTITUTE OF TECHNOLOGY LADKRABANG
ACADEMIC YEAR 2018

KMITL-2018-IC-M-004-016

STUDY OF T-JOINT SUBSTRUCTURE IN BUS BODY BY MEANS OF BENDING TEST

SAGPICHEST SARINYAVAJN

A THESIS REPORT SUBMITTED IN PARTIAL FULFILLMENT
OF THE REQUIREMENTS FOR THE DEGREE OF
MASTER OF ENGINEERING IN AUTOMOTIVE ENGINEERING
INTERNATIONAL COLLEGE
KING MONGKUT'S INSTITUTE OF TECHNOLOGY LADKRABANG
ACADEMIC YEAR 2018
KMITL-2018-IC-M-004-016

THESIS TITLE	Study of T-joint substructure in bus body by means of bending test
STUDENT NAME	Mr. Sagpichest Sarinyavajn
STUDENT ID	57610025
DEGREE	Master of Engineering
PROGRAME	Automotive Engineering
ADVISOR	Dr.Chi-na Benyajati
CO-ADVISOR	Asst.Prof.Dr. Panya Kansuwan
CO-ADVISOR	Prof. Dr. Massaki Okuma

ABSTRACT

This research will focus on a T-joint substructure of a bus body with a significance to a bending test. T-joint configurations were obtained from actual bus assembler in Thailand and were subjected to a bending load from in-house test rigs operated with 25kN Universal Tensile Machine. The objective was to improve a current structural joint configuration employed by a local assembler, in terms of weight and strength. The results from joint specimens with different joining techniques and designs would be initially used as a guideline prior to a substructure test for further validation.

This study was to investigate different joining configurations on T-joint of thin steel beams with thickness 5 mm which are commonly used in a bus structure under static in-plane bending load. Four different joining technique were investigated. the strength of the joint is playing a key role in overall deformation that a stronger joint could lead to more deforming in component, whereas a weaker joint might lead to more deforming near a joint area. The alternative joint was reduced 40-55 percent of the weld materials and reduce the deformation that occurs from the orientation of seam weld inside the T-joint component.

The result can be applied to other buses component like roof structures. the design of the Rig test will be applied to a larger scale of specimens.

ACKNOWLEDGEMENT

The authors would like to thank Thailand Advance Institute of Science and Technology, Tokyo Institute of Technology (TAIST-Tokyo Tech) and National Science and Technology Development Agency (NSTDA) for providing full scholarship. This study has been conducted as part of a research project in the Light Weight Engineering Laboratory, National Metal and Material Technology Center (MTEC) , Phanthong alliance Co., LTD and KMITL International College.

I would like to express my special gratefulness to Dr. Chi-na Benyajati, major advisor, Light Weight Engineering Laboratory, for his generous support, technical guidance, and encouragement all the time during the research work. I would like to direct my gratitude to my advisor, Assistant Professor Dr. Panya Kansuwan, department of Mechanical Engineering, KMITL and Professor Dr. Masaaki Okuma, department of Mechanical and Aerospace Engineering, Tokyo Tech, for kind advice and suggestions. I would like to thank Panthong alliance Co., LTD, for provide specimens for this experiment.

Finally, I would like to give this success to my parent who always stand by me, and have infinite faith in my research work

Sagpichest Sarinyavajn

July 2019

TABLE OF CONTENTS

LIST OF TABLES

Table **Page**

LIST OF FIGURES

Figure **Page**

LIST OF SYMBOLS

σ_b	Bending stress
β	Brace-chord ratio
Pe	Crushing resistance
d	Diameter of the rivet hole
C_T	Efficiency Coefficient of T- joint connection
η	Efficiency of the riveted joint
N	Maximum force for T-joint under in-plane bending load
σ t	Permissible tensile stress for the plate material.
p	Pitch of the rivets
σ	Principal stress
S_{sy}	Shear strength at yielding
τ	Shear Stress
P_s	Shearing resistance
t0,t1	Thickness of chord and brace
fy0,fy1	Tensile stress at yield point
P_t	Tearing resistance
t	Thickness of the plate
σ_e	Von-Mises effective stress
b0,b1	Width of chord and brace

LIST OF DEFINITIONS

ASTM	American Society for Testing and Materials
BR	Blind Rivet
BHR	Blind Hermetic Rivet
CAD	Computer Aided Design
CIDECT	Committee for International Development and Education on Construction of Tubular structures
CHS	Circular Hollow Square Section
CG	Center of gravity
COUR	Closing up rivet
GMAW	Gas Metal Arc Welding Process
HAZ	Heat Affected Zone
IIW	International Institute of Welded
MIG	Metal Inert Gas Welding
MAG	Metal Active Gas
RHS	Rectangular Hollow square section
SHS	Square Hollow Section
SMAW	Shielded Metal Arc Welding
SSPR	Thickness of the plate
UTM	Universal Tensile Machine
UVX	Universal Video Extensometer

CHAPTER 1

INTRODUCTION

1.1 Background

Buses are one of the main vehicles for public transportation in many countries. accidents due to land traffic are a major problem. Whether it is injury or disability Death and loss of property In addition, land-based accidents are considered one of the top causes of death in many countries. There are 4 types of accidents caused by land transport: 1) Frontal Impact is an accident caused by the front of the car before the front door has been damaged by kinetic energy. That happens to be changed to a collapsing phase that occurs with the vehicle structure 2.) Side Impact is an accident caused by damage to the door and side walls of the vehicle due to being affected by other vehicles or objects. 3.) Rear Impact is an accident caused by the rear area of the car from the refueling door to the end of the car being damaged due to being affected by other cars or other objects. In which the three incidents of the above are caused by two conditions Is that the car collides with other cars or obstructions, causing the structure to collapse and the passenger or driver moving to affect various objects within the car and 4.) the last type of accident is Rollover, which this type of accident usually occurs in large buses or trucks and this accident that can cause more damage than other types of road traffic accidents. The main cause of this type of accident due to the loss of the balance of the car when turning the curve on the steep slope, which will result in damage to the side of the structure including the roof is damaged. The size of buses usually varies between 8-12m in length. The bus configuration was first determined by iterative topology optimizations for 4 design variables, i.e., pillar structure, side structure, roof structure and floor structure. The Bus structures manufactures have to concern about the safety of passengers. Therefore, the strength of bus structure is an

important factor for the bus structure design and production process. Various type of beam steels are normally used in a bus structure. Different joints are designed to assemble these steels together. Welding is a joining technique widely used in the bus structures fabrication. Although the welding process is properly, controlled, the strength of the bus structure at welded joint areas are decreased because of peculiarities such as inhomogeneous material, welding residual stress and weld geometry (D.Radaj,1996).

These peculiarities cause difficulty in stress evaluation at welded joints. Moreover, most bus structures in Thailand are designed base on past experiences of engineer in a company but those experiences might not enough for passenger safety . Engineering knowledge need to be applied in the effective bus structure design. Computer Aided Design (CAD) and Computer Aided Engineering (CAE) are tools to evaluate the stress on the bus structure under many loading conditions . S.Manokruang (2012) presented the bus structure design using Computer Aided Design (CAD) for analysis It was found that a wireframe structure such as shown in Figure 1.1. It could be analyzed using beam elements Furthermore, many studies found that maximum stress is normally occurred at welded joints. As previously stated, stresses at welded joints are difficult to evaluate . Useful recommendations of welded structure are also given guideline, e.g. International Institute of welded (IIW)(A.Hobbacher,2008), Eurocode(European Committee for standardization,1993). These recommendations are assigned to thick structure with thickness higher than 5mm. However, the bus structure are assembly of thin steel beams. G. Savaidis(2000) and A. Fokikidis(2007), studied various welded joints from bus structure . In addition, S.T. Lie(2000) studied stress concentration factor and Reduction Factor (FAR) of welded square hollow section T-

joint under axial and pure bending .The close form solutions with weld geometry are presented using T-joint model.

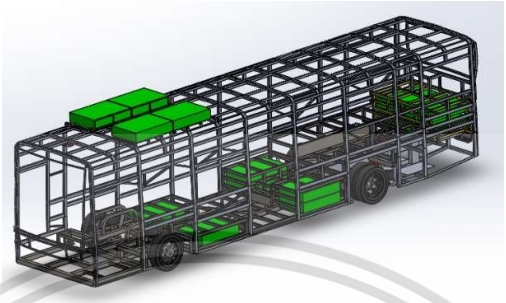

Figure 1.1 Bus Structure wireframe

Rollover accidents are a significant and growing contributor to this statistic. A rollover crash is a vehicular accident that is by nature, very violent as this type of crash is far more likely to result in the loss of life. While rollovers occur only in about three percent of all serious crashes, they account for about 30 percent of people killed while traveling in passenger vehicles. This research needs to study the substructure of buses. Conventional bus structure has been analyzed in this research. When an accident occurs, this Substructure part will have an important piece that helps secure passengers. As shown in Figure 1.2

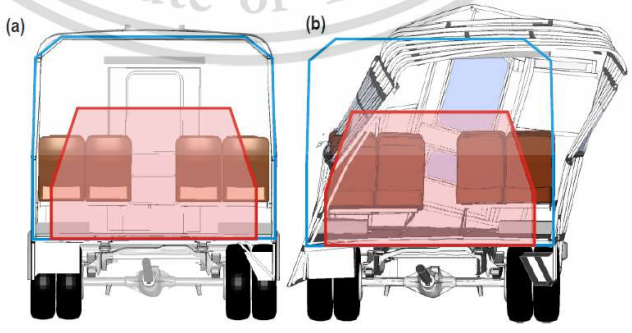

Figure 1.2 Simulation of Rollover behavior on bus structure

In general, the Rollover behavior test will use a full-scale bus structure for as shown in figure 1.3.

Figure 1.3 Full scale Rollover test

In general, the Rollover behavior test will use a full-scale bus structure for as shown in figure 1.3. In this study will present the test method, which tests only the important parts which will be separated into *3* main parts.

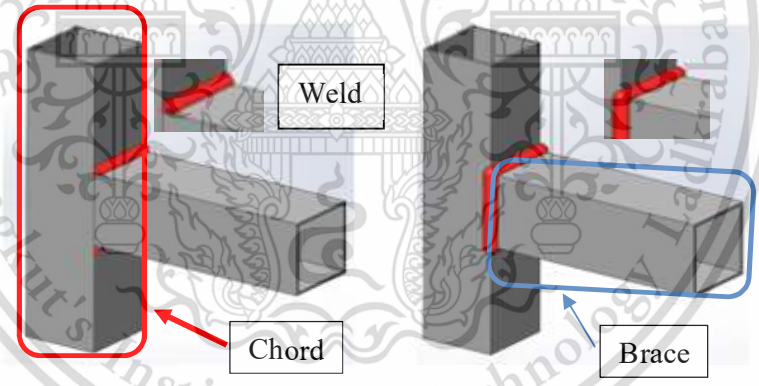

Figure 1.4 Welded T-joint

The stiffness of joints could be increased by reinforcements. Many joints in structures are normally reinforced by the plate steel . However, there is a welded joint in a bus structure is interesting . The square hollow steel are applied to prepare welded T-joint specimens a shown in Figure 1.4. The scope of this study was investigate different welding configurations position on T- joint of thin steel beams with thickness less than 5 mm commonly used in a bus structure under static in-plane bending.

1.2 Research Objective

1. To investigate and analyze the quality of weld on T- joint structure.
2. To investigate the behavior deformation for each weld type on substructure under the rollover situation.
3. To improve and develop alternative joint for substructure.
4. To select an appropriate joining of substructure.

1.3 Scope of Research

1. Design test rig that perform bending behavior on T-joint structure.
2. Perform deformation behavior on specimens for each weld type
3. Develop alternative joint and compare to each weld type

CHAPTER 2

LITERATURE REVIEW

2.1 Metal Deformation Failure

The microscopic yielding mechanism in ductile material is understood to be due to relative sliding of materials atoms within their lattice structure. This sliding is caused by shear stresses and is accompanied by distortion of the shape of the part. Thus the yield strength in shear S_{sy} is strength parameter of the ductile material used for design purposes (www.cadthai.com/article/4508/1/criteria_1.html)

2.1.1 Maximum shear stress theory (Tresca's Yield Theory)

The Maximum Shear Stress theory states that failure occurs when the maximum shear stress from a combination of principal stresses equals or exceeds the value obtained for the shear stress at yielding in the uniaxial tensile test.

At yielding, in an uni-axial test, the principal stresses are 1 = Sy; 2 = 0 and 3 = 0. Therefore the shear strength at yielding

$$S_{sy} = \frac{[1-(2\ or\ 3=0)]}{2} \tag{2.1}$$

Therefore $$S_{sy} = \frac{S_y}{2} \tag{2.2}$$

To use this theory for either two or three-dimensional static stress in homogeneous, isotopic, ductile materials, first compute the three principal stresses ($\sigma 1, \sigma 2, \sigma 3$) and the maximum shear stress τ_{13} as

$$\tau_{max} = \frac{(\sigma_1 - \sigma_2)}{2} = \frac{(\sigma_{p\,max} - \sigma_{p\,min})}{2} \tag{2.3}$$

Then compare the maximum shear stress to the failure criterion.

$$\tau_{max} \leq S_{sy} \text{ or } \frac{(\sigma_{p\,max} - \sigma_{p\,min})}{2} \leq S_{sy} \quad (2.4)$$

The safety factor for the maximum shear-stress theory is given by

$$N = \frac{S_{sy}}{\tau_{max}} \quad (2.5)$$

$$\tau_{max} < \tau_{cr} = \frac{\sigma_{yp}}{2} \quad (2.6)$$

N = Safety factor

τ_{max} = Maximum Shear Stress on specimens

τ_{cr} = Critical Shear Stress (Material properties)

σ_{yp} = Tensile Stress at Yield point (Material properties from tensile test)

2.1.2 Maximum distortion energy theory (von Mises-Hencky's Theory)

Distortion energy theory states that failure by yielding under a combination of stresses occurs when the energy of distortion equals or exceeds the energy of distortion in the tensile test when the yield strength is reached."

According to theory failure criteria is

$$S_y = [\sigma_1^2 + \sigma_2^2 + \sigma_3^2 - \sigma_1\sigma_2 - \sigma_2\sigma_3 - \sigma_3\sigma_1]^{1/2} \quad (2.7)$$

For two dimensional stress state ($\sigma_2 = 0$), the equations reduces to

$$S_y = [\sigma_1^2 + \sigma_3^2 - \sigma_3\sigma_1]^{1/2} \quad (2.8)$$

The von-Mises effective stress (σ_e) also sometimes referred to as equivalent stress is defined as the uniaxial tensile stress that would create the same distortion energy as is created by the actual combination of applied stresses.

$$\sigma_e = [\sigma_1{}^2 + \sigma_2{}^2 + \sigma_3{}^2 - \sigma_1\sigma_2 - \sigma_2\sigma_3 - \sigma_3\sigma_1]^{1/2} \quad (2.9)$$

$$\sigma_e = [\sigma_1{}^2 + \sigma_3{}^2 - \sigma_3\sigma_1]^{1/2} \quad (2.10)$$

In terms of applied stresses in coordinate directions

$$\sigma_e = [\sigma_{xx}{}^2 + \sigma_{yy}{}^2 - \sigma_{xx}\sigma_{yy} + 3\tau_{xy}{}^2]^{1/2} \quad (2.11)$$

Safety factor for distortion

$$N = \frac{S_y}{\sigma_e} \quad (2.12)$$

2.2 Welding Theory

Connecting the work pieces together with the welding process can choose from several methods of welding depends on the design of the work types of materials, work, strength, welding ability in that process The impact on the workpiece, etc. How to choose which method Can be considered as follows (Prof. SR. Satish Kumar and Prof. A.R. Santha Kumar, 2010)

2.2.1 Welding with Shielded Metal Arc Welding: SMAW

Is the process of connecting the metal together by using heat from the arc between the work piece and the welding wire cover the heat flux for about 5,000 degrees Celsius to melt the workpiece metal.

2.3 MIG Welding

Gas metal arc welding covered Is a welding process that is used to replace welding with an electrical wire. The flux can be welded in various metals, especially thick aluminum. In 1948, the gas arc welding process was covered. Well known and widely used in trade. In the beginning, this welding process is used for welding aluminum and using inert gas. Which is called MIG (Metal Inert Gas Welding) and later developed the use of CO2 gas when O2 is gas covered to weld carbon steel and low alloy steel The United States Welding Association calls this connection the GMAW (Gas Metal Arc Welding). Most of Japan and Europe call the welding process that uses CO2 to cover the mag (MAG), which comes from the term metal active gas. Because CO2 gas when passing the arc will change to active gas that is sensitive to the reaction.

Principles of metal arc gas welding (GMAW) welding method, gas metal arc welding

2.3.1 Gas Metal Arc Welding process(GMAW)

GMAW that receives heat from the arc between the welding wire and the workpiece Is a solid bare welding wire that is continuously fed into the arc area, acting as a metal to fill and melt. The melting pond will be covered with gas to prevent the formation of air.

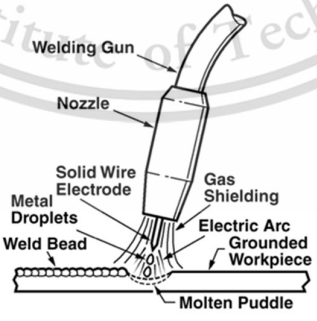

Figure 2.1 Gas metal arc welding Process (GMAW)

(Source : http://www.supradit.com/contents/metal/Data/5/1.html)

2.3.1.1 Advantage (GMAW compared with other weld processes)

1.) There is very little slag produce so its post weld cleaning is minimal.

2.) This process can be used in every position which is an advantage over the SAW welding process.

3.) Being that the electrode is a continuous wire it allows for long welds without the need to stop.

4.) It can be Automated for high production with repeatable parts.

5.) GMAW can have high travel speeds and deposition rates if it is compared to Shielded Metal Arc Welding (Stick/SMAW), which can save money on down time

6.) It is a process that is sometimes considered to be easier to learn than other processes.

7.) The Process is Capable of welding Dissimilar metals.

2.3.1.2 Limitation ((GMAW compared with other weld processes)

1.) The welding machine itself is more complex than the SMAW power supplies, which leads to an increase in equipment costs.

2.) Due to the size of the GMAW Gun it makes it hard to reach into smaller areas.

3.) Also, there is a lot of heat that is radiated off the process that can cause discomfort.

4.) The Shielding Gas can be blown away from the weld pool causing many issues.

5.) The whip should not be coiled while welding is being performed, because of possible undesirable feeding issues.

6.) Not Suitable for field area or outside the building. Because the wind may blow covering gas from the Arc area (It should be made a wind shelter).

2.3.2 Application for MIG

Implementation In the process of welding all metal arc gas the welding wire will be fed to the welding head with an automatic system. That can control the feed speed. For shaking welding head depends on the Semi-automatic welding system being a semi-automatic welding process. Which the welding control device is controlled by manually except wire feed.

2.4 Welding design

Welding is a very commonly used permanent joining process. Thanks to great advancement in welding technology, it has secured a prominent place in manufacturing machine components. A welded joint has following advantages:

1.) Compared to other type of joints, the welded joint has higher efficiency.
An efficiency > 95 % is easily possible.

2.) Since the added material is minimum, the joint has lighter weight.

3.) Welded joints have smooth appearances.

4.) Due to flexibility in the welding procedure, alteration and addition are possible.

5.) It is less expensive.

6.) Forming a joint in difficult locations is possible through welding.

The advantages have made welding suitable for joining components in various machines and structures.

2.4.1 Types of welded joints

2.4.1.1 Lap or fillet joint

obtained by overlapping the plates and welding their edges. The fillet joints may be single transverse fillet, double transverse fillet or parallel fillet joints as shown in figure 2.2

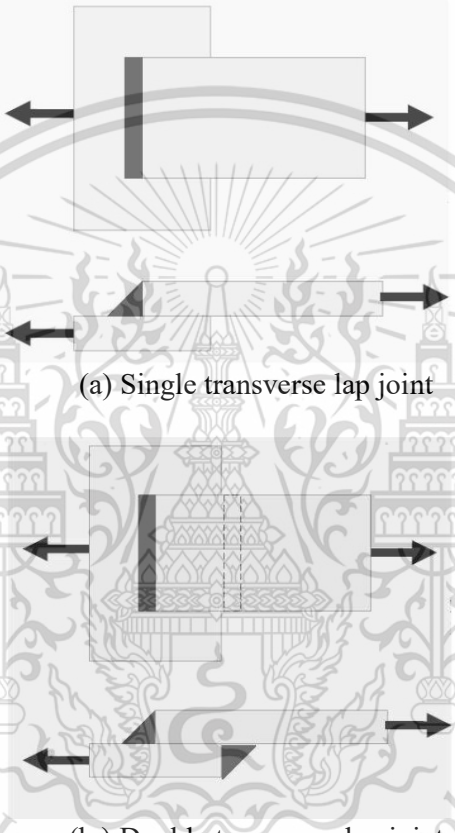

(a) Single transverse lap joint

(b.) Double transverse lap joint

(c.) Parallel lap joint

Figure2.2 Different types of lap joint

(Source: Design of steel structures. Indian Institute of Technology Madras,2010)

2.4.1.2 Butt joint

Formed by placing the plates edge to edge and welding them. Grooves are sometimes cut (for thick plates) on the edges before welding. According to the shape of the grooves, the butt joints maybe of different types as shown in figure 2.3.

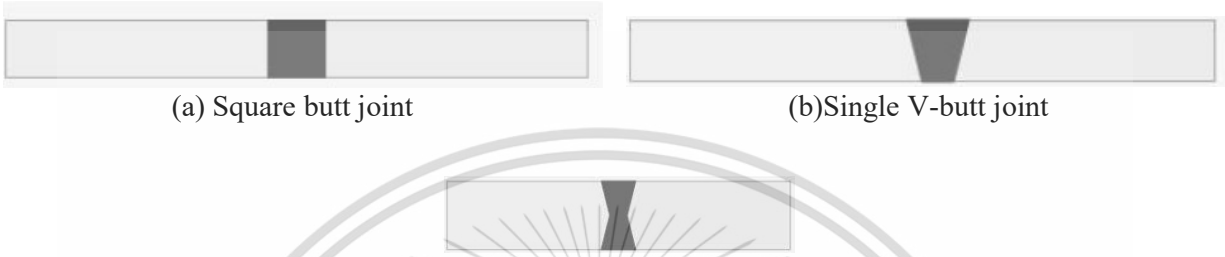

(a) Square butt joint

(b)Single V-butt joint

(c) Double – V butt joint

Figure 2.3 Different types of butt joints

(Source: http://ecoursesonline.iasri.res.in/mod/page/view.php?id=125520)

2.4.2 Strength of weld: in-plane loading

There are different forms of welded joints, subjected to in-plane loading under tension.

2.4.2.1 Transverse fillet weld

Figure 2.4*a* shows a double transverse fillet weld under tension. It is assumed that the section of the weld is an isosceles right-angled triangle, ABC, i.e. 45o fillet weld (Fig.2.4b).

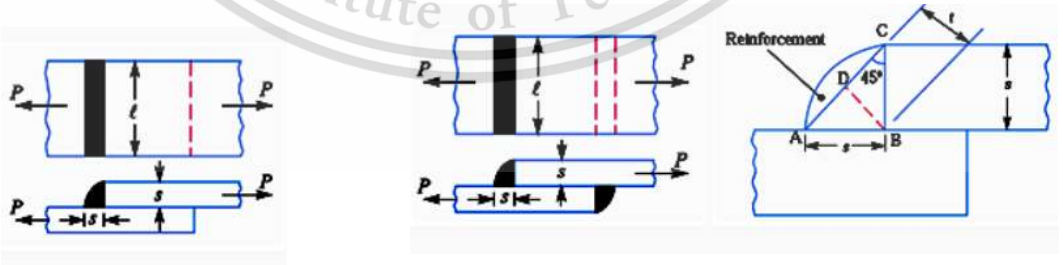

(a) (b)

Figure 2.4 Double transverse fillet weld

(Source: http://ecoursesonline.iasri.res.in/mod/page/view.php?id=125520)

The length of each side (AB=BC) is known as leg length or size of the weld. The minimum cross-sectional dimension, BD (at 45o from the plate surface or edge) is termed as throat thickness. Transverse fillet welds are assumed to fail in tension across the throat.

Let t = thickness of the plate or size of the weld

l = length of the weld

σ t = allowable tensile stress

From the geometry of Fig. 2.4b,

Throat thickness, BD$(=h) = t \sin 45° = \frac{t}{\sqrt{2}}$ (2.13)

Resisting throat area = $hl = \frac{tl}{\sqrt{2}}$ (2.14)

Tensile strength of the joint = $\frac{tl}{\sqrt{2}} \sigma$ t = $\sqrt{2}tl\sigma$ t , for double fillet (2.15)

2.4.2.2 Parallel fillet weld

Figure 2.5a shows a double parallel fillet weld under tension. Parallel fillet welds are assumed to fail in shear across the throat.

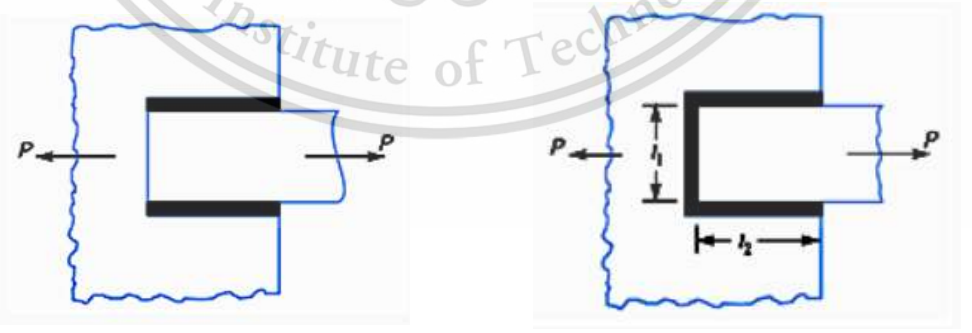

(a) Double parallel fillet weld (b) Combination of transverse and parallel fillet weld

Figure 2.5 Parallel weld
(Source: http://ecoursesonline.iasri.res.in/mod/page/view.php?id=125520)

Let τ = allowable shear stress for the weld material

Resisting throat area = $\frac{tl}{\sqrt{2}}$ (2.16)

Shear strength of the joint = $\frac{tl}{\sqrt{2}}\tau$, for single fillet (2.17)

= $\frac{2tl}{\sqrt{2}}$ $\sqrt{2}\,tl\tau$, for double fillet (2.18)

2.4.2.3 Butt weld

Fig. 2.6a shows a single V-butt joint under tension.

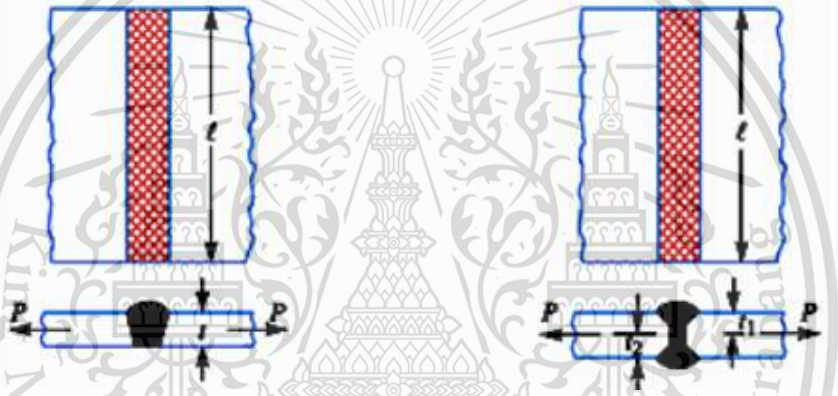

(a) (b)

Figure 2.6 Butt joints under tension

(Source: http://ecoursesonline.iasri.res.in/mod/page/view.php?id=125520)

In case of single V-butt weld, the throat thickness of the weld is considered to be equal to the plate thickness, *t*. Hence,

tensile strength of the joint = $tl\sigma_t$ (2.19)

Where, *l* = length of the weld = width of the plate.

Figure 2.15b shows a double V-butt joint under tension.

Let $h1$ = throat thickness at the top

$h2$ = throat thickness at the bottom

Then tensile strength of the joint = ($h1$ + $h2$) l σ t (2.20)

2.4.2.4 Fillet welds under bend loading

Figure 2.7 shows a double parallel fillet weld, subjected to bending load, P. The joint is symmetric about the neutral plane.

Area resisting bending on the tensile (compressive) side,

$$\text{throat area} = \quad A = 2\,t\,l \tag{2.21}$$

where , t = size of the weld

This applied load may be considered as a load P directly acting on the joint through the CG and a bending moment of magnitude P.e acting on the joint. 1st one will lead to direct shear stress and the 2nd will lead to a bending stress.

$$\text{Direct Shear Stress} = \frac{P}{A} = \frac{P}{2t} \text{ x } l(\text{b+t})\ \sigma_t \tag{2.22}$$

$$\text{Bending Stress} = \sigma_b = \frac{My}{I} \tag{2.23}$$

Where y = distance of the point on the weld from the neutral axis

I = Moment of inertia of the weld section

Maximum tensile and shear stress may be calculated as:

$$\sigma_{t\,max} = \left(\frac{\sigma_{tb}}{2}\right)^2 + \sqrt{\left(\frac{\sigma_{tb}}{2}\right)^2 + \tau^2} \tag{2.24}$$

$$c = \sqrt{\left(\frac{\sigma_{tb}}{2}\right)^2 + \tau^2} \tag{2.25}$$

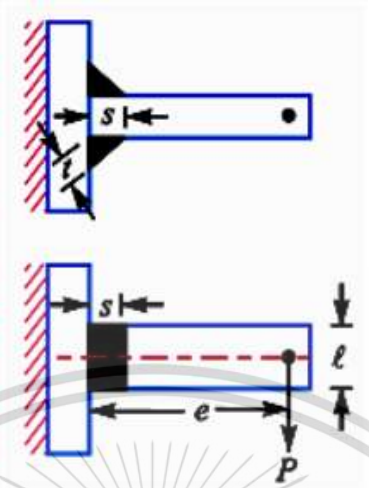

Figure 2.7 Fillet welds under bending load

(Source: http://ecoursesonline.iasri.res.in/mod/page/view.php?id=125520)

2.4.2.5 Weld joint under eccentric loading

A more general case of eccentric loading is shown in Fig. 2.8. Here, the fillet welds are subjected to the action of a load, P acting at a distance, *e* from the centre of gravity of the weld system. To understand the effect of eccentric load, P; introduce two equal and opposite forces, P1 - P2 (=P) and passing through G, the centre of gravity of the weld system, as shown.

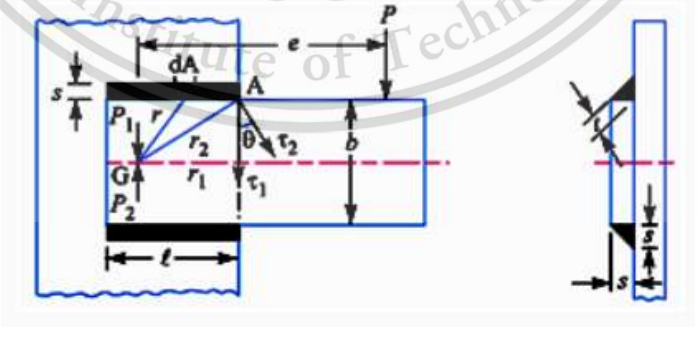

Figure 2.8 Eccentric Loading

(Source: http://ecoursesonline.iasri.res.in/mod/page/view.php?id=125520)

The effect of $F1(=F)$ is to produce direct or primary shear stress, τ_1, and the effect of P - $P2$ ($=P$-P) is to produce twisting moment, Pe; resulting in secondary shear stress, τ_2 in the welds.

Primary shear stress, $$\tau_1 = \frac{P}{A} = \frac{P}{2tl} \quad (2.26)$$

Secondary shear stress, $$\tau_1 = \frac{Mr}{J} \quad (2.27)$$

Where r = distance of the point on the weld from the CG

J = Polar moment of inertia of the weld section

r is calculated from the geometry for the farthest point of the weld from the CG.

2.5 T-joints rectangular hollow section design

The structural advantage of hollow sections has become apparent to most designer, particularly for structural members loaded in compression or torsion. Circular hollow sections (CHS) have a particularly pleasing shape and offer very efficient distribution of steel about the centroidal axes, as well as the minimum possible resistance to fluid, but specialized profiling is needed when joining shapes together. As a consequence, rectangular hollow sections (RHS) have evolved as a practical alternative, allowing easy connections to the flat face, they are very popular for columns and trusses. so, this study was designed base on RHS.

According to **C**ommittee for **I**nternational **D**evelopment and **E**ducation on **C**onstruction of **T**ubular structures (CIDECT) standard, the connection ultimate moment capacity in tests is typically recorded, and Korol rt al even developed an empirical formula for estimating the maximum connection moment, but this moment typically occurs at excessively large connection deformation. Thus, for all practical design purposed, the moment capacity of a connection can be determined in a manner similar to that used for axially-load RHS T-joints, whereby the strength is characterized

by an ultimate bearing capacity or by a deformation or rotation limited. This design approach is more apparent if one considers the possible failure modes for such connection, which are shown in Figure 2.9 presume that neither the welds nor the members themselves are critical (e.g. local buckling of the vertical part is precluded). Chord shear failure (d) has not actually been observed in any test, so analytical solutions for failure modes (d) are not considered herein.

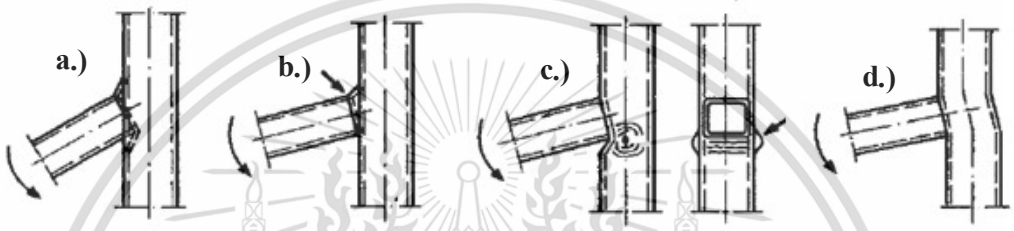

Figure 2.9 Possible failure modes for RHS connections loaded by in-plane load a.) Chord face yielding b.) Tearing in Chord c.) Crippling of the chord side walls d.) Chord shear failure

(Source: CIDECT design guide for rectangular hollow section joints under predominantly static loading, Jeffrey A. Packer,1992)

According to CIDECT standard, a typical welded T-joint is shown in figure 2.10 where a brace is welded to a chord. Symbols used in this formula are defined on figure 2.10. Efficiency of T-connection will show in figure 2.11.

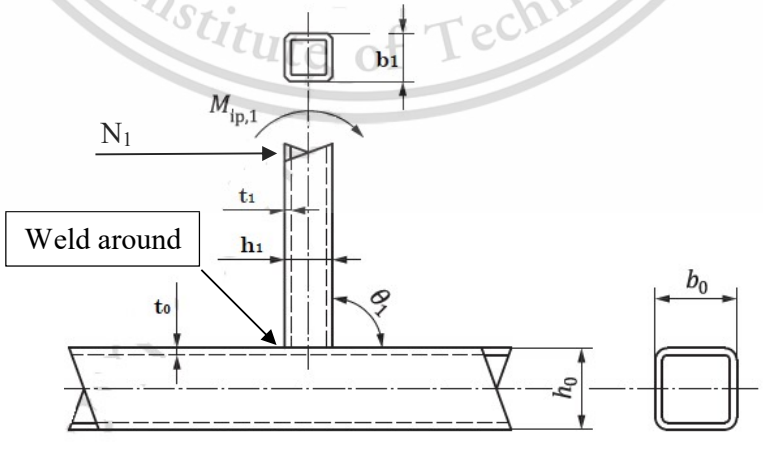

Figure 2.10 T-joint (RHS) with brace in-plane bending load

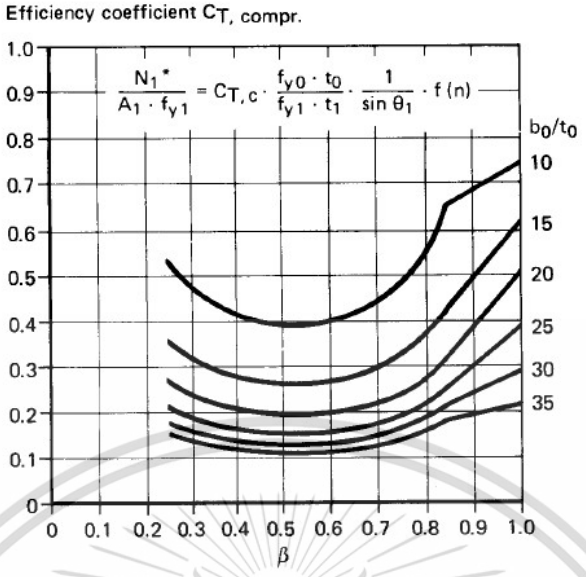

Figure 2.11 Relation chart between Efficiency coefficient and Brace-Chord ratio of T-joint connection

(Source : CIDECT standard guide design 3)

brace-chord width ratio

$$\beta = \frac{b_0}{t_0} = \frac{b_1}{t_1} \tag{2.28}$$

Where β = Brace-Chord ratio

b = Width of Brace and Chord (mm)

t = Thickness of Brace and Chord (mm)

Maximum allowable force

$$N_1 = A_1 . f_{y1} . C_T . \frac{f_{y0} . t_0}{f_{y1} . t_1} . \frac{1}{sin\theta} \tag{2.29}$$

Where N = Maximum force for T-connection (kN)

A = Section area on Hollow section tube (mm^2)

C_T = Efficiency coefficient from Chart

f_y = Yield Stress of brace and chord (MPa)

2.6 Tension test

According to the test method Samples that will be tested will be pulled slowly. And then record the value of stress and stress caused plotted as a curve shown in Figure 2.12 Graph showing stress and strain relationships the size and shape of the piece. There are different tests depending on the type of material. Various standards of testing such as standards Of ASTM (American Society of Testing and Materials), BS (British Standards), JIS (Japanese Industrial Standards) or even TIS (Industrial Product Standards Thai) has determined the size and shape of the test piece in order for the results of the test to be reliable with the speed to increase the action.

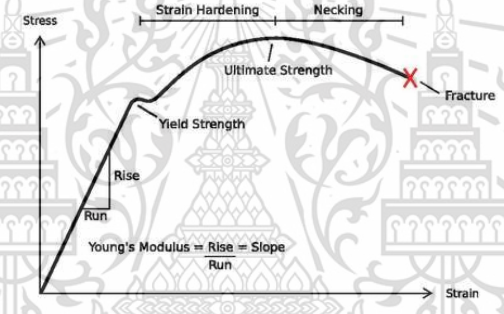

Figure 2.12 Stress and Strain Relationship

The first stage is the linear elastic region. The stress is proportional to the strain, that is, obeys the general Hooke's law, and the slope is Young's modulus. In this region, the material undergoes only elastic deformation. The end of the stage is the initiation point of plastic deformation. The stress component of this point is defined as yield strength (or upper yield point, UYP for short).

The second stage is the strain hardening region. This region starts as the strain goes beyond yielding point, and ends at the ultimate strength point, which is the maximal stress shown in the stress-strain curve (tensile strength, T.S., also sometimes referred to as the ultimate tensile strength, D.T.S.). In this region, the stress mainly

increases as material elongates, except that there is a nearly flat region at the beginning. The stress of the flat region is defined as the lower yield point (LYP) and results from the formation and propagation of Lüders bands. Explicitly, heterogeneous plastic deformation forms bands at the upper yield strength and these bands carrying with deformation spread along the sample at the lower yield strength. After the sample is again uniformly deformed, the increase of stress with the progress of extension results from work strengthening, that is, dense dislocations induced by plastic deformation hampers the further motion of dislocations. To overcome these obstacles, a higher resolved shear stress should be applied. As the strain accumulates, work strengthening gets reinforced, till the stress reaches the tensile strength.

The third stage is the necking region. Beyond tensile strength, a *neck* forms where the local cross-sectional area becomes significantly smaller than the average. The necking deformation is heterogenous and will reinforce itself as the stress concentrates more at small section. Such positive feedback leads to quick development of necking and leads to fracture. Note that though the pulling force is decreasing, the work strengthening is still progressing, that is, the true stress keeps growing but the engineering stress decreases because the shrinking section area is not considered. This region ends up with the fracture. After fracture, percent elongation and reduction in section area can be calculated.

2.7 Rivet design

Often small machine components are joined together to form a larger machine part. Design of joints is as important as that of machine components because a weak joint may spoil the utility of a carefully designed machine part. Mechanical joints are broadly classified into two classes viz., non-permanent joints and permanent joints. Non-permanent joints can be assembled and dissembled without damaging the

components. Examples of such joints are threaded fasteners (like screw-joints), keys and couplings etc.

Permanent joints cannot be dissembled without damaging the components. These joints can be of two kinds depending upon the nature of force that holds the two parts. The force can be of mechanical origin, for example, riveted joints, joints formed by press or interference fit etc, where two components are joined by applying mechanical force. The components can also be joined by molecular force, for example, welded joints, brazed joints, joints with adhesives etc. Not until long ago riveted joints were very often used to join structural members permanently. However, significant improvement in welding and bolted joints has curtained the use of these joints. Even then, rivets are used in structures, ship body, bridge, tanks and shells, where high joint strength is required. Riveted joints are mainly of two types

2.7.1 Lap joints

The plates that are to be joined are brought face to face such that an overlap exists, as shown in figure 2.13 Rivets are inserted on the overlapping portion. Single or multiple rows of rivets are used to give strength to the joint. Depending upon the number of rows the riveted joints may be classified as single riveted lap joint, double or triple riveted lap joint etc. When multiple joints are used, the arrangement of rivets between two neighboring rows may be of two kinds. In chain riveting the adjacent rows have rivets in the same transverse line. In zig-zag riveting, on the other hand, the adjacent rows of rivets are staggered.

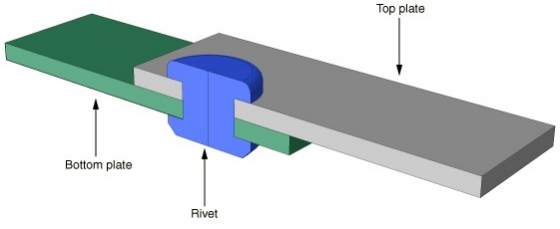

Figure 2.13 Lap joint

2.7.2 Butt joints

A butt joint is that in which the main plated are kept in alignment butting (i.e. touching) each other and a cover plate (i.e. strap) is placed either on one side or both sides of the main plates. The cover plate is then riveted together with the main plates. Butt joints are of the following two types

2.7.2.1 Single strap butt joint

The edges of the main plates butt against each other and only one cover plate is placed on one side of the main plates and then riveted together as shown in figure 2.14.

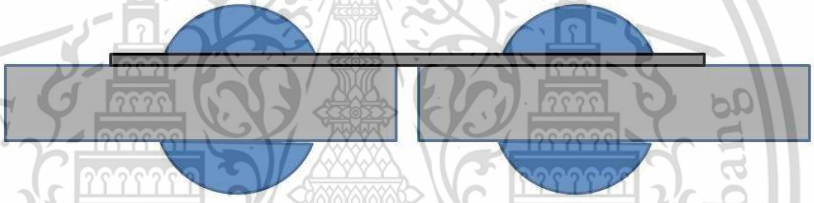

Figure 2.14 Single strap butt joint

2.7.2.2 Double strap butt joint

The edges of the main plates butt against each other and two cover plates are placed on both sides of the main plates and then riveted together as shown in figure 2.15.

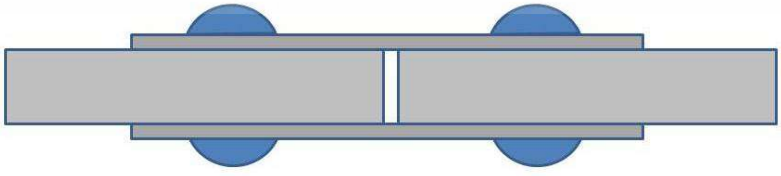

Figure 2.15 Double strap Butt joint

2.7.3 Other types of rivet

In addition to the above, following are the types of riveted joints depending upon the number of rows of the rivets.

2.7.3.1 Single Riveted joint

A joint that is in which there is a single row of rivets in a lap joint as shown in Figure 2.16(a). And there is a single row of the rivets on each side in abut joint as shown in figure 2.16.

2.7.3.2 Double riveted joint

A joint that in which there are two rows of rivets in a lap joint as shown in figure 2.16 (b), (c) and there are two rows of rivets on each side in a butt joint as shown in figure 2.16-2.20.

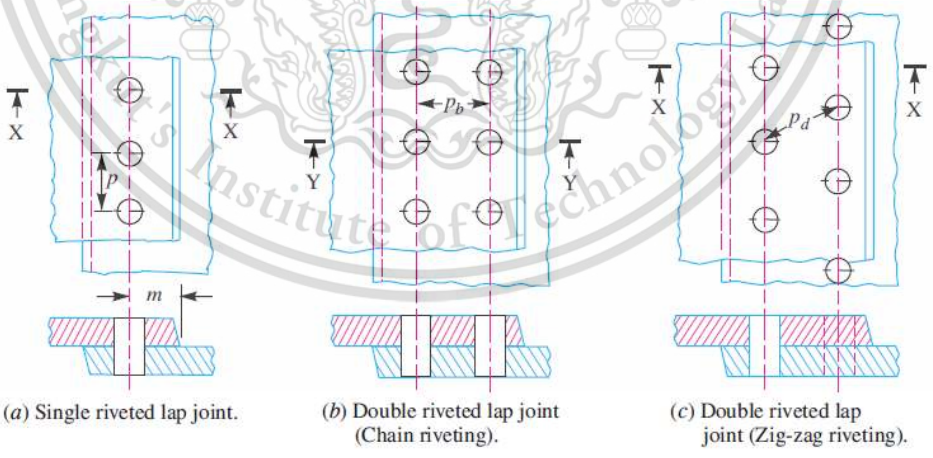

Figure 2.16 Single and double rivet lap joints.
(Source: A text book of machine design, chapter9 ,Riveted joints)

Similarly, the joints may be triple riveted, or quadruple riveted.

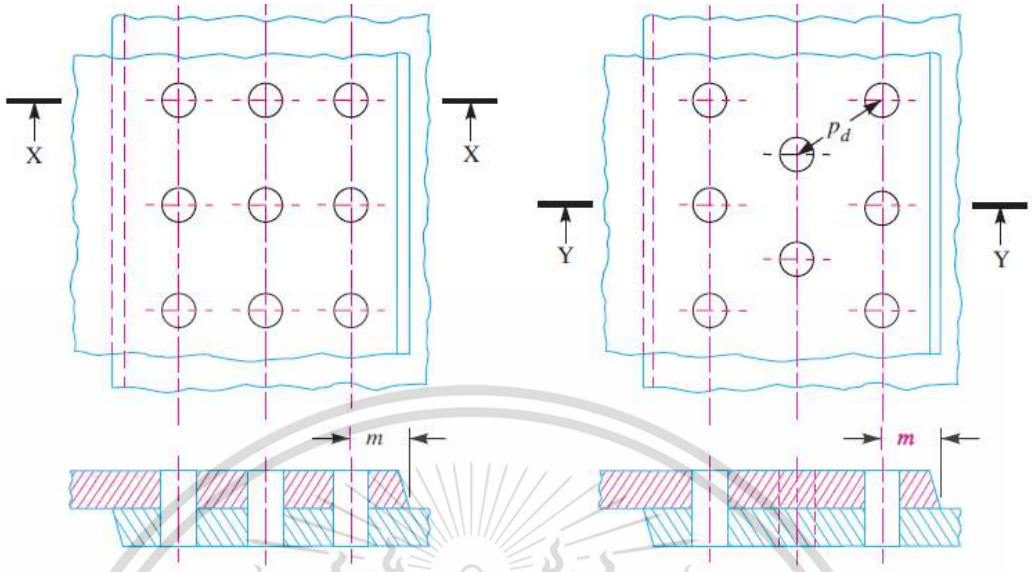

Figure 2.17 Triple rivet lap joint
(Source: A text book of machine design, chapter9 ,Riveted joints)

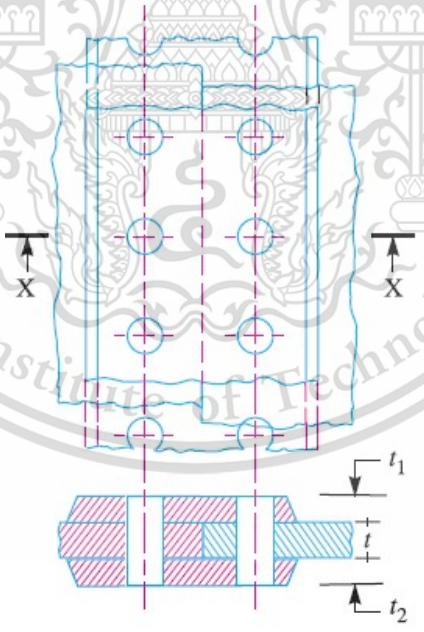

Figure 2.18 Single riveted double strap butt joint
(Source: A text book of machine design, chapter9, Riveted joints)

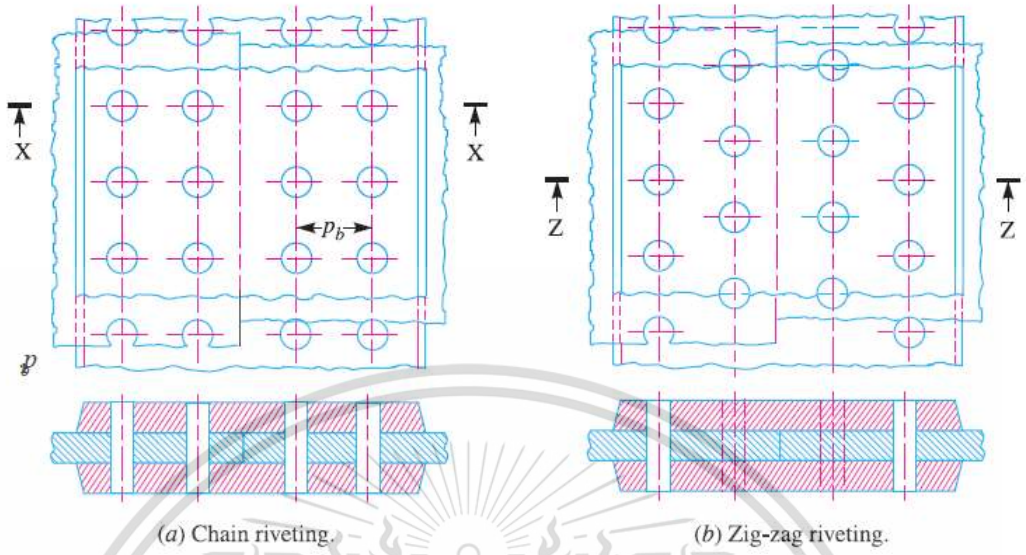

Figure 2.19 Double riveted double strap (equal) butt joints
(Source: A text book of machine design, chapter9 ,Riveted joints)

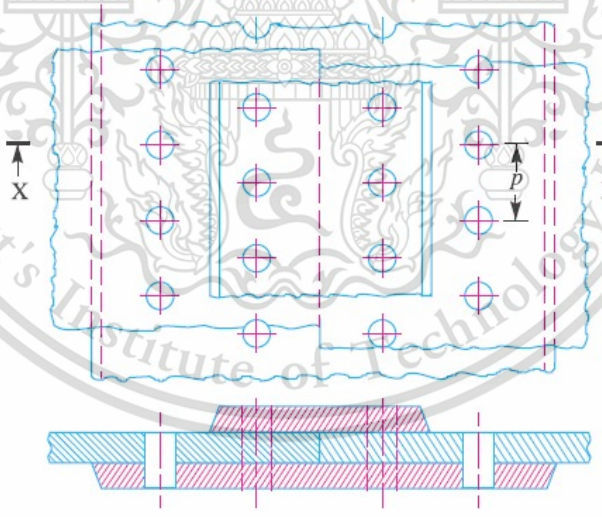

Figure 2.20 Double riveted double strap (unequal) butt joints with zig-zag riveting
(Source: A text book of machine design, chapter9 ,Riveted joints)

2.7.4 Important term used in rivet joints

The following terms in connection with the riveted joints are important from the subject point of view:

1.) **Pitch.** It is the distance from the Centre of one rivet to the Centre of the next rivet measured parallel to the seam as shown in Figure 2.21. It is usually denoted by p.

2.) **Back pitch.** It is the perpendicular distance between the Centre lines of the successive rows as shown in Figure2.22. It is usually denoted by p_b.

3.) **Diagonal pitch.** It is the distance between the centers of the rivets in adjacent rows of zig-zag riveted joint as shown in figure 2.23. It is usually denoted by p_d.

4.) **Margin or marginal pitch.** It is the distance between the center of rivet hole to the nearest edge of the plate as shown in Figure 2.23. It is usually denoted by m.

2.7.5 Failure of a riveted joint

2.7.5.1 Tearing of the plate at an edge

A joint may fail due to tearing of the plate at an edge as shown in figure2.18 (a). This can be avoided by keeping the margin, m = 1.5d, where d is the diameter of the rivet hole.

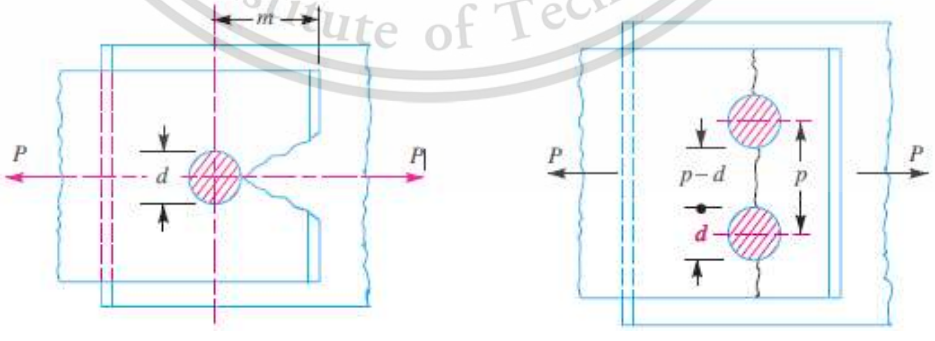

(a) Tearing of the plate an edge (b) Tearing of the plate across the rows of rivets

Figure 2.21 Tearing deformation
(Source: A text book of machine design, chapter9 ,Riveted joints)

2.7.5.2 Tearing of the plate across a row of rivets.

Due to the tensile stresses in the main plates, the main plate or cover plates mat tear off across a row of rivets as shown in figure 2.22(b). In such cases, we consider only one pitch length of the plate, since every rivet is responsible for that much length of the plate only

The resistance offered by the plate against tearing is known as tearing resistance or tearing strength or tearing value of the plate.

Let p = Pitch of the rivets,

d = Diameter of the rivet hole,

t = Thickness of the plate, and

σ_t= Permissible tensile stress for the plate material.

We know that tearing area per pitch length,

$$A_t = (p - d)t \tag{2.30}$$

Tearing resistance or pull required to tear off the plate per pitch length,

$$P_t = A_t \sigma_t = (p - d)t.\sigma_t \tag{2.31}$$

When the tearing resistance (P_t) is greater than the applied load (P) per pitch length, then this type of failure will not occur.

2.7.5.3 Shearing off the rivets.

The plates which are connected by the rivets exert tensile stress on the rivets,

And if the rivets are unable to resist the stress, they are sheared off as shown in figure2.22. It may be noted that the rivets are in single shear in a lap joint and in a single cover butt joint, as shown in figure 2.22. But the rivets are in double cover butt joint 2.23. The resistance offered by a rivet to be sheared off is known as shearing resistance or shearing strength or shearing value of the rivet.

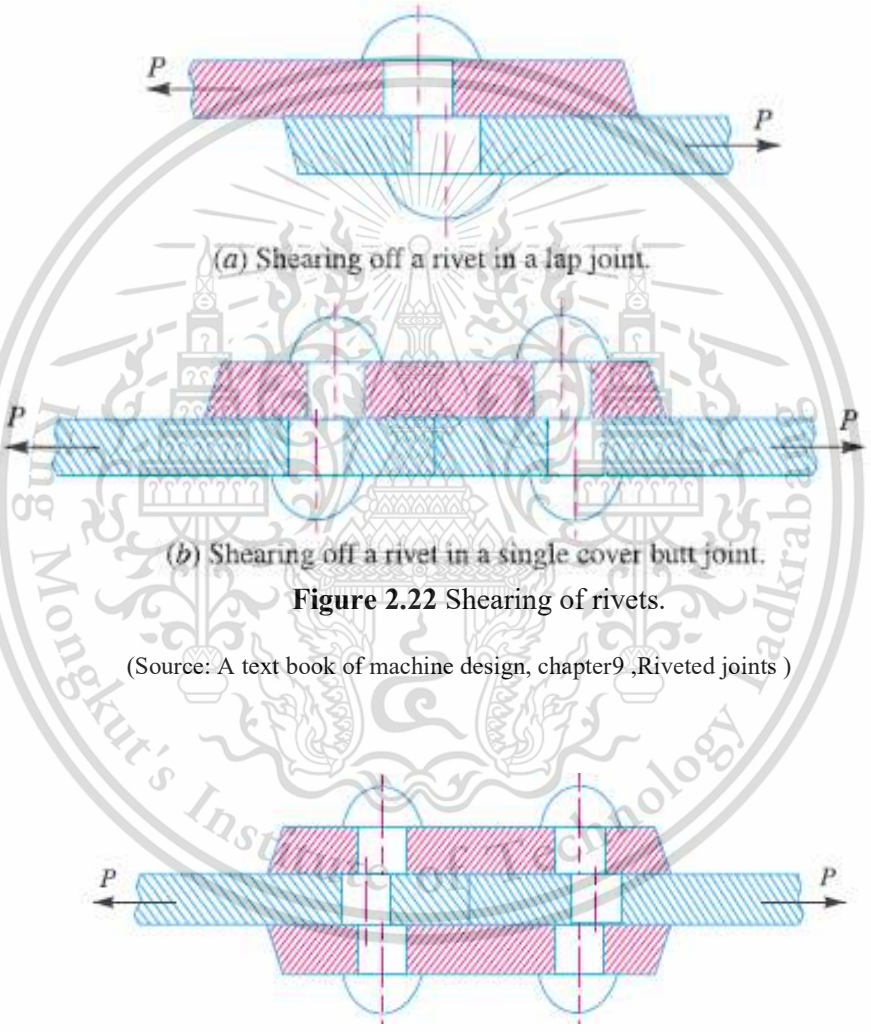

Figure 2.22 Shearing of rivets.

(Source: A text book of machine design, chapter9 ,Riveted joints)

Figure 2.23 Shearing off a rivet in double cover butt joint.
(Source: A text book of machine design, chapter9 ,Riveted joints)

Let d = Diameter of the rivet hole,

τ = Safe permissible shear stress for the rivet material,

n = Number of rivets per pitch length.

We know that shearing area,

$$A_s = \frac{\pi}{4} . d^2 \quad \text{(In single shear)} \quad (2.32)$$

$$= 2 . \frac{\pi}{4} . d^2 \quad \text{(double shear)} \quad (2.33)$$

$$= 1.875 . \frac{\pi}{4} . d^2 \quad \text{(double shear, Indian regulation)} \quad (2.34)$$

Shearing resistance or pull required to shear off the rivet per pitch length,

$$P_s = n . \frac{\pi}{4} . d^2 . \tau \quad \text{(single shear)} \quad (2.35)$$

$$= n . 2. \frac{\pi}{4} . d^2 . \tau \quad \text{(double shear)} \quad (2.36)$$

$$= n . 1.875. \frac{\pi}{4} . d^2 . \tau \quad \text{(double shear, Indian regulation)} \quad (2.37)$$

When the shearing resistance (P_s) is greater than the applied load (P) per pitch length, then this type of failure will occur.

2.7.5.4 Crushing of the plate rivets.

Sometimes, the rivets do not actually shear off under the tensile stress but were crushed as shown in figure 2.24. Due to this, the rivet hole becomes of an oval shape and hence the joint becomes loose. The failure of rivets in such a manner is also known as bearing failure. The area which resists this action is the projected area of the hole or rivet on diametral plane.

The resistance offered by a rivet to be crushed is known as crushing resistance or crushing strength or bearing value of the rivet.

When the crushing resistance (Pe) is greater than the applied load (P) per pitch length then this type of failure will occur.

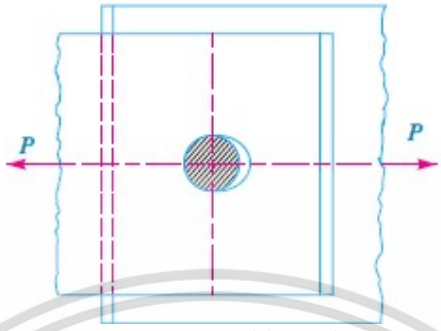

Figure 2.24 Crushing of a rivet
(Source: A text book of machine design , chapter9 ,Riveted joints)

2.7.6 Strength of a riveted joint

The strength of a joint may be defined as the maximum force, which it can transmit, without causing it to fail. P_t , P_s and P_c are the pulls required to tear off the plate, shearing off the rivet and crushing off the rivet. A little consideration will show that if we go on increasing the pull on riveted joint, it will fail when the least of these three pulls is reached, because a higher value of the other pulls will never reach since the joint has failed, either by tearing off the plate, shearing off or crushing off the rivet.

2.7.7 Efficiency of a riveted joint

The efficiency of riveted joint is defined as the ratio of the strength of riveted joint to the strength of the un-riveted or solid plate.

We have already discussed that strength of the riveted joint

= Least of P_t , P_s and P_c

Strength of the un-riveted or solid plate per pitch length,

$$P = p \, . \, t \, . \, \sigma_t \tag{2.38}$$

Efficiency of the riveted joint

$$\eta = \frac{\text{Least of } .P_t, P_s \text{ and } P_c}{p \, .t \, .\sigma_t} \tag{2.39}$$

Where p = Pitch of the rivets,

t = Thickness of the plate, and

σ_t = Permissible tensile stress of the plate material.

2.8 Literature Reviews

Sakkarin (2006) presented design and the development of double deck (standard No.4). The objective by study to the method of development the standard of double deck-bus type 8 wheels. At present, more than 80 percent is a bus that is built in local area and price is less than 50 percent, but the production process does not concern engineering analysis, so bus structure is unsafe for passenger. This research aims to develop and design 8-wheel bus (standard no.4) . The research was done by in spec and analysis to both chemical and mechanical properties of material. In chemical properties of structure had problem on assembly and found that weld joint not pass to standard property with lower on the tensile strength and bend test found that properties was fail. The dimension of chassis assembly was following to the law of transport department. Another development was developed to chassis structure assembly for extend along forward to the tail of chassis by add some bracket to stronger assembly.

Cho-Chung Liang (2009) presented optimization for rollover crashworthiness design of bus structure Bus superstructure was tested according to regulation No.66 By using LS-DYNA finite element software. The optimization was performed by the successive response surface method with LS-OPT. In the optimization problem, a design variable analysis focused on the energy absorption ability of bus frame components such as sidewall beam and roof. The objective was to minimize mass of bus structure and aimed to equalize the energy absorption of each component by changing the thickness. From the results, the mass of buss was increased by 1.6% while the deformation of bus structure is decreased by39.4 %.

Milad Moradi (2017) investigated the influence of various welding sequence schemes on the load bearing capacity of a S355 steel square hollow section (SHS)T-joint. The failure and the joint behavior under loading condition are analyzed. The FE-software ABAQUS AWI and SYSWELD v2014 are used for the thermo-mechanical simulation of the welding process. The type of welding process used is metal active gas (MAG) welding. A fillet weld with throat thickness of 5 mm is performed. In this research, the joints were all loaded under the same loading condition under brace concentric loading using a 2000 kN testing machine as shown in Figure 2.25. Four-Sequence type were performed in this research as shown in figure 2.26.

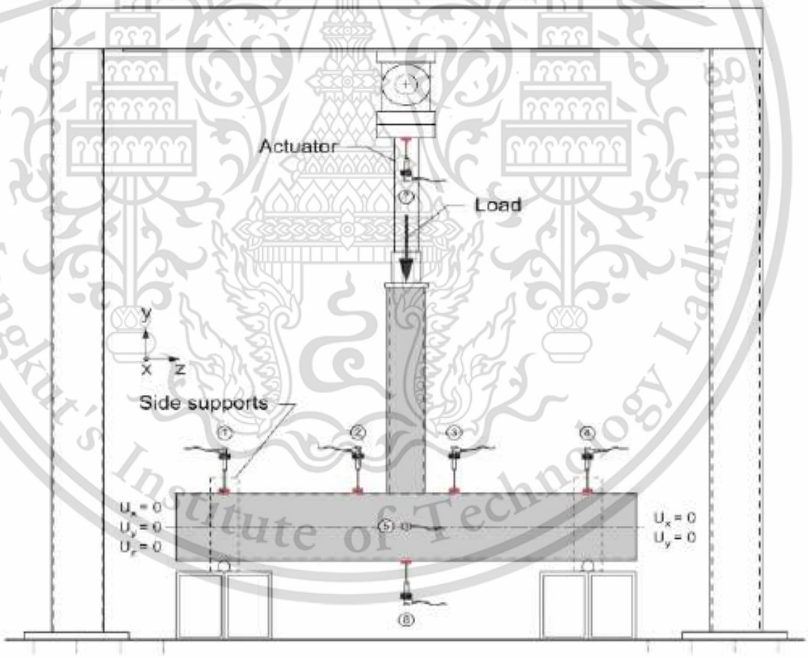

Figure 2.25 Compressive test configuration

(Source: Milad Moradi, A Study on the Influence of Various Welding Sequence Schemes on the Gain in Strength of Square Hollow Section Steel T-Joint, Journal of Welding and Joining, Vol.35No.4,2017)

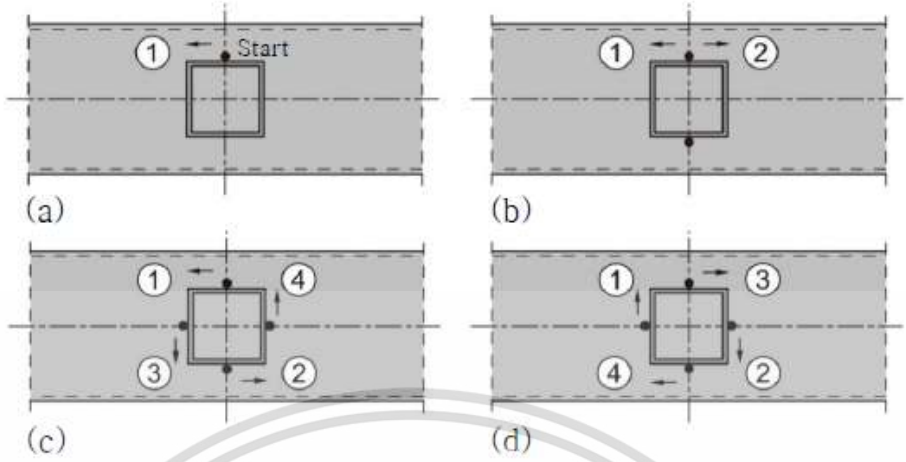

Figure 2.26 Weld sequence studied . (a) Right progressive welding, (b) double-phase progressive welding, (c) skip welding, (d) reverse skip welding

(Source: Milad Moradi, A Study on the Influence of Various Welding Sequence Schemes on the Gain in Strength of Square Hollow Section Steel T-Joint, Journal of Welding and Joining, Vol.35No.4,2017)

The results in terms of stresses were compared and many similarities have been found between the solutions offered by the two commercial software used. Measured results of longitudinal and transverse stresses have shown that various weld sequence schemes can lower the magnitude of residual stresses especially around the weld toe and in the heat affected zone. Progressive welding sequence was the strongest. Gain in strength drops by increasing the number of start and end points, reaching a maximum value of -10 % when 8 start and end points are involved. The number of start and end points were highly influence the overall behavior of the joints. Further experimental and numerical investigations are needed especially with focus on the areas between start and end points where the stress concentration tend to shape.

C.K. Lee (2013) investigated on the residual stress distributions near the weld toe of high strength steel box section T-joints is conducted. Two specimens fabricated by welding at ambient temperature and at preheating temperature of 100° C were studied. The effects of preheating on the residual stress distribution near the weld toe of the T-joint were investigated by applying the standard ASTM hole-drilling method. The ASTM hole-drill method was employed to measure residual stress at critical locations of the joint near the chord weld toe. It is found that preheating is beneficial and can effectively reduce the magnitude of residual stress. For the residual stress distributions, It is found that residual stress at the corners of the joint are higher than at other positions for both specimens and the transverse component is the dominating residual stress component.

L.Han(2006) presented effect of specimen configuration on the mechanical behavior of self-piercing riveted, multi-layer joints in aluminium alloys was conducted. It has observed that the specimen configuration had a significant effect on the strength and failure mechanism of self-piercing riveted multi-layer joint. Two configurations were prepared in this research as shown in figure2.27. From the results, the G111 group of samples exhibited the highest joint strength and energy absorption, while the G21 samples exhibited the worst behavior. Secondary bending is a major contributor of failure for the G21 and G12 single-shear lap joints. Due to the absence of secondary bending, the double-shear joints of the G111 configuration therefore had superior shear performance.

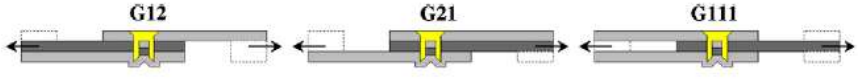

(a) Configuration for shear test

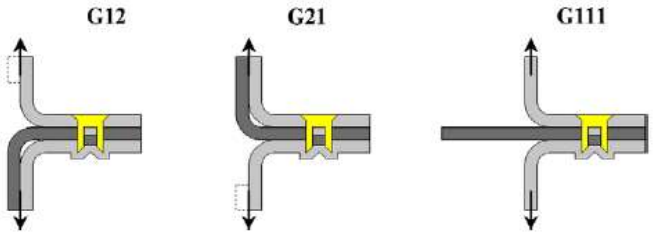

(b) Configuration for peel test

Figure2.27 Illustration of specimen Configurations

Source: L.Han, Mechanical behavior of self-piercing riveted multi-layer joints under different specimen configurations ,Material and Design 28 , 2007

Jacek Mucha (2015) investigated the mechanical behavior and failure of riveted joints determined and compared between the lap joint unilateral tensile test and shear test In this research, four types of riveted joints were used: aluminium-steel blind rivet (BR), aluminium-steel blind hermetic rivet (BHR) , aluminium alloy rivet fir closing up (COUR) and Solid self -piercing steel rivet (SSPR) as shown in figure 2.28. The rivets had the same diameter of the cylindrical part (d_r = 4 mm), while the remaining geometry was selected for the total thickness of joined sheets (d_{tot} = 4mm). The specimens were prepared with dimensions included in ISO standard (2013) as shown in figure 2.29.

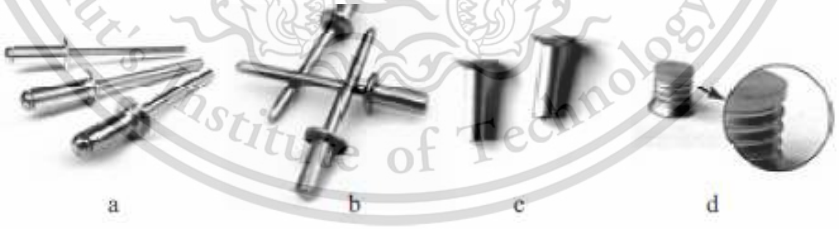

Figure 2.28 Fasteners used in riveting joints: (a) aluminum-steel BR; (b) aluminum-steel BHR; (c) aluminum alloy COUR; (d) steel SSPR.

(Source: Jacek Mucha, Mechanical Behavior and Failure of riveting joints in in tensile and shear tests, Strength of Materials, Vol. 47, No. 5,2015)

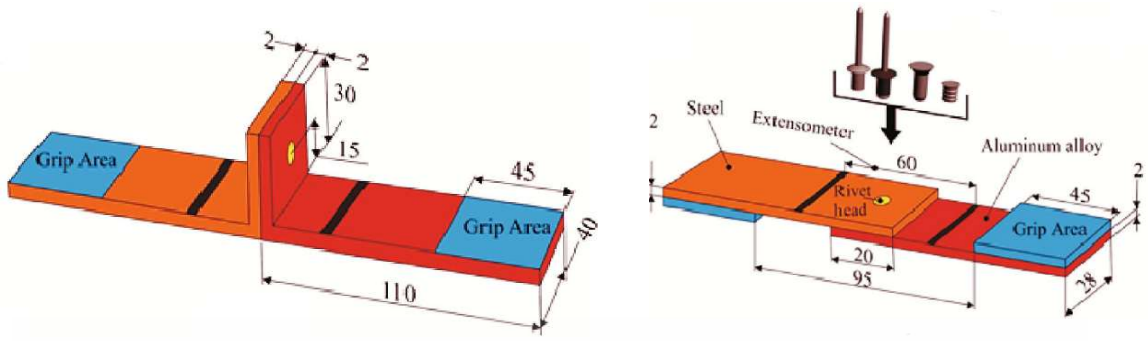

(a) (b)

Figure 2.29 The specimen geometry and the rivet position in the hybrid connection: (a) T-shaped specimen joint; (b) lap joint.

(Source: Jacek Mucha, Mechanical Behavior and Failure of riveting joints in in tensile and shear tests, *Strength of Materials, Vol. 47, No. 5,*2012)

From the results, the highest value of the shear force was obtained for the SSPR joints, and the lowest one for the joint with the closing-up rivet. The capacities of a tensile load transfer are lower than those of a shear transfer. In tensile tests, the maximum values of the joint fracture force were observed for the steel sheets joined by the blind hermetic rivet as shown in figure 2.30a and 2.30b.

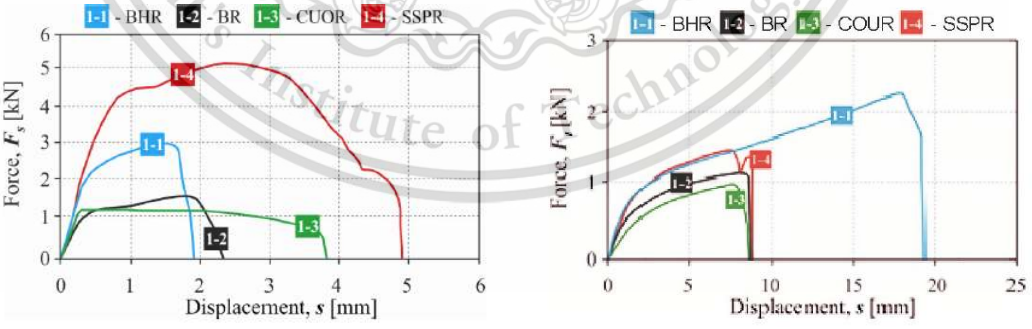

(a) (b)

Figure 2.30 The joint force characteristic of steel sheet:: (a) shear test; (b) tensile test

(Source : Jacek Mucha, Mechanical Behavior and Failure of riveting joints in in tensile and shear tests, *Strength of Materials, Vol. 47, No. 5,*2012)

Peter Pastucha (2015) was developed alternative joint for bus structure. One of the eventual solutions of fatigue crack problem and avoid HAZ effect zone consists in the replacement of some weld connection by the shape fasteners. The creation of these joints is possible thanks to the laser technology used at the material dividing that enable to create complex contours with high precision (Hussein H.M.A., 2012 and Kinik,2015). The example of new designed shape fastener (assembled and decomposed state) is in Figure 2.31.

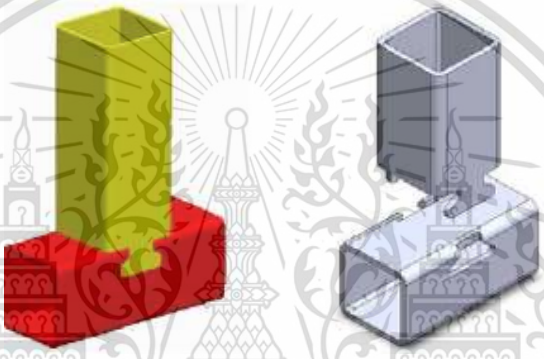

Figure 2.31 New Design of the shape fastener (Assembled and decomposed state)

(Source: Shape Fastener of the bus skeleton testing , Peter pastucha , 2015)

The design of this research has been arranged in specified shapes based on the design philosophy. This arrangement has used to be safe for occupants and to sustain extreme conditions can be matched on the road. Utilization of new connection, when it satisfies the safety regulations, should enable to reduce time of the bus frame production in the future. In spite of the fact that fasteners presented in this research was suitable for practical using, the tests and achieved results can be considered a first step to improve production efficiency.

Jarmo Havula (2018) was studied moment-rotation behavior of welded tubular high strength steel for T-joint. $\beta = b1/b0 \geq 0.85$, i.e., when chord face bending governs the deformation of the specimen. Joints with fillet and butt welds are considered. Figure2.32 presents the typical moment-rotation relationship for a hollow section joint with $\beta \geq 0.85$. In the figure, $M_{pl,exp}$ and $M_{u,exp}$ denote platic and ultimate moment resistances, respectively; S_j,ini and Sj,h denote initial and hardening rotational stiffness, respectively; φu denotes rotation corresponding to ultimate resistance. The rotation capacity of all specimens complies with the requirements for tubular joints, even using welds smaller than full-strength welds. The experimental results show that the size of fillet welds has a significant influence on the structural behavior of joints, increasing their bending resistance and rotational stiffness.

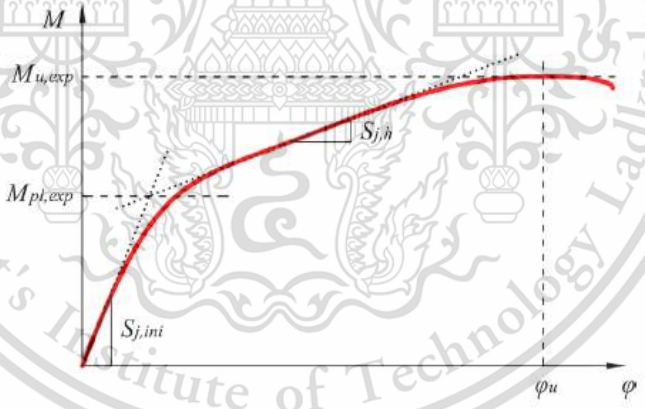

Figure 2.32 Typical M- φ relationship for hollow section T joint with $\beta \geq 0.85$

(Source: Jarmo Havula, Marsel Garifullin, Moment-rotation behavior of welded tubular high strength steel T joint)

Kosteski (2003) was study finite element method-based yield load determination procedure for hollow structural section connections. the ultimate deformation limit of 3%$b0$ proposed by Lu et al.(1994) and adopted by the International Institute of Welding (IIW) Sub commission XV-E is the most widely accepted ultimate deformation limit being used by researchers to define and compare the strength of welded HSS connections. However, as this 3%$b0$ ultimate deformation limit gains wider acceptance in the international research community, the original development of this ultimate deformation limit should be reviewed to prevent its misuse. A notional deformation limit-based criterion was described to determine the capacity of welded HSS connections that do not exhibit a clearly defined peak load or even yield load. Alternatively, several methods for determining the "yield load" from load-deformation curves that do not exhibit a distinct yield load have been proposed. This so-called yield load can then be used to define the limit state capacity of the connection. Figure 2.33 shows a sample experimental load-deformation curve for a welded HSS T-connection exhibiting a ductile chord flange failure mode.

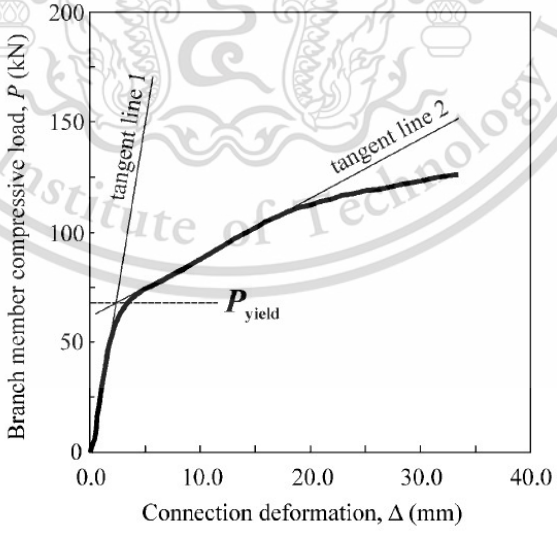

Figure 2.33 Example of bi-linear yield load approximation method by Zhao and Hancock

(Source: N. Kosteski, "finite element method based yield load determination procedure for hollow structural section connections, Journal or constructional steel research,2003)

CHAPTER 3

RESEARCH METHODOLOGY

This chapter explains the reviewing work process methodology as shown in figure 3.1. In general, the structure of the bus will be tested. Test organization will select at least 6 structures, which are roof pieces, sidewalls and the base floor of the two sides of the bus structure as shown in Figure 3.2. From the existing structure that consists of a rectangular steel box with a size of 50 * 50 mm which thickness is 2 mm by the MIG welded method, where the size of the weld is according to the Amp and Volt used in the welding process. In this study, T-joint connection was selected to determine the deformation behavior and strength of welded type. After reviewing existing joints in the bus structure, 3 different types of welding position in the welded joint were to be studied .

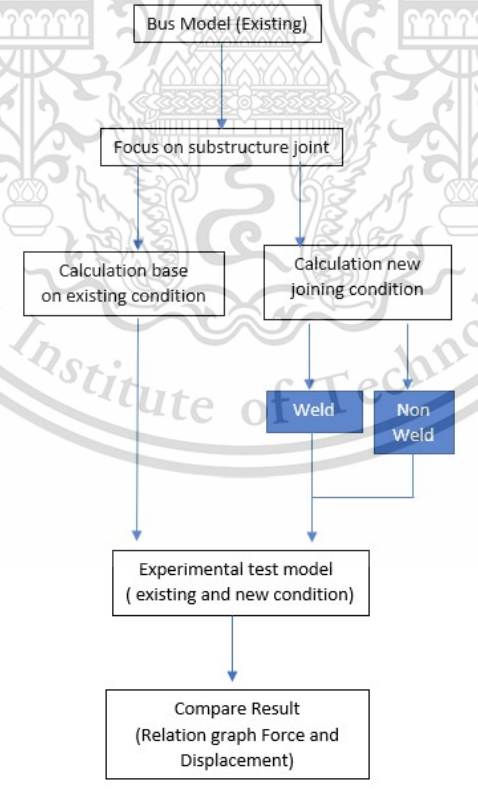

Figure 3.1 Work Flow process

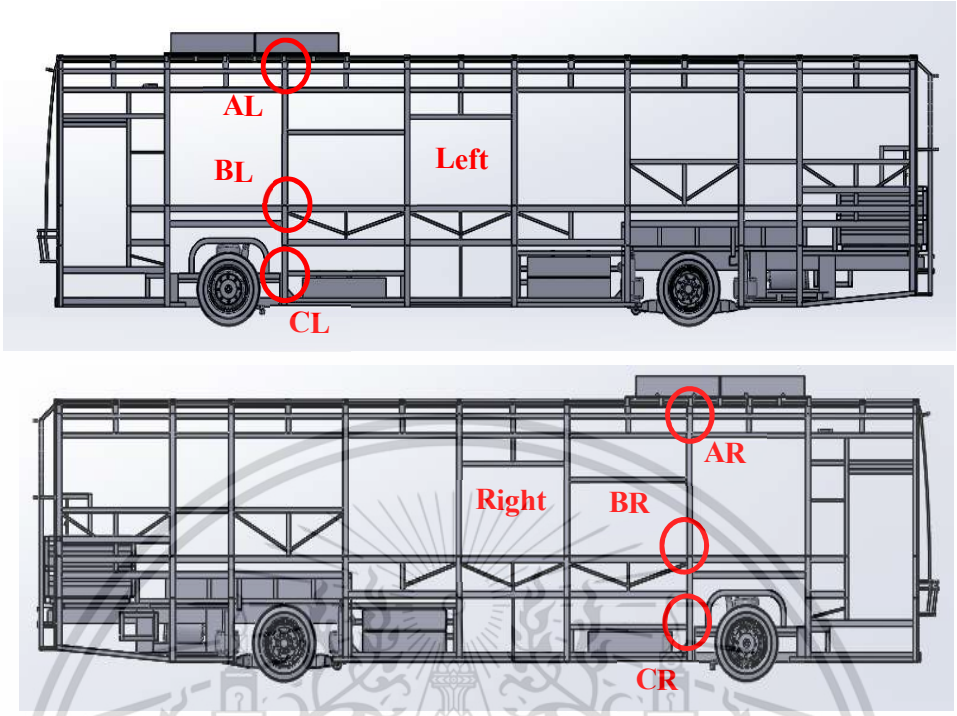

Figure 3.2 Joint test selection (Left and Right Side)

3.1 Test rig

A test rig has been created to perform bending deformation behavior under Rollover Condition . According to the study of structural deformation, it was found that the damage behavior caused by the accident rollover was bending behavior on the bus substructure. CAD model of test rig has shown in figure 3.3 ,3.4 and actual test rig has shown in figure 3.5.

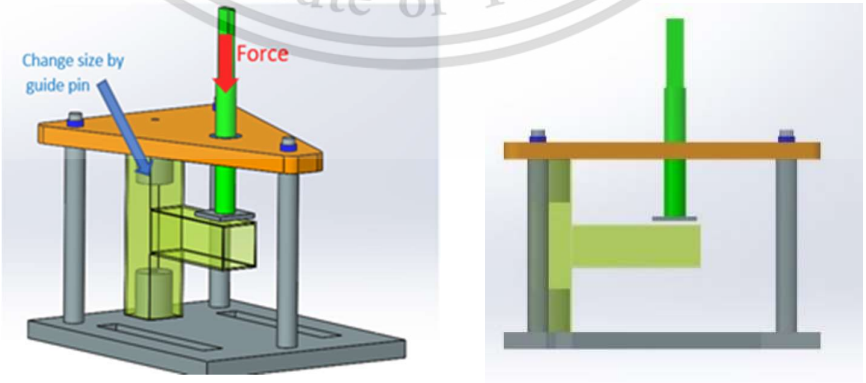

Figure 3.3 CAD model of test rig

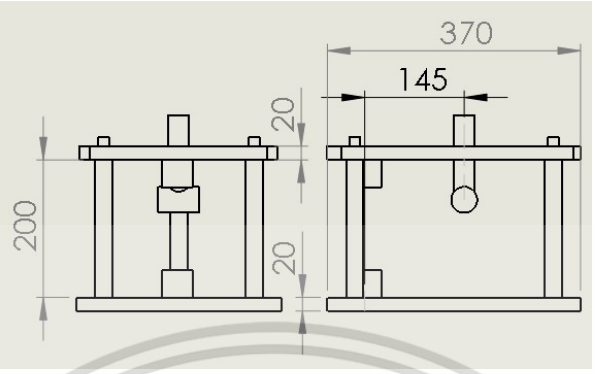

Figure 3.4 Dimension of test rig

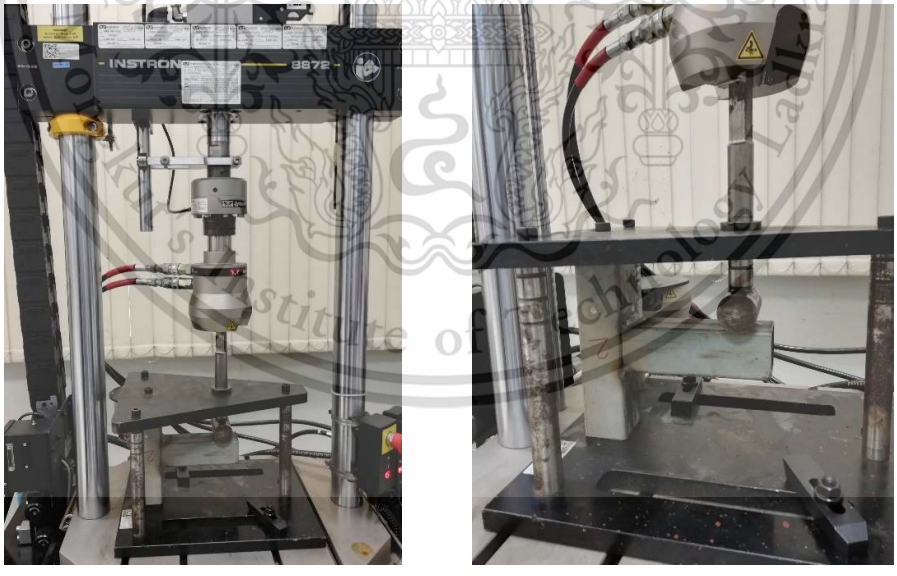

Figure 3.5 Actual test rig

3.2 Experimental tool

3.2.1 Universal Tensile Machine (UTM)

Instron 8872, Fatigue Testing Systems machine with Up to ±25 kN axial force capacity, has been used to this experimental as shown in figure 3.6. This machine will send force through the test rig to specimens.

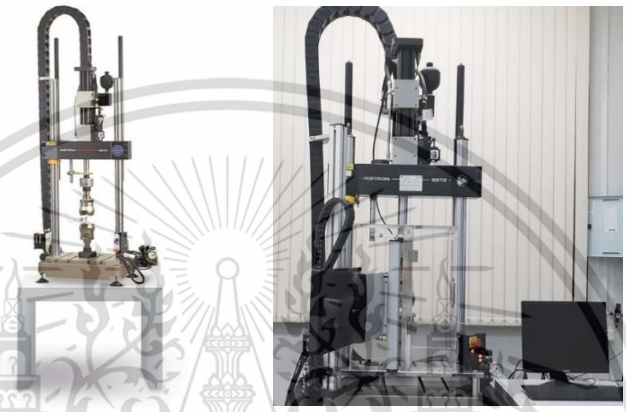

Figure 3.6 Instron 8872
(Source :https://www.instron.co.th/th-th/products/testing-systems/dynamic-and-fatigue-systems/servohydraulic-fatigue/8872-table-top)

3.2.2 Universal Video Extensometer (UVX)

UVX (AVE2), The fully-integrated device easily adapts to the normal fluctuations of environmental condition in this test . The device dramatically reduces errors from thermal and lighting variations that are common in most labs. This machine was used for investigation of plastic zone as shown in figure 3.7 and 3.8.

Figure 3.7 Universal Video Extensometer

(Source : https://www.instron.us/en-us/products/testing-accessories/extensometers/non-contacting-video/extensometers/2663-901)

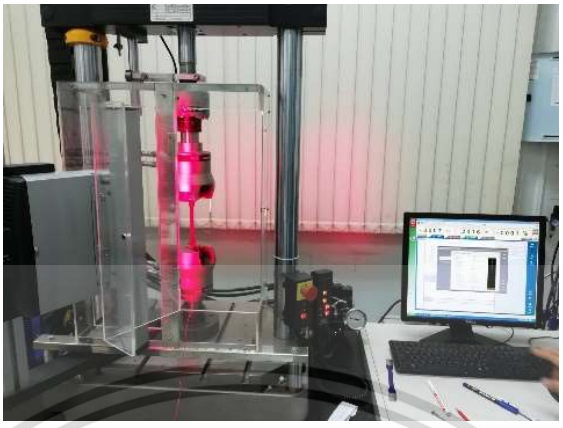

Figure 3.8 Universal Video Extensometer setup

(Source : https://www.instron.us/en-us/products/testing-accessories/extensometers/non-contacting-video/extensometers/2663-901)

3.2.3 Strain gauge

A Strain gage (sometimes refered to as a Strain Gauge) is a sensor whose resistance varies with applied force; It converts force, pressure, tension, weight, etc., into a change in electrical resistance which can then be measured. When external forces are applied to a stationary object, stress and strain are the result. Stress is defined as the object's internal resisting forces, and strain is defined as the displacement and deformation that occur. Table 3.1 and Figure 3.9 are shown specification of strain gages that used in this experiment. this equipment will be used with data acquisition system in next bullet.

Table 3.1 Strain gages Specification

Kyowa Strain Gages	
Type	KFG-5-120-C1-11L5M2R
Gage Factor (24°C,50%RH)	2.07 ±1.0%
Gage Length	5 mm
Gage Resistance	119.6 ± 0.4Ω
Temp. Coeff.	+0.008 % / °C

Figure 3.9 Strain gages

3.2.4 Data acquisition system

The displacement in elastic area on specimens was kept by data acquisition system. The hardware which used in the experiment were SIRIUSi with STG function as shown in Figure 3.10. the software was DEWESoft X3 as shown in figure 3.11 which collect data from strain gage in real time.

Figure 3.10 data acquisition hardware

(Source: https://download.dewesoft.com/list/manuals-brochures)

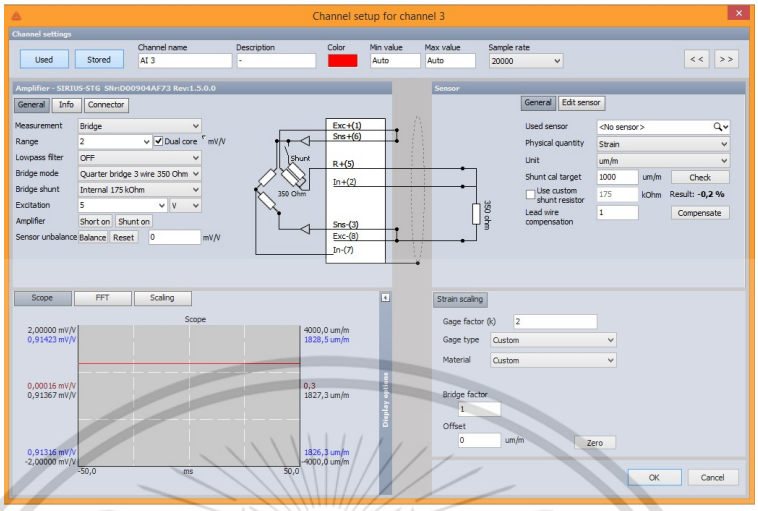

Figure 3.11 DEWEsoft X3 software

3.3 Material properties test

For material properties test, ASTM/E8 standard has been used to perform a specimens as shown in figure 3.12 The experiments were carried out using Universal Video Extensometer (UVX). This machine will be applied tensile force on specimens. Strain gages has been used to collect elastic zone data and UVX to collect plastic zone data.

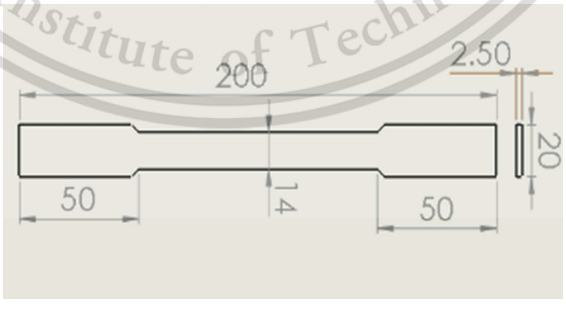

Figure 3.12 Dimension specimens follow ASTM /E8 standard

Strain gages have been attached on specimens as shown in figure 3.13. This experiment will use Universal Tensile Machine (UTM) with Universal Video Extensometer (UVX) for applied tension force and measure extension of specimens. Equipment setup was shown in figure 3.14.

Figure 3.13 Strain gages with specimens for tensile test

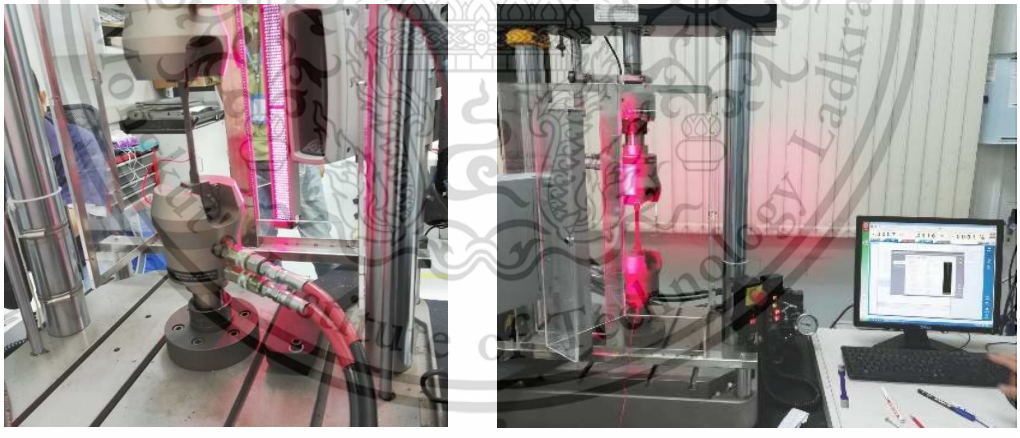

Figure 3.14 Experiment setup with UTM and UVX

Stress-Strain curve will be a result for this experiment as shown in figure 3.15

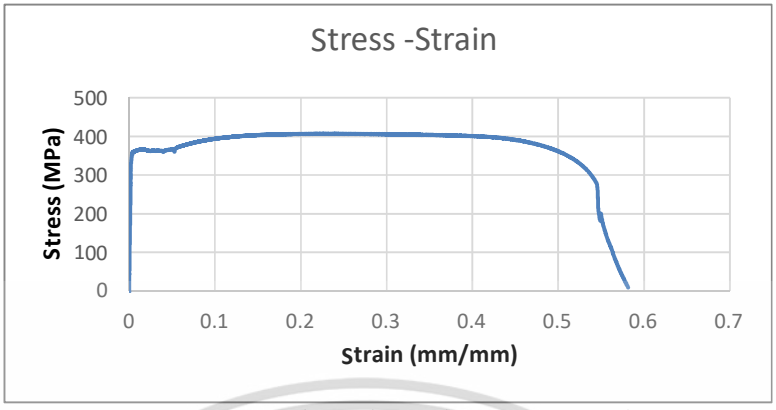

Figure 3.15 Result as shown in Stress – Strain curve

3.4 Weld equipment

MT-12(shown in figure3.16b) is high quality solid welding wire, it is copper coated mild steel welding wire suitable for 100% CO2 and Argon & CO2 mixed gas protective welding. It has stable feed ability, good welding seams, less spatters and excellent welding process properties as shown in table 3.2. Welding Machine setup value as shown in table 3.3

Table 3.2 Weld material specification

Weld material (MT-12)	
Equivalent spec.	JIS Z3312 YGW12 AWS A5.18 ER0S-6
Diameter	0.9 mm
Yield Strength	465 MPa
Tensile Strength	570 MPa

Table 3.3 Welding setup value

MIG350 DC inverter	
Voltage (V)	17 V
Current (A)	70 A

(a)

(b)

Figure 3.16 Welding equipment

3.5 T-joint Test

According to CIDECT standard, Maximum force for T-joint will calculation from existing model for fully welded connection . Parameter was shown in table 3.4.

Table3.4 Parameter value for Maximum force allowable formula

Parameter	Value
b_0, b_1	1
f_{y0}, f_{y1}	344
C_T	0.389
t	50
Θ	90

$$\beta = \frac{b_0}{t_0} = \frac{b_1}{t_1} \tag{3.1}$$

$$N_1 = A_1 . f_{y1} . C_T . \frac{f_{y0} . t_0}{f_{y1} . t_1} . \frac{1}{sin\Theta} \tag{3.2}$$

So, the result of this formula (N) is 23.76 kN. Uniaxial Tensile Machine Intron 25kN has been provide for this experimental.

T-joint structure has been selected for represent substructure deformation under roll over situation . T- joint specimens were made by square hollow beam steel with geometry as shown in figure 3.17.

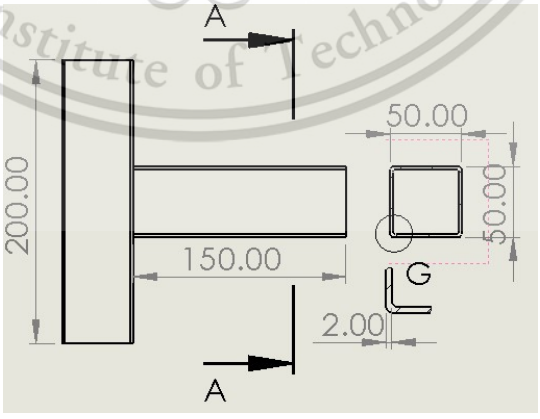

(a) Drawing of T-joint

(b) example for T-joint

Figure 3.17 T-joint (3D)

In this experiment, SIM SOLID (Altair software) has been used to create a simple weld model as shown in figure 3.18 . Maximum stress has located at corner area . Shear stress has distributed on corner area around the weld boundary as shown figure 3.19. Therefore, Corner welded should be considered in this experiment.

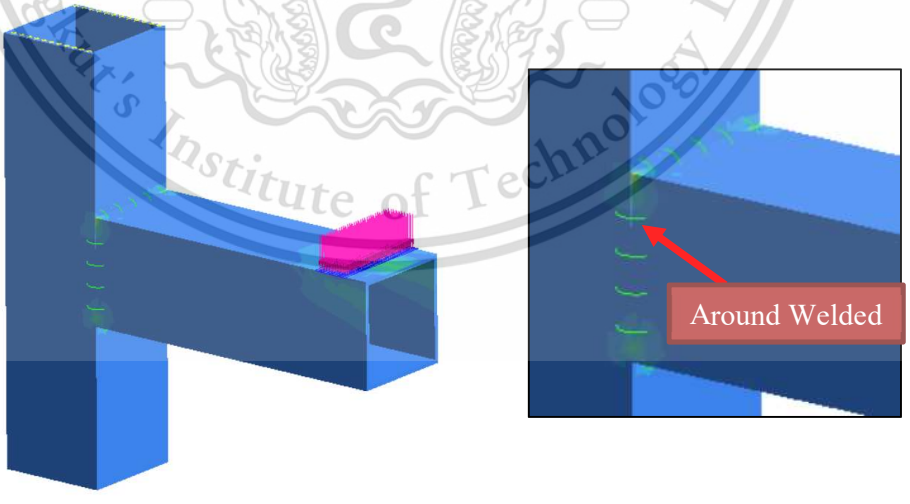

Figure 3.18 Simple model of weld (around welded)

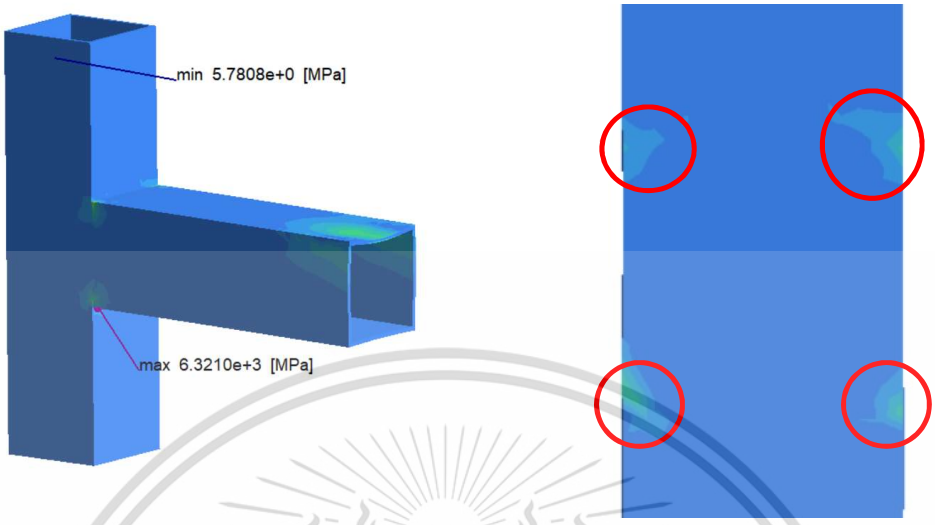

Figure 3.19 Stress distribution at corner area

Three Specimen types were provide in this study as shown in Figure 3.20 (a-c). The weld profile and the specimen preparation were carried out in accordance with Thai bus assembler.

3.5.1 Around welded

Around weld joint was a perfect joint which is obtained by the fusion around of the edges of the two to be joined together. This is the most common connection of bus structures. This specimen was studied deformation behavior.

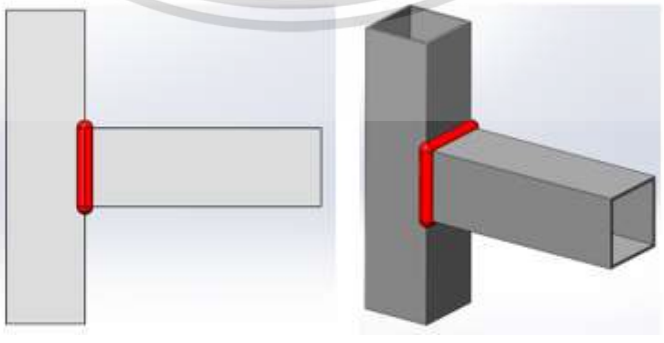

Figure 3.20a Around welded joint

3.5.2 2-Sided welded

2-sided welded was a permanent joint which is obtained by fusion 2 sides of both edges joint. This type was created to study the deformation behavior and find ways to reduce the cost of welds.

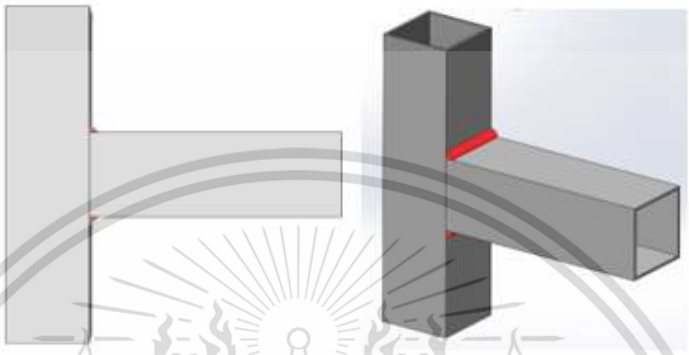

Figure 3.20b 2-Sided welded joint

3.5.3 Corner welded

This type was combined from around welded and 2-side welded to study Deformation behavior, improve and develop a new welding method that was stronger or equal to other types. 4 sizes of weld length were prepared for this experiment ie. 5 mm, 7 mm, 13mm and 15 mm as shown in the figure. mm, 7 mm, 13mm and 15 mm as shown in the figure 3.20c and 3.20d.

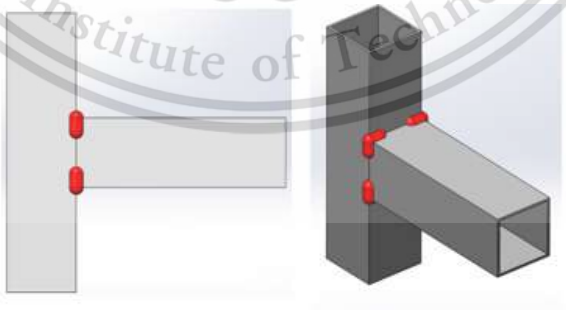

Figure 3.20c Corner welded joint

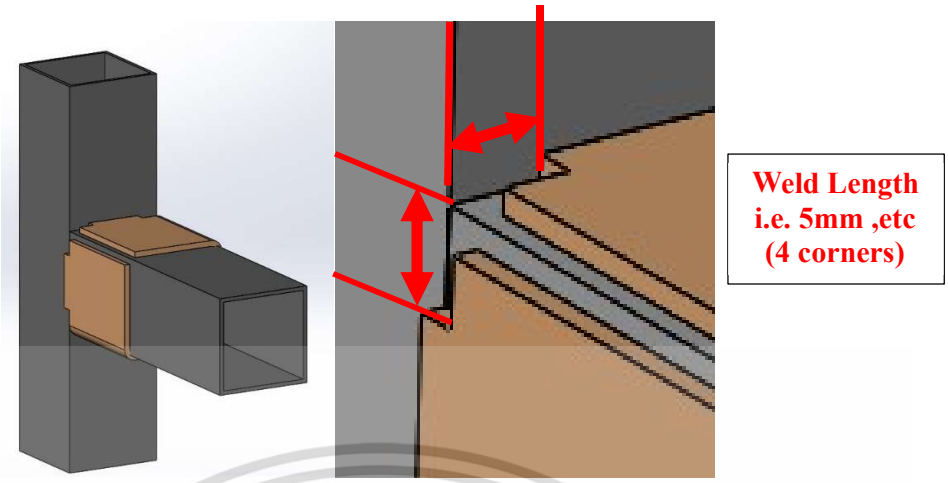

Figure 3.20d Weld length variable

3.6 Alternative joint

There are many types of the buses in the world; they differ in various indicators such as the size, power and construction. The skeleton of the investigated bus is created by steel that are usually welded using Metal Active Gas Method. The base material of square hollow (or rectangle) steel is the low-carbon steel. The basic dimensions of the profiles are 50x50 mm thickness 2 mm. One of the eventual solutions of this problem consists in the replacement of some weld connection by rivet joint. Rivet joint has been developed to replace welding type. Single strap butt joint has been used to this joint as shown in figure 3.21.

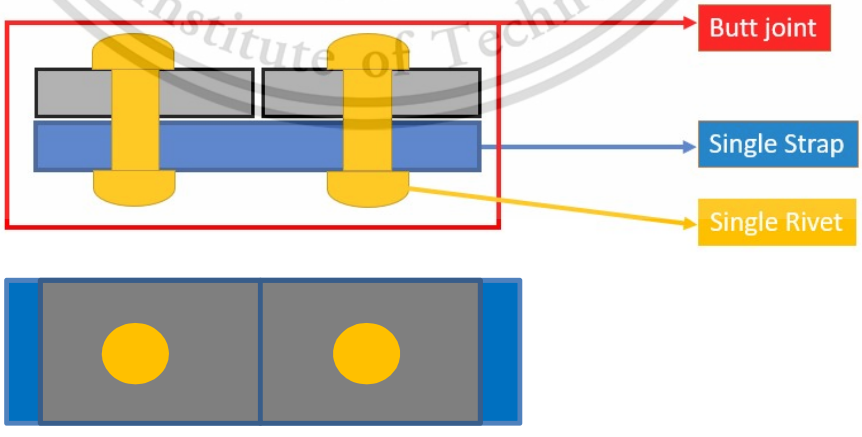

Figure 3.21 Single Strap Single rivet butt joint

3.6.1 Single riveted tensile test

All specimens were prepared with dimensions included in ISO 12996 standard (2013) as shown in figure 3.20. Stainless Steel blind rivet (BR)has been used to this specimen. The rivets had the same diameter of the cylindrical part (d = 4.8mm), while the remaining geometry was selected for the total thickness of joined sheets (d_{tot}=4mm). This experiment was determined a maximum shear tensile stress and Tensile stress for selected rivet as shown in figure 3.22 . Applied force and displacement curve will be results for this experiment as shown in figure 3.23.

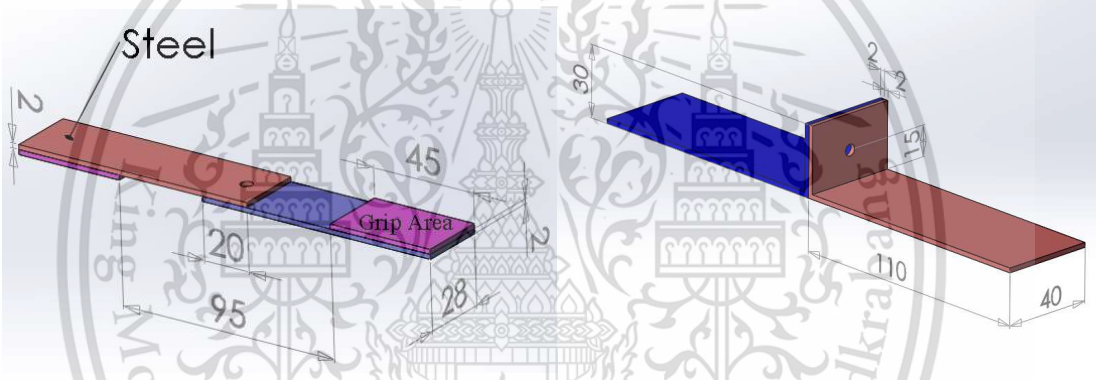

Figure 3.22 Single rivet specimen configuration

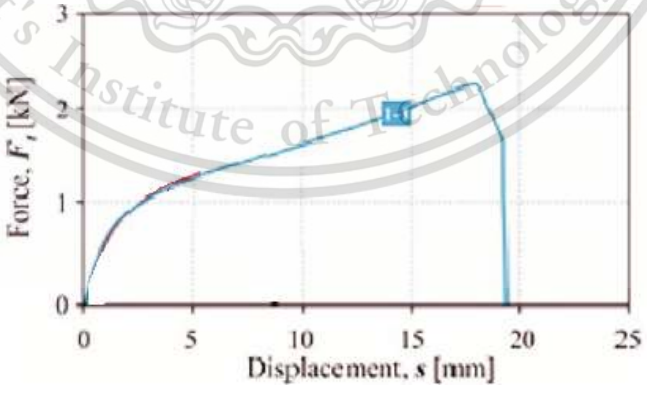

Figure 3.23 Relation graph between force and displacement for tensile test

3.6.2 T-joint with rivet configuration

According to previous test, Selected rivet will be applied to T-joint design. Rivet joint bracket has been created for this experiment as shown in figure 3.24.

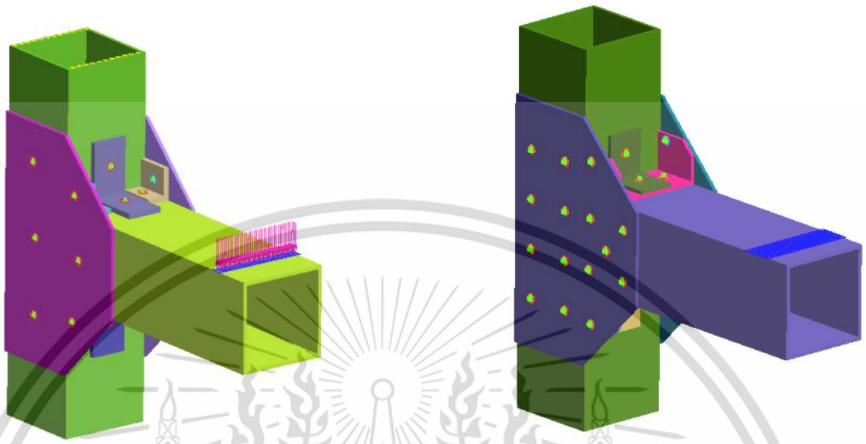

Figure 3.24 3D model of riveted design

Blind rivet break stem open type has been selected for this test as shown in figure 3.25. Because this type is easy to use and can be found in local stores.

Figure 3.25 blind rivet stem open type

(Source : POP rivet system Catalog ; https://www.mavin.com/pdf/AD610ABS.pdf)

The stiffness of joints could be increased by reinforcements. Many joints in structures are normally reinforced by the plate steel. this experiment provided 3 types 1.) Rivet with 2 reinforcement bracket. (R1) 2.) Rivet with 1 reinforcement bracket. (R2) 3.) Rivet no reinforcement bracket (R3) as shown in figure 3.26. Bracket1 was designed to support shear load. bracket 2 was designed to support tensile load

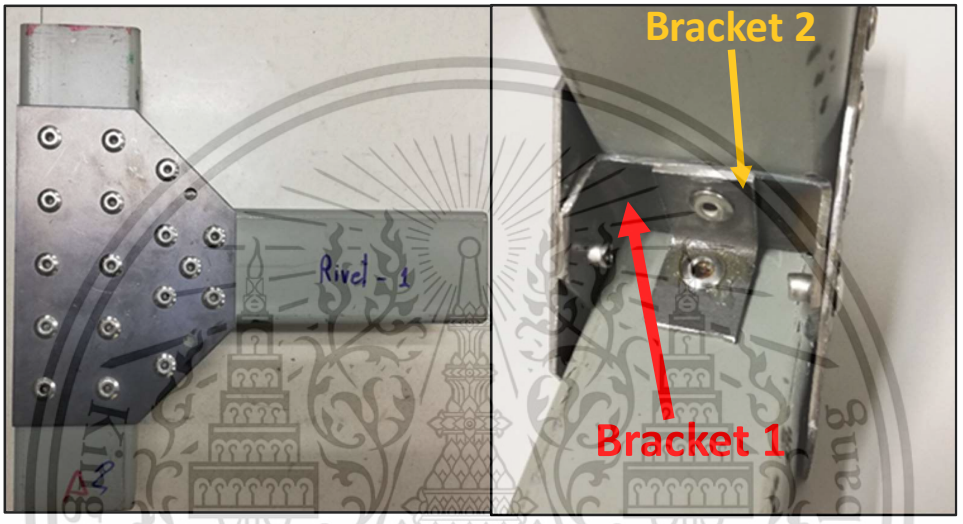

a.) Rivet joint with 2 reinforcement (R1)

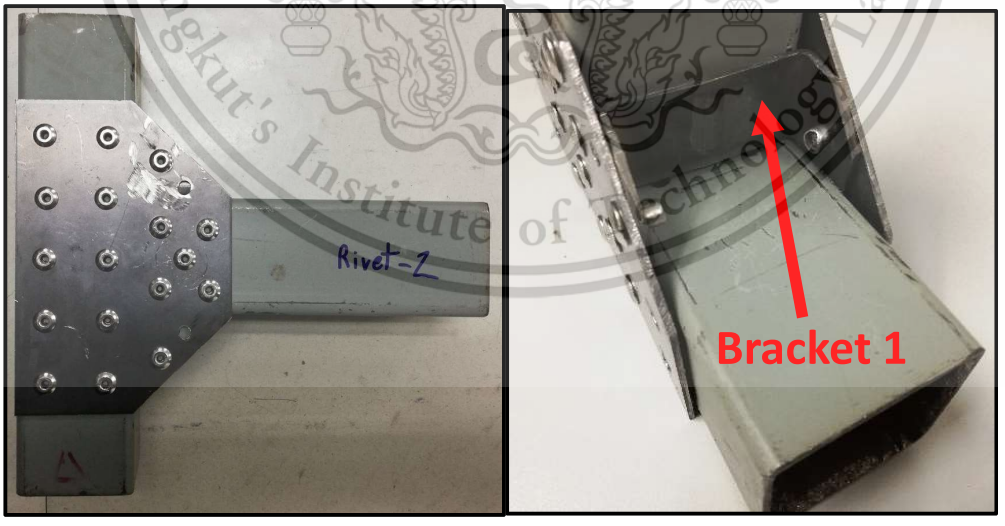

b.) Rivet joint with 1 reinforcement R2

Figure 3.26 Reinforcement bracket

Rivet design will use previous load from welding type. Design process for rivet joint will shown in figure 3.27.

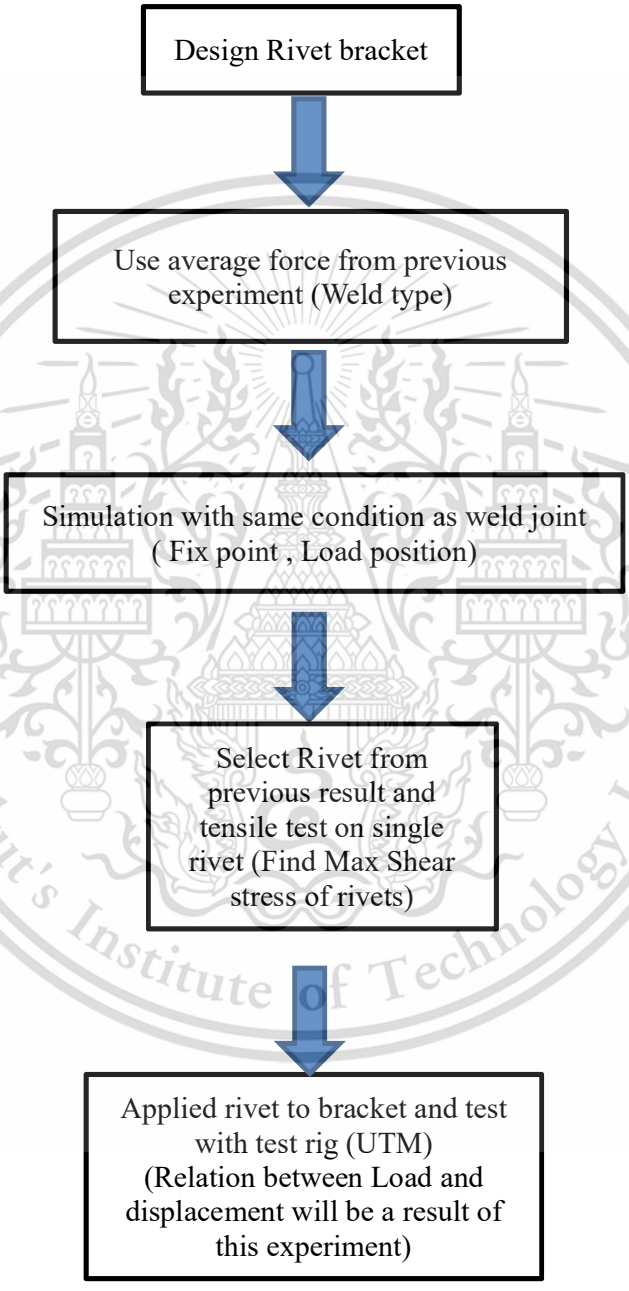

Figure 3.27 Design process for rivet joint

3.6.2.1 Rivet system design

Twenty kN force has been applied for rivet system design as shown in figure3.28. Because of Efficiency of rivet system, Double rivet Butt joint has been selected for this design as shown in Table 3.5. Dimension of rivet system was shown in figure 3.29.

Table 3.5 Efficiency of butt joint rivet

Type of Joint	Average Efficiency (%)	Maximum Efficiency (%)
Single Riveted	55-60	63.3
Double Riveted	70-83	86.5

(Source : Unit 3 Riveted joint design ; Machine Design version 7 wiley)

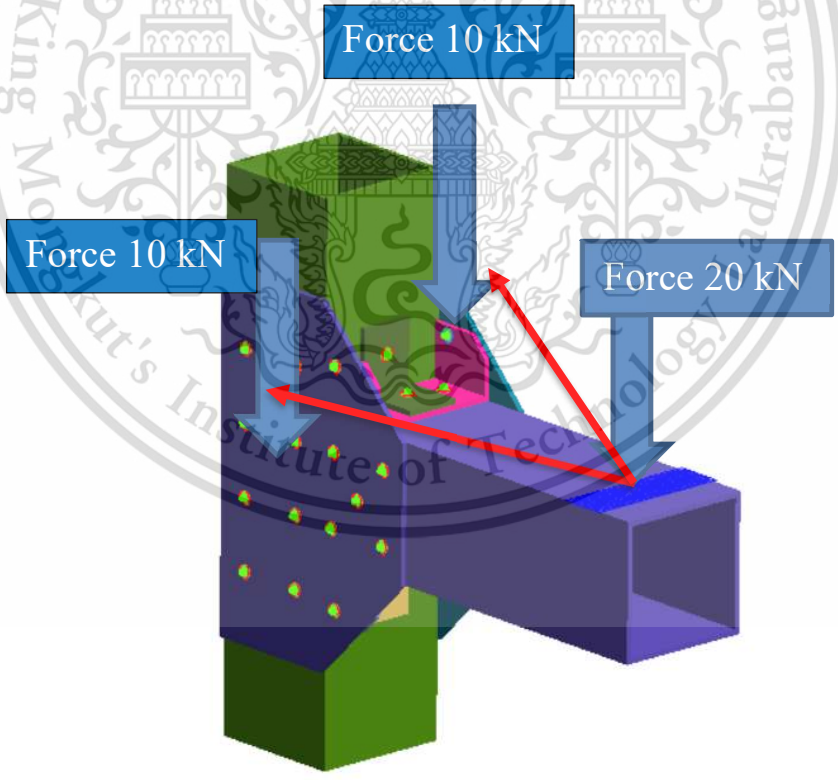

Figure 3.28 Applied force for rivet system

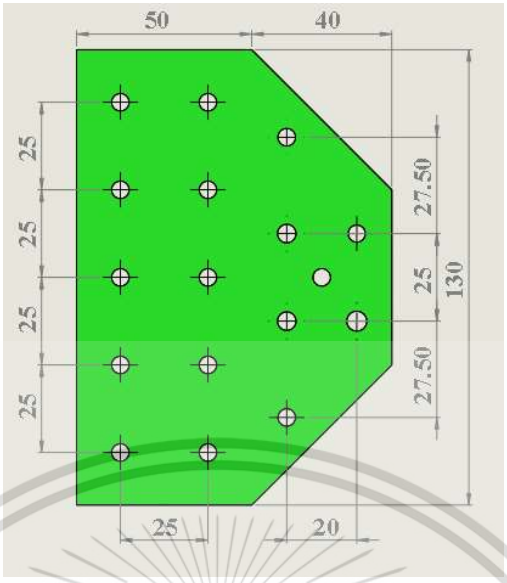

Figure 3.29 Dimension of rivet system

According to theoretical rivet design, The force F1,F2.etc. on individual rivets as shown in figure3.30. For satisfying condition of equilibrium, components of forces in vertical direction should sum up to zero. If the force F1, F2. Etc. make angle Θ_1, Θ_2 etc. respectively with y-axis then

$$F_1 \cos \Theta_1 + F_2 \cos \Theta_2 + \ldots + Fn \cos \Theta_n = 0 \qquad (3.3)$$

The force is acting at a L mm from vertical line through the centroid as shown in Figure 3.31.

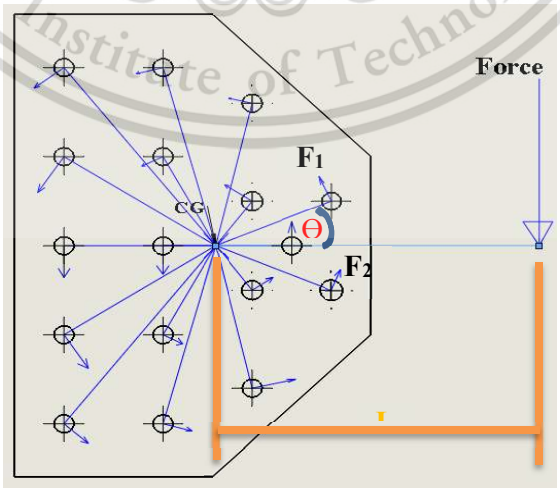

Figure 3.30 Force diagram for rivet system

According to F1 position

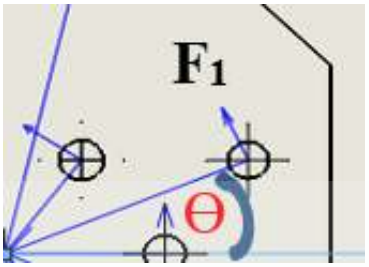

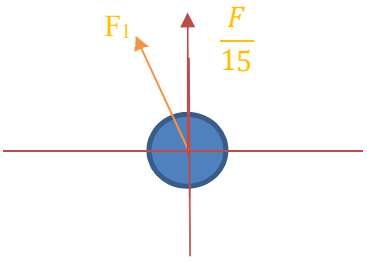

Figure 3.31 Rivet diagram

The net force on each rivet will be the resultant of $\frac{F}{15}$ and F1 ,F2 etc. Apparently, the largest magnitude will occur where the angle between two force is minimum. The angle is minimum Θ = 25 ° in rivet 1.

The resultant of two forces R1 and R2 with angle between them being Θ is given by

$$R = \sqrt{{R_1}^2 + {R_1}^2 + 2R_1R_2cos\Theta} \tag{3.4}$$

With τ as permissible shearing stress and *d* as diameter of rivet

$$R = \frac{\pi}{4}d^2\,\tau \tag{3.5}$$

So, result for this design is d= 4.35 mm ≈ 5 mm

In this calculation assumed that all rivets have same diameter. Hence all rivets will have diameter of 5 mm each.

3.6.2.2 Rivet selection

From the previous calculation, diameter for rivet is 5 mm. Rivet size has been selected by Pop riveting systems catalog as shown in figure 3.32. Diameter that near the calculation is 4.8 mm. According to red box, grip range that appropriate for this experiment is 3.2 - 6.4mm (Design thickness is $t_{total} = 4$ mm). Two material types of rivet have been provided i.e. Steel and Stainless Steel .

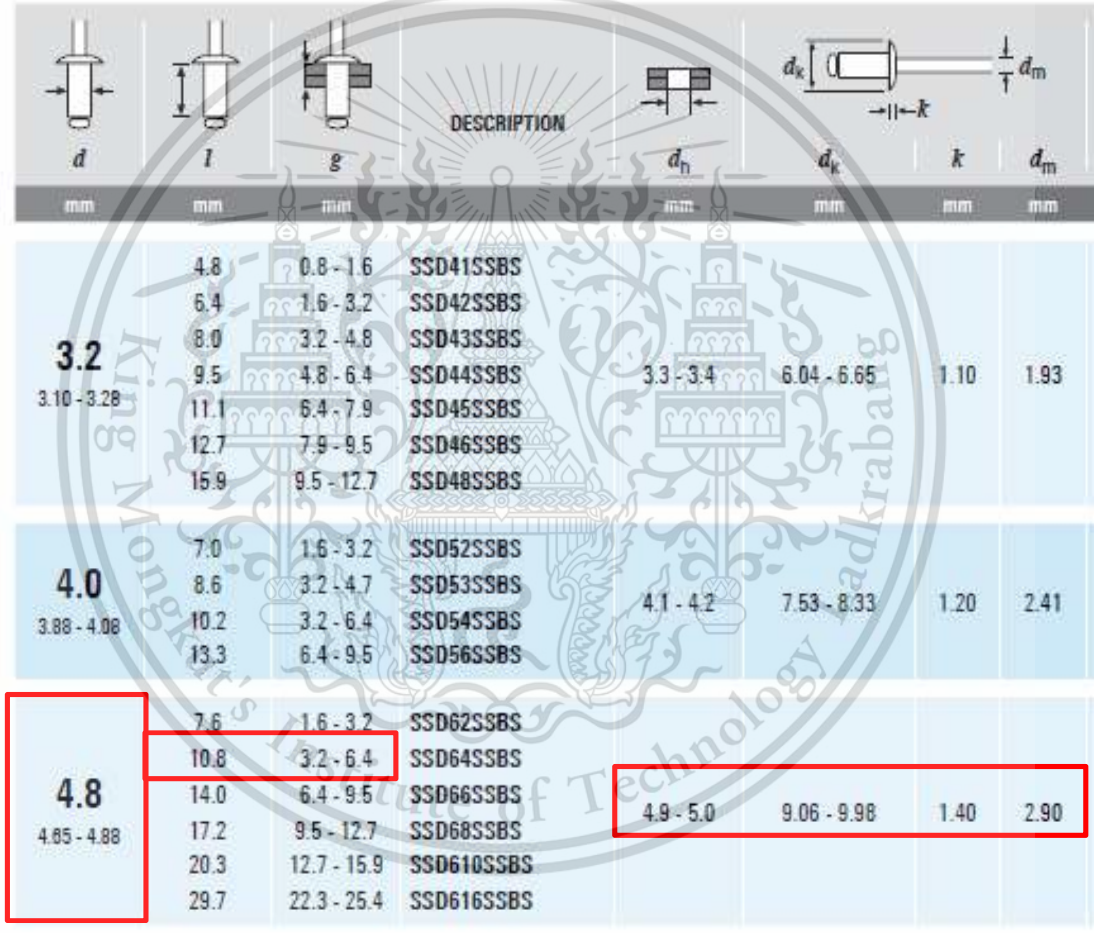

d mm	l mm	g mm	DESCRIPTION	d_h mm	d_k mm	k mm	d_m mm
3.2 (3.10 - 3.28)	4.8	0.8 - 1.6	SSD41SSBS	3.3 - 3.4	6.04 - 6.65	1.10	1.93
	6.4	1.6 - 3.2	SSD42SSBS				
	8.0	3.2 - 4.8	SSD43SSBS				
	9.5	4.8 - 6.4	SSD44SSBS				
	11.1	6.4 - 7.9	SSD45SSBS				
	12.7	7.9 - 9.5	SSD46SSBS				
	15.9	9.5 - 12.7	SSD48SSBS				
4.0 (3.88 - 4.08)	7.0	1.6 - 3.2	SSD52SSBS	4.1 - 4.2	7.53 - 8.33	1.20	2.41
	8.6	3.2 - 4.7	SSD53SSBS				
	10.2	3.2 - 6.4	SSD54SSBS				
	13.3	6.4 - 9.5	SSD56SSBS				
4.8 (4.65 - 4.88)	7.6	1.6 - 3.2	SSD62SSBS	4.9 - 5.0	9.06 - 9.98	1.40	2.90
	10.8	3.2 - 6.4	SSD64SSBS				
	14.0	6.4 - 9.5	SSD66SSBS				
	17.2	9.5 - 12.7	SSD68SSBS				
	20.3	12.7 - 15.9	SSD610SSBS				
	29.7	22.3 - 25.4	SSD616SSBS				

Figure 3.32 Rivet details catalog

3.6.2.3 Design validation

From the previous calculation , SIM SOLID (Altair software) has been used to create a simple weld model as shown in figure 3.33. Condition for this experiment will show in table 3.6.

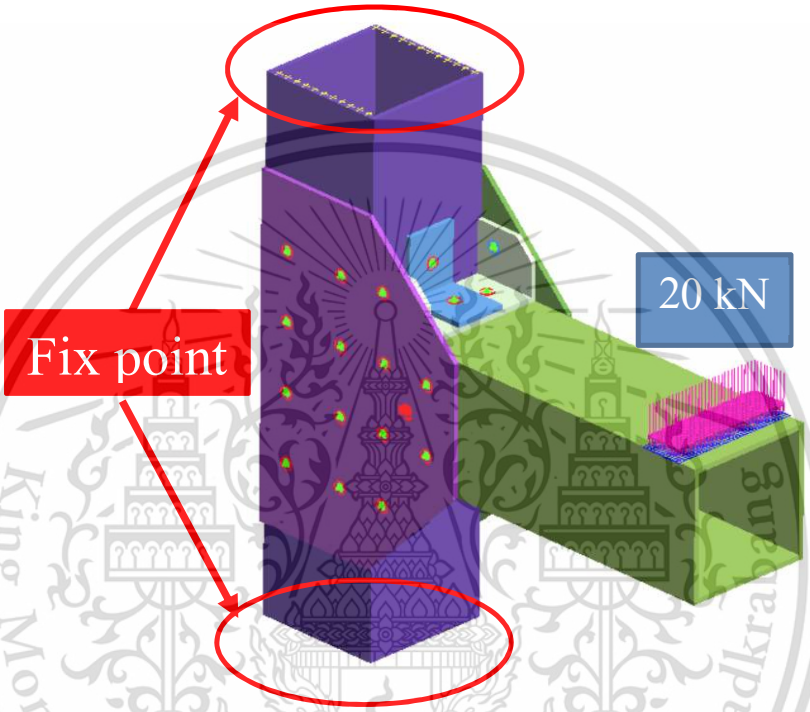

Figure 3.33 Rivet Joint Condition Setup

Table 3.6 Simulation Condition

MATERIAL	Steel (SS400)
LOAD	20 kN
CONTACT ON EACH COMPONENT	Slide no friction
RIVET SIZE	4.8 mm (Selected rivet)

From the result , two positions that resist tensile stress loading as shown in figure 3.33.

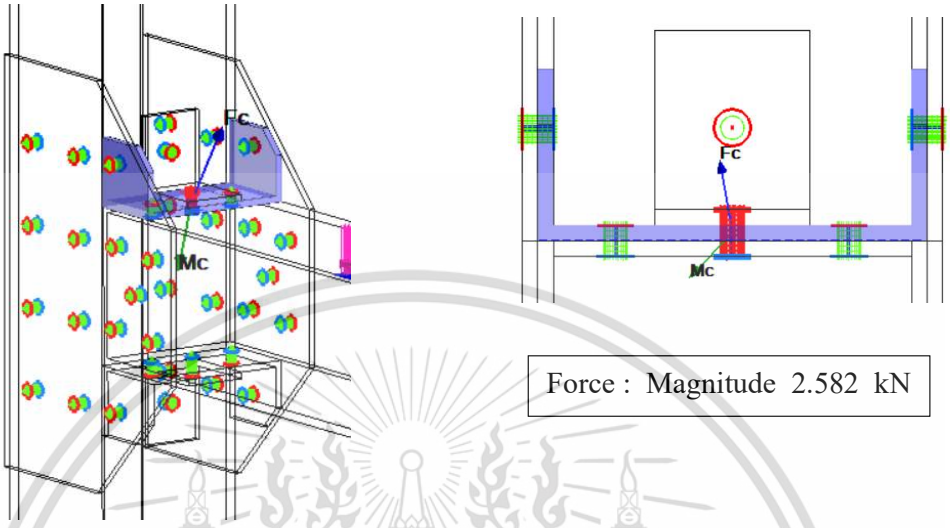

a.) Upper rivet for tensile

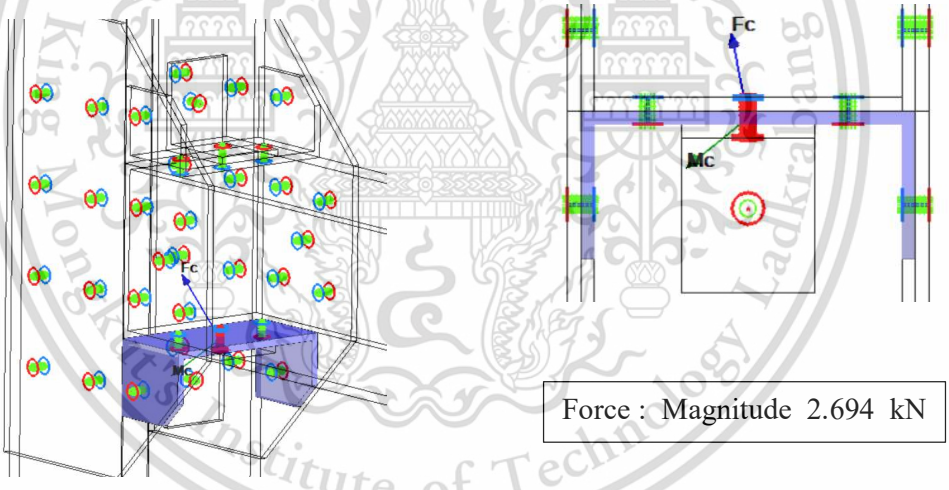

b) Bottom rivet for tensile

Figure 3.34 Rivet for Tensile stress

Other rivets were shear stress resistant. Maximum shear stress has the same position with previous calculation as shown in Figure 3.35. This rivet can be used as standard criteria in the rivet system design and selected rivet for the entire specimens.

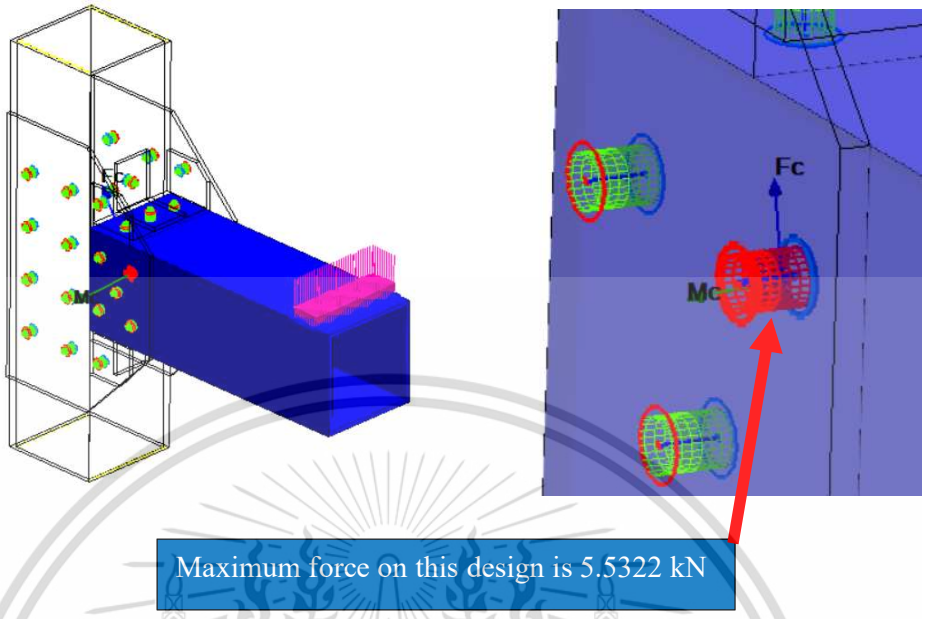

Figure 3.35 Maximum shear stress position for rivet

According to the simulation results were compared to the single rivet actual results. this result will select the appropriate size of rivet for this design.

CHAPTER 4

RESULTS AND DISCUSSION

4.1 Material Properties test

4.1.1 Base metal test

The obtained stress and strain of all specimens were plotted in Figure 4.1.All specimens showed similar value as summarized in Table 4.1. Images of tested specimens with resulting deformation and fracture damage are shown in Figure 4.2.

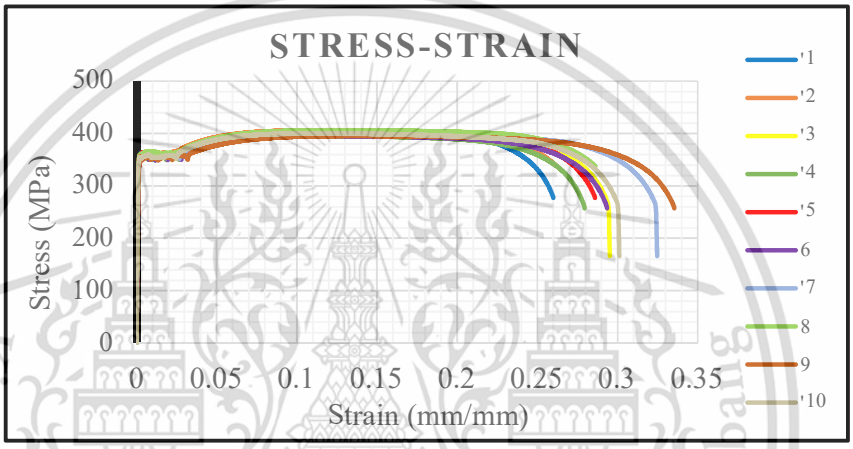

Figure 4.1 Material properties test results

Table 4.1 Experimental result (Material properties for base metal)

Specimen	Tensile Strength (Mpa)	Young Modulus (Gpa)
1	400	195
2	396	191
3	404	197
4	406	196
5	415	202
6	410	200
7	401	198
8	385	185
9	412	211
10	405	205
Average	403.4	198
Standard Deviation(S.D)	8.64	7.22

(a) Before test

(b) After test

Figure 4.2 Specimens before and after test

4.1.2 Rivet tensile test

For the experiment, the sheet materials were made of Steel SS400 and thickness of each sheet was the same (2mm). Two experiments were provided for this test; shear stress , tensile stress for single rivet. For material selection of rivet, three materials were provided with same diameter size 4.8mm, which are stainless steel, steel and aluminum. All materials performed a same shearing failure as shown in figure 4.3. From the results of the experiment, it was found that the stainless steel was the strongest, followed by steel and aluminum respectively. The experimental result for 3 material type was shown in figure 4.4 and table 4.2. So, Stainless steel has been used to rivet joint specimens.

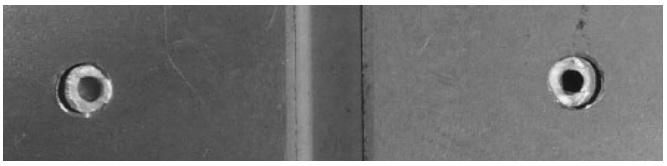

Figure 4.3 Shearing failure on each material type

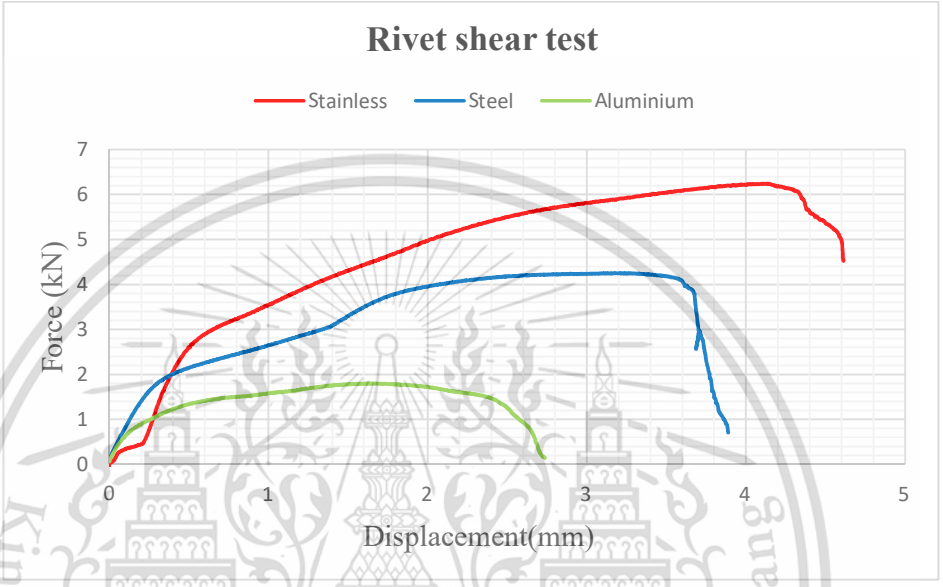

Figure 4.4 Rivet shear test result with 3 material

Table 4.2 Rivet test result with 3 material

4.1.2.1 Shear stress test

Specimens	Shear Strength (MPa)	Shear Stress at Yield (MPa)	Maximum Force (kN)
Stainless Steel	313.24	246.42	6.24
Steel	299.66	183.97	4.25
Aluminum	89.15	32.19	1.80

The obtained force and displacement of all specimens were plotted in Figure 4.5. All specimens showed similar value as summarized in Table 4.3. Images of tested specimens with resulting deformation and fracture damage are shown in Figure 4.6. The results showed that the steel plates that were tested were stronger than the rivet pins. because rivet had deformed.

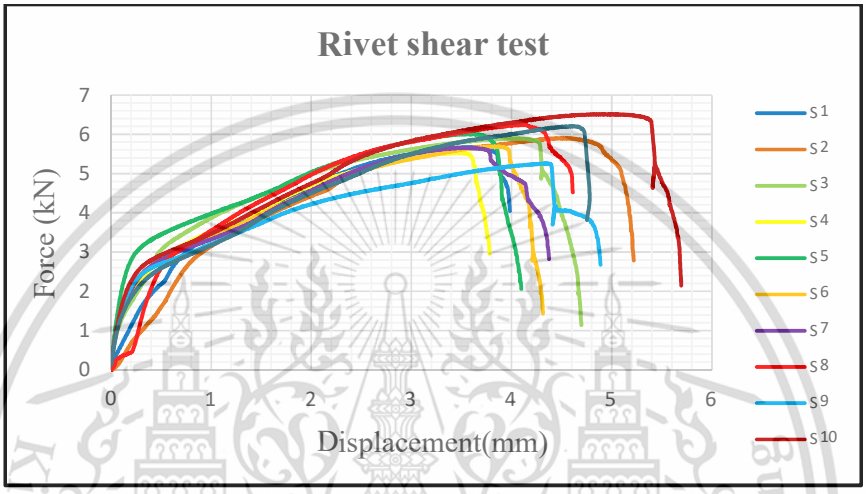

Figure 4.5 Rivet Shear Stress Test Result

(a) Before test

(b) After test

Figure 4.6 Rivet specimens before and after test

Table 4.3 Summarize result for shear stress

Specimens	Shear Strength (MPa)	Shear Stress at Yield (MPa)	Maximum Force (kN)
1	313.24	246.42	5.67
2	326.03	250.25	5.90
3	325.73	249.97	5.89
4	305.42	252.33	5.52
5	332.13	265.89	6.01
6	314.37	252.33	5.68
7	312.74	216.76	5.66
8	344.83	284.83	6.24
9	290.63	280.98	5.26
10	359.90	346.18	6.51
AVG	322.502	264.59	5.834
Standard Deviation (S.D)	19.91	34.44	0.36

4.1.2.2 Tensile stress test

The obtained force and displacement of all specimens were plotted in Figure 4.7. All specimens showed similar value as summarized in Table 4.3. Images of tested specimens with resulting deformation and fracture damage are shown in Figure 4.8a. In most cases (three out of four specimens) the mechanism of fracture implies a pull-out of the rivet head from bottom sheets (Figure 48b). Another case, the tubular part of a rivet exhibited a failure (figure 4.8c). The results showed that the rivets can resist shear stress more than tensile stress.

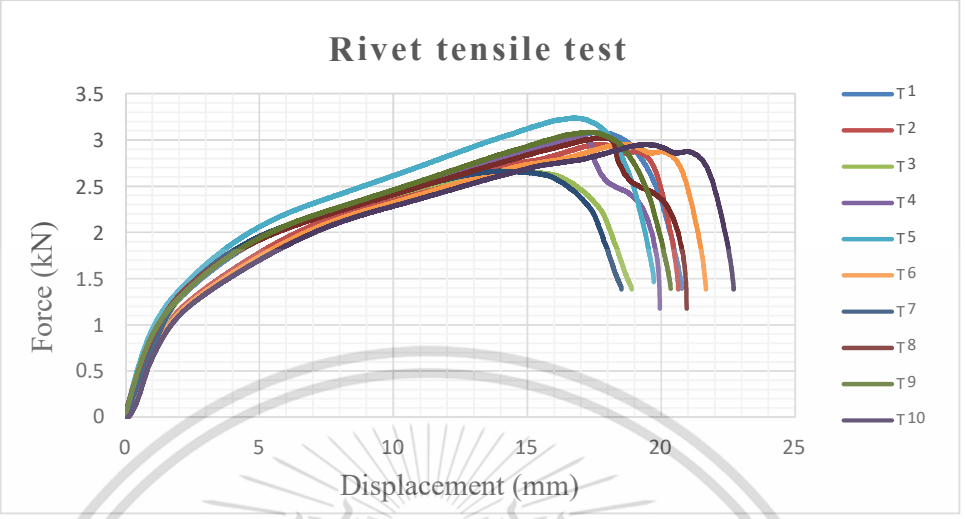

Figure 4.7 Rivet tensile stress test result

Table 4.4 Summarize result for tensile stress

Specimen	Tensile Strength (Mpa)	Tensile Stress at Yield (Mpa)	Maximum Force (kN)
1	170.48	78.35	3.08
2	163.13	78.86	2.95
3	157.19	79.68	2.66
4	147.2	76.08	3.03
5	171.25	79.42	2.66
6	165.98	78.8	3.24
7	160.11	77.56	2.95
8	155.2	76.19	3.03
9	159.35	77.85	3.08
10	167.2	78.65	2.95
Average	161.71	78.144	2.96
Standard Deviation (S.D)	7.45	1.24	0.18

a) Before test

b.) After test

c.) Rivet crack

Figure 4.8 Failure behavior of rivet

4.2 T-joint configuration result

4.2.1 Around welded joint

The vertical load versus displacement curves of all around-welded-joint specimens were plotted in Figure 4.9. Due to the deformation behavior and load results of specimen type. The results could be divided into 2 groups. The first group is A1-1, A1-2, A1-3 and the second group is A2-1, A2-2, A2-3

It could be seen that the specimen group 2nd was stronger than group 1st due to the buckling behavior deformation observe from the Chord tube as shown in Figure 4.10 and 4.11. Furthermore, according to 1st group, the position of seam weld inside the tube has also seem to affected the strength of the joint specimens shown in Figure 4.12.

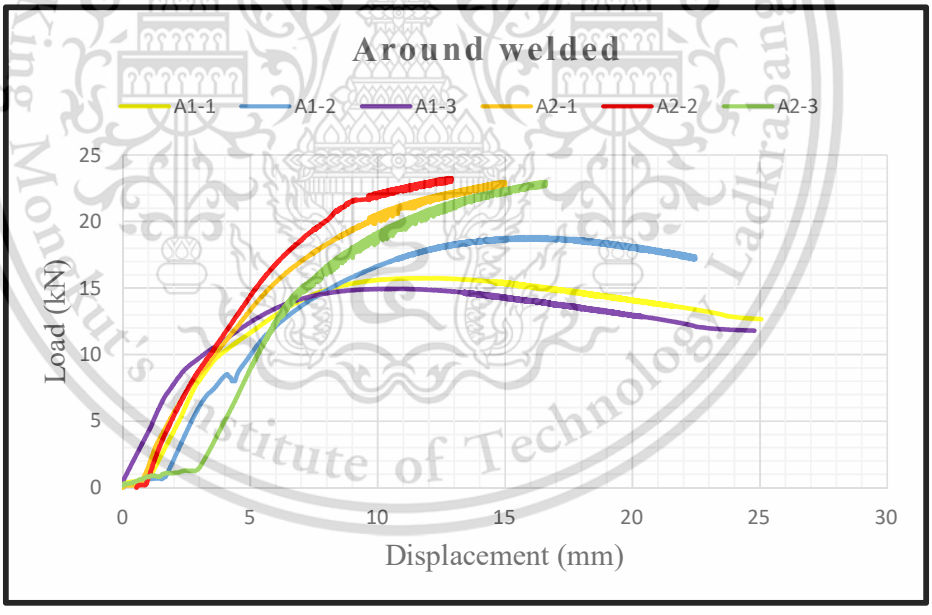

Figure 4.9 Around welded test result

Figure 4.10 Deformation behavior for around welded group 1

Figure 4.11 Deformation behavior for around welded group 2

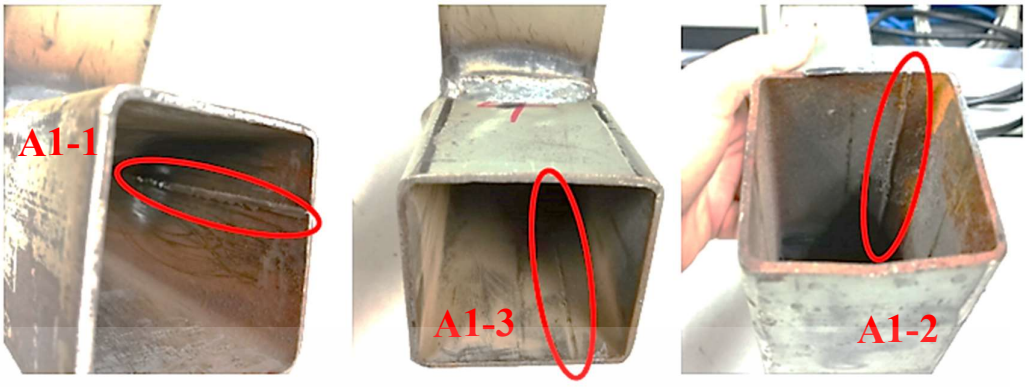

Figure 4.12 Different seam welded positions on an internal surface of vertical structural steel member in T-joint specimens

Specimen group 2 cannot perform damage to the specimen due to the safety limit of UTM machine. So, yield load approximation method (Zhao Ling,2018) has been used to create criteria for both groups as shown in figure 4.13 and table 4.5 will summarize all around welded specimen data.

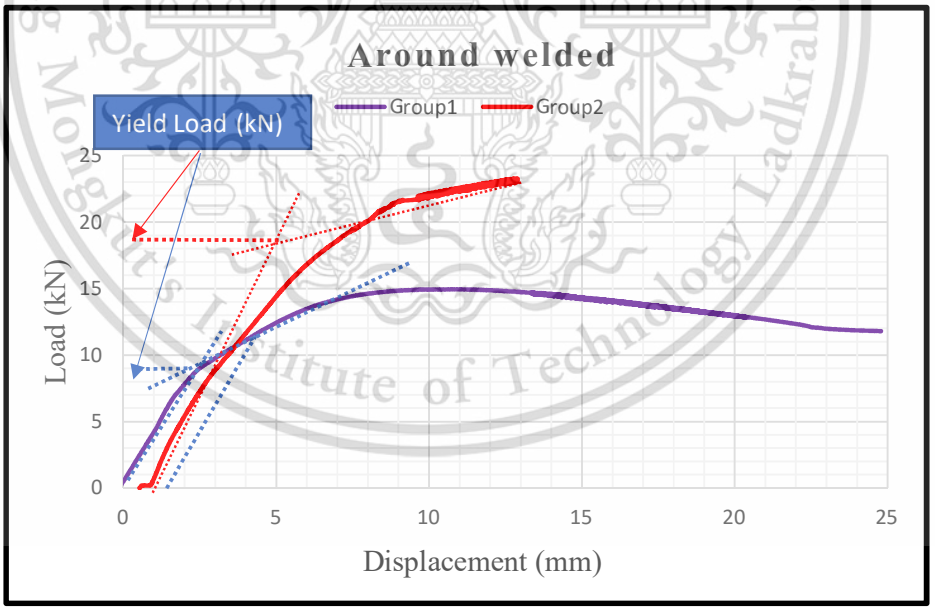

Figure 4.13 Yield load from load-displacement curve for around welded

Table 4.5 Summarize of Yield load and Maximum load of around weld specimen

Specimens	Yield load (kN)	Maximum Load(kN)
A1-1	9.15	15.75
A1-2	9.55	18.83
A1-3	8.95	14.95
A2-1	20.05	22.97
A2-2	18.95	23.27
A2-3	18.15	22.95
Average	14.21	19.79
Std. Dev.	5.42	3.82

4.2.2 2-Sided welded joint

The vertical load versus displacement curves of all 2Side welded specimens are plotted in Figure 4.14. Due to the deformation behavior and load results of specimen type. The results showed that specimens could be divided into 2 groups. the first group is S1-1, S1-2, S1-3 and second group is S2-1, S2-2, S2-3.

It could be seen that the specimen group 2nd was stronger than group 1st because the second group due to the tearing observe from the Chord tube as shown in Figure 4.15 and 4.16.

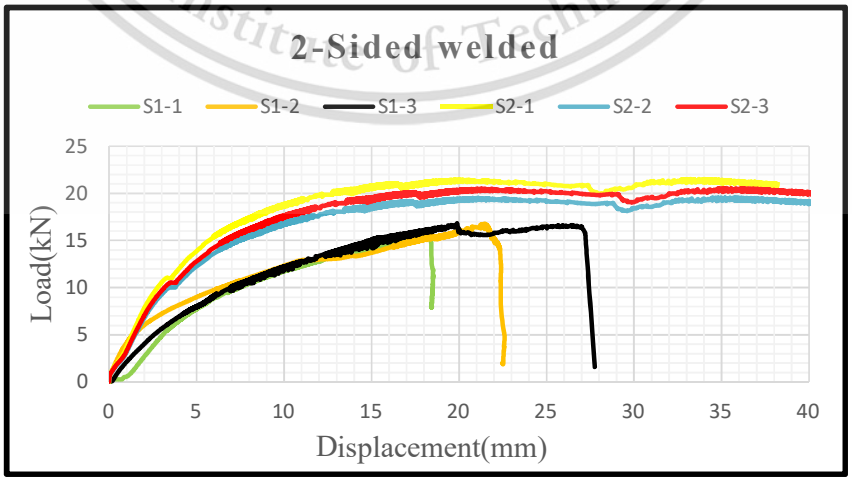

Figure 4.14 2-Sided welded result

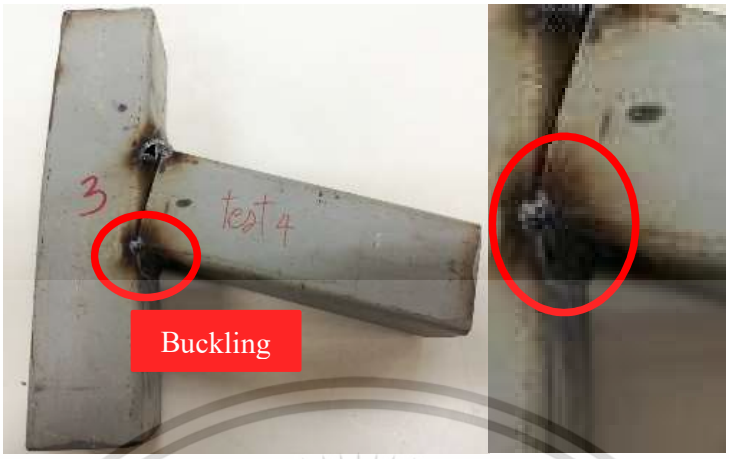

Figure 4.15 Deformation behavior for 2-sided welded group1

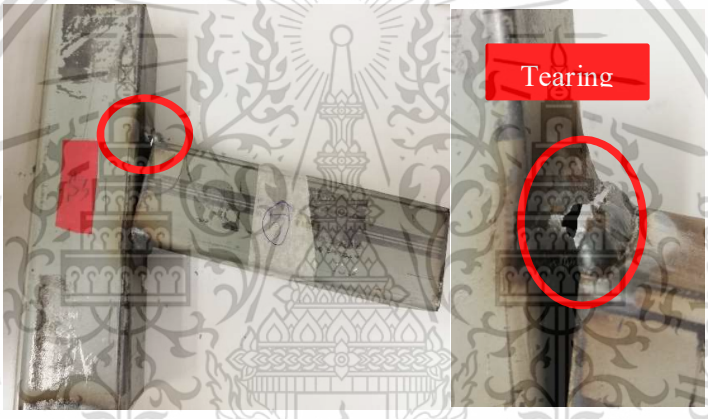

Figure 4.16 Deformation behavior for 2-sided welded group2

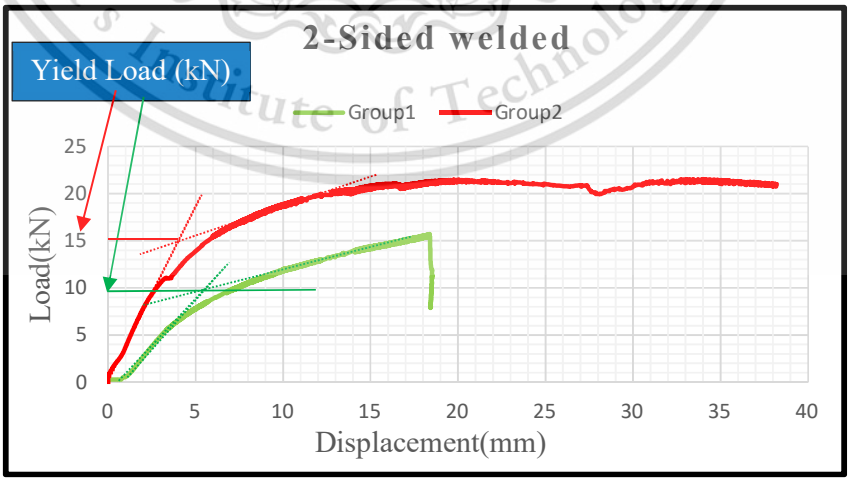

Figure 4.17 Yield load from load-displacement curve for 2sided welded

According to 2-sided weld result, Approximation method has been applied to determine Yield load as shown in figure 4.17 and table 4.6.

Table4.6 Summarize of Yield load and Maximum load of 2-sided weld specimen

Specimens	Yield load (kN)	Maximum Load(kN)
S1-1	9.55	15.71
S1-2	9.65	16.77
S1-3	10.05	16.83
S2-1	16.20	21.51
S2-2	14.50	19.59
S2-3	15.02	20.54
Average	12.50	18.49
Std. Dev.	3.06	2.37

4.2.3 Corner Welded Joint

The vertical load versus displacement curves of all corner-welded-joint specimens were plotted in Figure 4.18,4.20 and 4.22. Due to this specimen type, specify the size of the welding. The results could be divided into 2 groups. The first group(small size), which has a weld size of 5 and 7 mm, is CS-1, CS-2, CS-3, CS-4, CS-5, CS-6 and the second group (Large size) ,which has a weld size of 11 and 15 mm, is CL1-1, CL1-2, CL1-3, CL2-1, CL2-2, CL2-3, CL3-1, CL3-2, CL3-3, CL4-1, CL4-2, CL4-3 respectively.

According to the small size (5mm and 7mm), this type does not find any failure of base metal as shown in figure 4.19. this type does not found any failure of base metal and the 7mm specimen was stronger than the 5mm .

On the other hand, Large size (11mm, 15mm) was found that buckling and tearing Failure at Chord tube. From the results of the experiments of both sizes, we will separate into 2 groups, the first group is CL1 and CL3. The second group is CL2 and CL4. The 2nd is stronger than group 1st due to the buckling behavior deformation and tearing on weld toe observe from the Chord tube as shown in Figure 4.23 and 4.24.

Specimen group CL4 cannot perform damage to the specimen due to the safety limit of UTM machine. So yield load approximation method has been used to create criteria for both groups as shown in figure 4.20, 4.25 and table 4.7a,b.

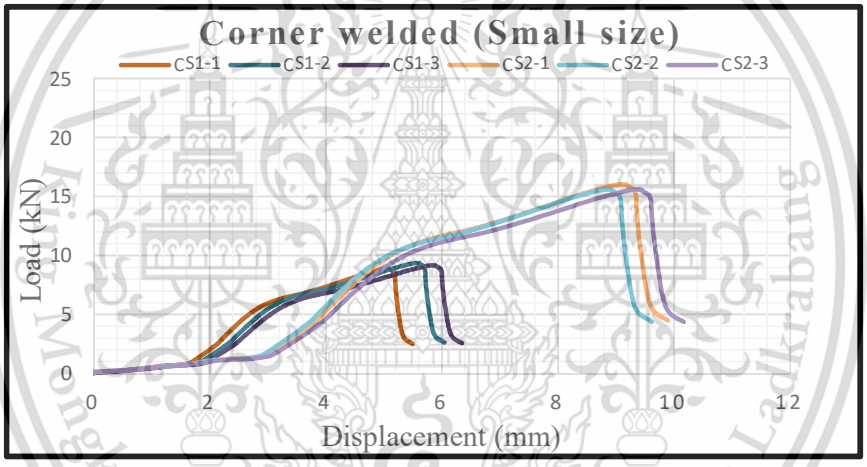

Figure 4.18 Corner welded result (small size)

Figure 4.19 Deformation Behavior for Corner weld (small size)

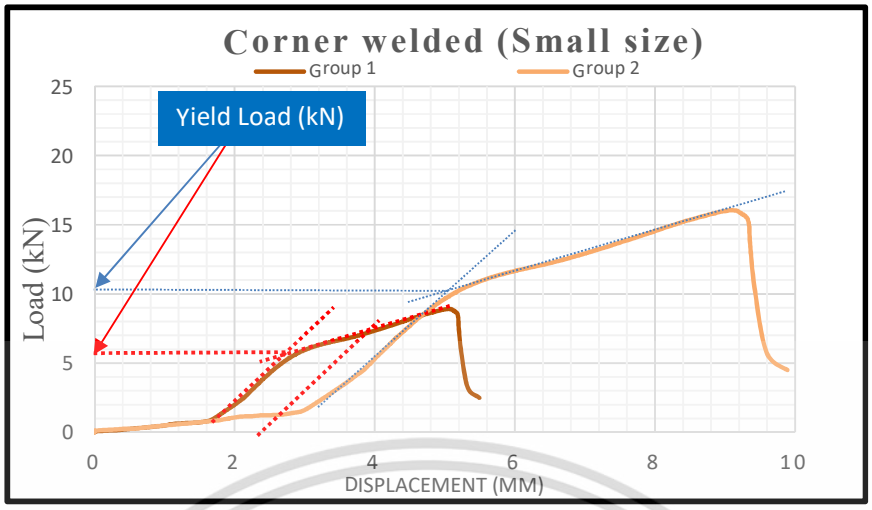

Figure 4.20 Yield load from load-displacement curve for corner welded (Small)

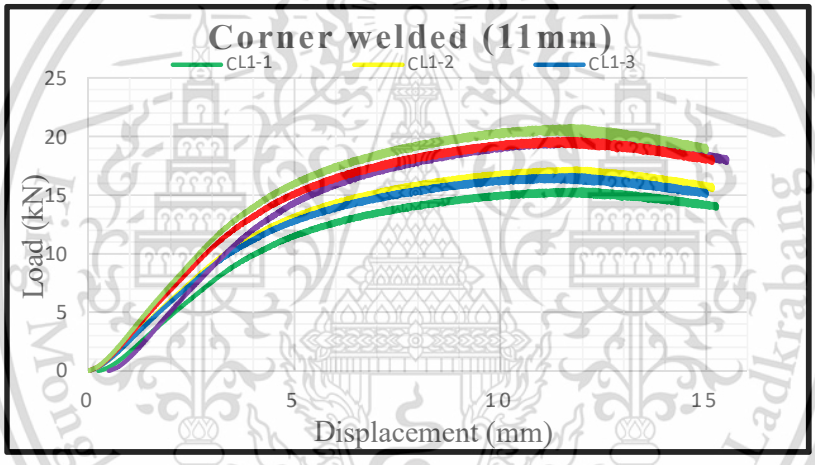

Figure 4.21 Corner welded result (Large size :11mm)

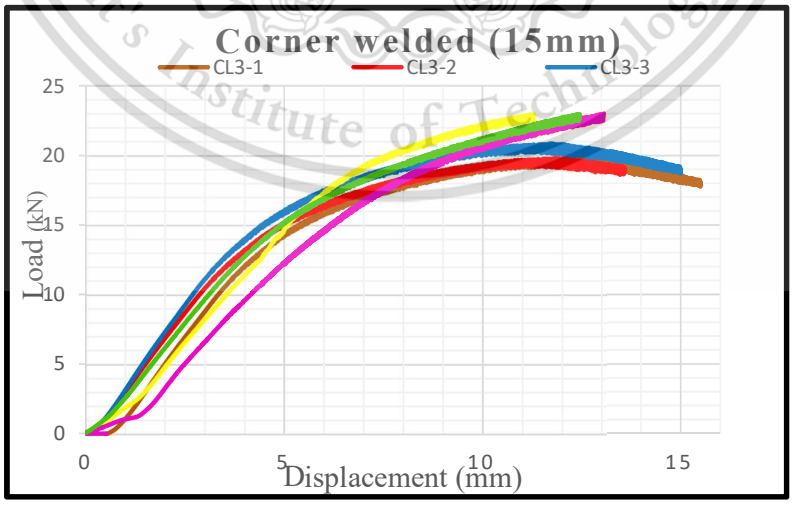

Figure 4.22 Corner welded result (Large size:15 mm)

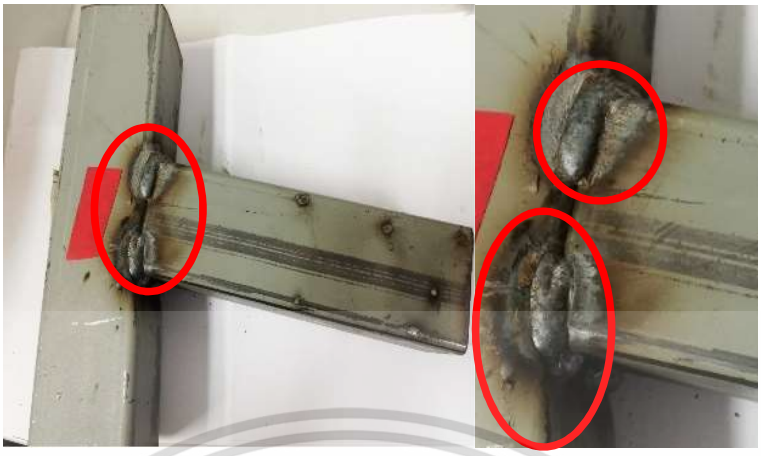

Figure 4.23 Deformation behavior for corner weld group 1 (Large size)

Figure 4.24 Deformation behavior for corner weld group 2 (Large size)

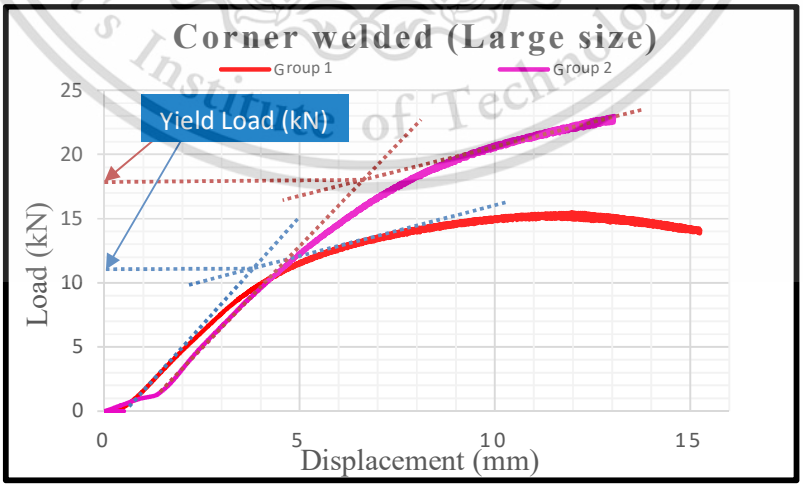

Figure 4.25 Yield load from load-displacement curve for corner welded (Large)

Table 4.7a Summarize of yield load and maximum load of corner weld (small)

Specimens	Yield load (kN)	Maximum Load (kN)
CS1-1	5.65	8.92
CS1-2	5.6	9.37
CS1-3	5.58	9.18
CS2-1	10.01	15.06
CS2-2	10.05	15.61
CS2-3	9.55	14.88
Average	7.74	12.17
S.D.	2.34	3.31

Table 4.7b Summarize of yield load and maximum load of corner weld (Large)

Specimens	Yield load (kN)	Maximum Load (kN)
CL1-1	12.25	15.48
CL1-2	12.4	17.26
CL1-3	12.55	16.71
CL2-1	14.2	19.84
CL2-2	14.55	20.89
CL2-3	14.6	19.84
CL3-1	15.5	15.49
CL3-2	15.6	16.75
CL3-3	15.5	16.71
CL4-1	16.25	22.94
CL4-2	16.8	21.3
CL4-3	16.65	21.6
Average	14.74	18.74
Std. Dev.	1.62	2.61

4.2.4 Rivet joint Result

The vertical load versus displacement curves of all Rivet joint specimens were plotted in Figure 4.26. In this experiment was prepared 3 specimens type as follows: 1.)two reinforcement (R1) 2.)one reinforcement (R2) 3.)No reinforcement (R3) as shown in figure 4.27.

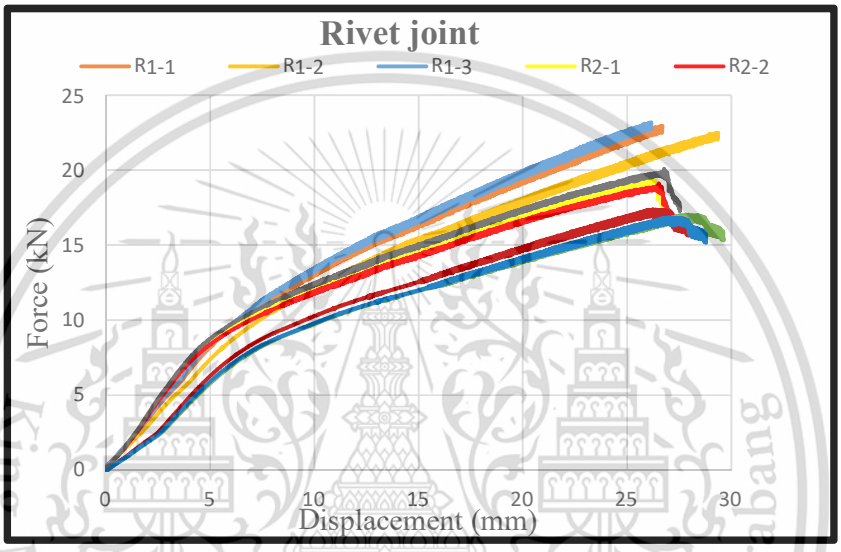

Figure 4.26 Rivet joint result

a) Rivet with two reinforcement (R1)

b) Rivet with one reinforcement (R2)

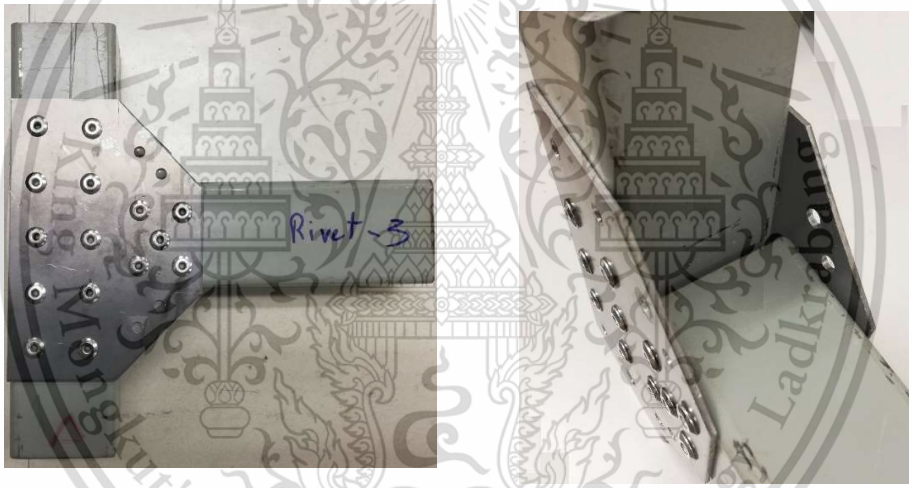

c) Rivet no reinforcement (R3)

Figure 4.27 Rivet joint specimens

From the result, Rivet joint that combined with two reinforcement has no failured of a rivet as shown in figure 4.28. Others joint were deformed at the same position rivet as calculation as shown in figure 4.29 and 4.30..

Figure 4.28 Deformation behavior of rivet joint with two reinforcement (R1)

Figure 4.29 Deformation behavior of rivet joint with one reinforcement (R2)

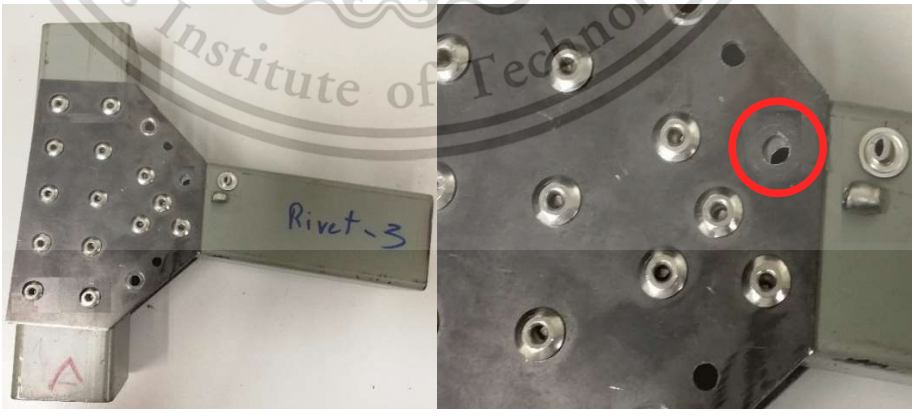

Figure 4.30 Deformation behavior of rivet with no reinforcement(R3)

Specimen group R1 cannot perform damage to the specimen due to the safety limit of UTM machine. So yield load approximation method has been used to create criteria for both groups as shown in figure 4.31 and table 4.8.

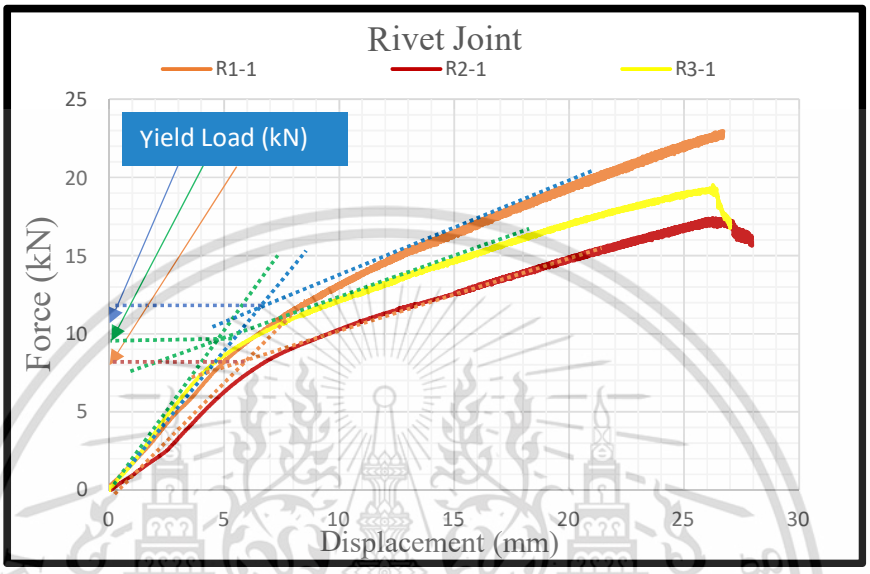

Figure 4.31 Yield load from load-displacement curve for rivet joint

Table 4.8a Summarize of yield load and maximum load of rivet joint (R1)

Specimens	Yield load (kN)	Maximum Load(kN)
R1-1	14.20	22.95
R1-2	14.30	22.49
R1-3	15.20	23.16
Average	14.57	22.87
Std. Dev.	0.55	0.34

Table 4.8b Summarize of yield load and maximum load of rivet joint (R2)

Specimens	Yield load (kN)	Maximum Load (kN)
R2-1	11.05	19.51
R2-2	11.05	19.12
R2-3	11.40	20.09
Average	11.17	19.57
Std. Dev.	0.20	0.49

Table 4.8c Summarize of yield load and maximum load of rivet joint (R3)

Specimens	Yield load (kN)	Maximum Load(kN)
R3-1	9.55	17.39
R3-2	9.65	17.04
R3-3	10.05	16.87
Average	9.75	17.1
Std. Dev.	0.27	0.27

According to the experimental results of the test, it can be seen that the damaged position was the same as the manual calculation and simulation result as shown in figure 4.32.

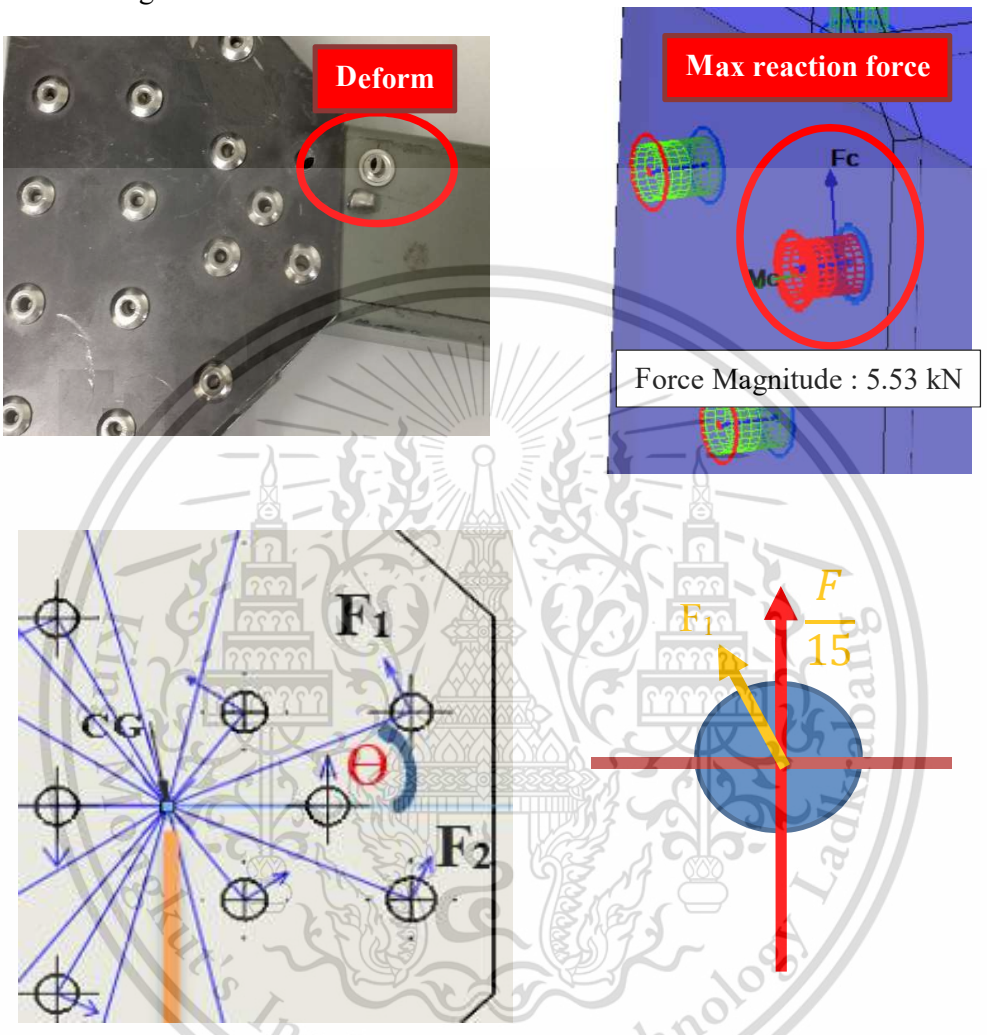

Figure4.32 Compare experimental, simulation result and design calculation

4.3 Compare each type

Based on the results of all the experiments, if we compare with the average of the maximum action force, the result will be inaccurate due to the fact that some of the results are not the highest value because Safety limit of the UTM machine, so this experiment was using the yield point, which is determined from the equation and approximation method by using relation graph between Force and displacement as shown in figure 4.33 and table 4.9

According to table1 , rivet joint(R1) was sthe strongest followed by corner weld(large) and around weld as compared with averaged yield load. The displacement of the rivet joint was more than others. because the hole diameter was larger than the rivet diameter size, which is following the standard. If rivet joint has a clearance, it will change the stress as shown in figure 4.34. To make the rivet tight, it could be improved by using an automatic tool.

Table 4.9 Average for all results

Specimen	Averaged Maximum Load (kN)	Averaged Yield Load (kN)
Around	19.79	14.21
2-Side	18.49	12.50
Corner(Large)	18.74	14.74
Corner(Small)	12.17	7.74
Rivet (R1)	22.87	14.57
Rivet (R2)	19.57	11.17
Rivet (R3)	17.10	9.75

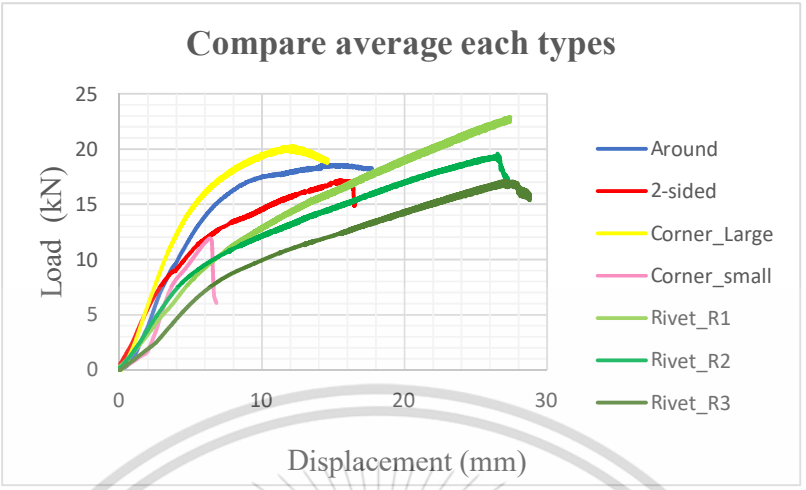

Figure 4.33 Load and displacement comparison 4 type

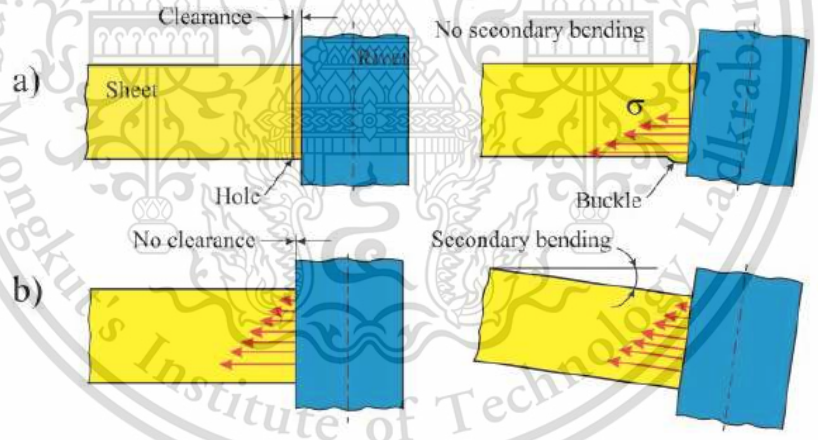

Figure 4.34 Rivet stress diagram a) with clearance b) without clearance

(Source: Jacek mucha, the structure of strength of riveted joints determined in the lap joint tensile shear test, acta mechanica et automatica, 2015

According to welding types, It can be seen that around welded, corner welded (large size) and Riveted joints (R1) have a similar result. This experiment measures the volume of welding material from Engineering CAD program. Therefore, this experiment can be concluded that material cost can reduce the by changing the welding type where the strength is still similar to the existing type as shown in table 4.10.

Table4.10 Summarize of weld material volume

Specimens	Average Yield Load (kN)	Weld material (cm^2)	Deviation from around weld (cm^2 ,%)
Around welded	14.21	6.41	0
2-Sided welded	12.50	1.96	- 69.42 %
Corner welded (Large, 11mm)	14.74	2.85	- 55.54 %
Corner welded (Large, 15mm)	14.74	3.79	- 40.87 %

The results of the experiment are found around the welded, with the greatest motion deviation, followed by 2-sided welding, Corner weld and rivet joint respectively as shown in table4.11.

Table 4.11 Comparison of Standard Deviation for each type

Specimens	SD (Yield load)	SD (Max load)
Around	5.42	3.82
Corner (S)	2.34	3.31
Corner (L)	1.62	2.61
2-sided	3.06	2.37
Rivet (R1)	0.55	0.34
Rivet (R2)	0.20	0.49
Rivet (R3)	0.27	0.27

4.4 Discussion

In this topic was discussed with 2 part 1.) welding joint, this part was explained the deformation parameter that affects the strength of specimens joint. 2.) Rivet joint validation, this part was explained the comparing deformation between equation, simulation and experiment specimens

4.4.1 Welding joint

According to welding experimental type results, 2-parameter that was believed to significantly major effect on the strength of T-joint specimens were the orientation of seam weld inside the steel tube member and welding size. This research also found 3 types of deformation as shown in figure 4.35. the elastic bending of the brace (figure 4.35a), the elastic buckling of the chord (figure 4.35b) and the tearing deformation of the joint (figure 4.35c).

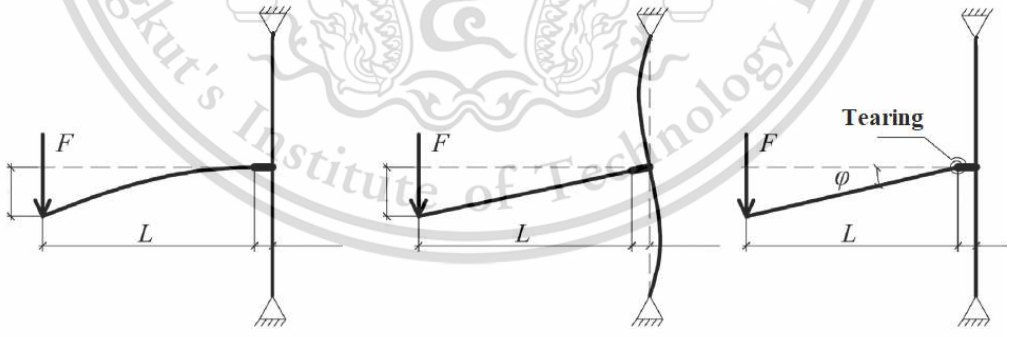

a) b) c)

Figure 4.35 Behavior of joint under loading: (a) bending of brace component; (b) buckling of chord; (c) tearing deformation of joint

4.4.1.1 Orientations of seam welded on square hollow tube

Podaný (2012) was study characteristic of plasticity and strength of tubes material. Due to the lower ductility of tensile samples the position of welded wall with respect to the plane of the bend is important . Figure 4.36 were illustrated three orientations of welded walls including the distribution of the engineering strain. Inside seam weld reflects the tensile test results as shown in figure 4.37. Their specimen having the seam weld, exhibit lower ductility, but higher strength

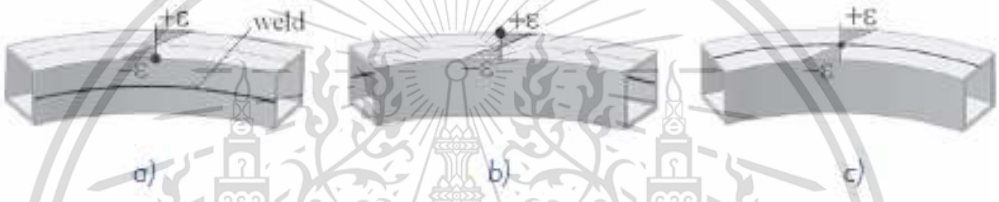

Figure 4.36 Correlation between the strain distribution and weld position

(Source: K. Podaný "Mechanics of Square tubes bending and cross section distorsion" Brno University of Technology, Faculty of Mechanical Engineering,2010)

Figure 4.37 Plane and three-dimensionally bend

(Source : K. Podaný "Mechanics of Square tubes bending and cross section distorsion" Brno University of Technology, Faculty of Mechanical Engineering,2010)

Seam weld has been found on the square hollow tube. The orientation of seam weld inside a square hollow tube was shown in figure4.38, table 4.12 and 4.13

Table 4.12 Orientation of seam weld inside hollow box (chord component)

Chord Component								
Type			Deformation group	Specimen No.	Seam Weld Position			
					I	II	III	IV
Around Weld			Buckling on chord	1-1	✓			
				1-2	✓			
				1-3			✓	
			Bending on brace	2-1		✓		
				2-2				✓
				2-3		✓		
2-Side Weld			Buckling on chord	1-1	✓			
				1-2	✓			
				1-3			✓	
			Tearing at weld	2-1		✓		
				2-2		✓		
				2-3				✓
Corner Weld	Small (5,7 mm)		Tearing at weld	S1-1				✓
				S1-2				✓
				S1-3	✓			
			Tearing at weld	S2-1				✓
				S2-2			✓	
				S2-3	✓			
	Large	Large1 (11mm)	Buckling on chord	L1-1	✓			
				L1-2	✓			
				L1-3			✓	
			Bending on brace	L2-1		✓		
				L2-2		✓		
				L2-3				✓
		Large2 (15mm)	Buckling on chord	L3-1	✓			
				L3-2			✓	
				L3-3	✓			
			Bending on brace	L4-1				✓
				L4-2		✓		
				L4-3		✓		

Table 4.13 Orientation of seam weld inside hollow box (brace component)

Brace Component								
Type			Deformation group	Specimen No.	Seam Weld Position			
					I	II	III	IV
Around Weld			Buckling on chord	1-1		✓		
				1-2				✓
				1-3		✓		
			Bending on brace	2-1			✓	
				2-2			✓	
				2-3	✓			
2-Side Weld			Buckling on chord	1-1		✓		
				1-2				✓
				1-3		✓		
			Tearing at weld	2-1				✓
				2-2		✓		
				2-3				✓
Corner Weld	Small (5,7 mm)		Tearing at weld	S1-1	✓			
				S1-2				✓
				S1-3		✓		
			Tearing at weld	S2-1	✓			
				S2-2				✓
				S2-3			✓	
	Large	Large1 (11mm)	Buckling on chord	L1-1		✓		
				L1-2				✓
				L1-3		✓		
			Bending on brace	L2-1			✓	
				L2-2	✓			
				L2-3			✓	
		Large2 (15mm)	Buckling on chord	L3-1		✓		
				L3-2		✓		
				L3-3				✓
			Bending on brace	L4-1			✓	
				L4-2	✓			
				L4-3			✓	

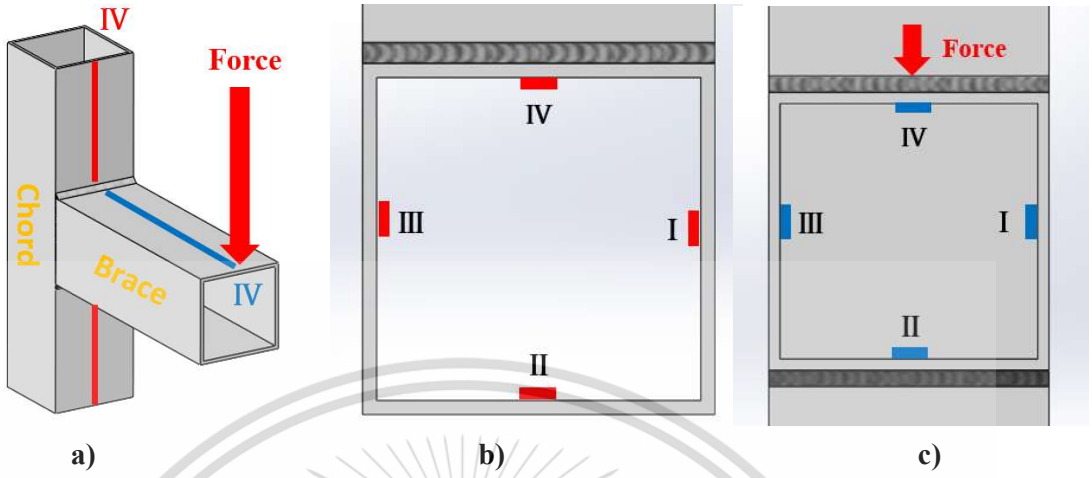

Figure 4.38 a) Diagram of seam weld on chord and brace b.) orientation on chord c.) orientation on brace

According to 3 deformations behaviour, the strength of a specimen was described by the orientation of seam weld inside a square hollow tube. For bending deformation on the brace component, the orientation that affected this behavior was II, IV position of the chord and I, III position of the brace as shown in figure 4.39.

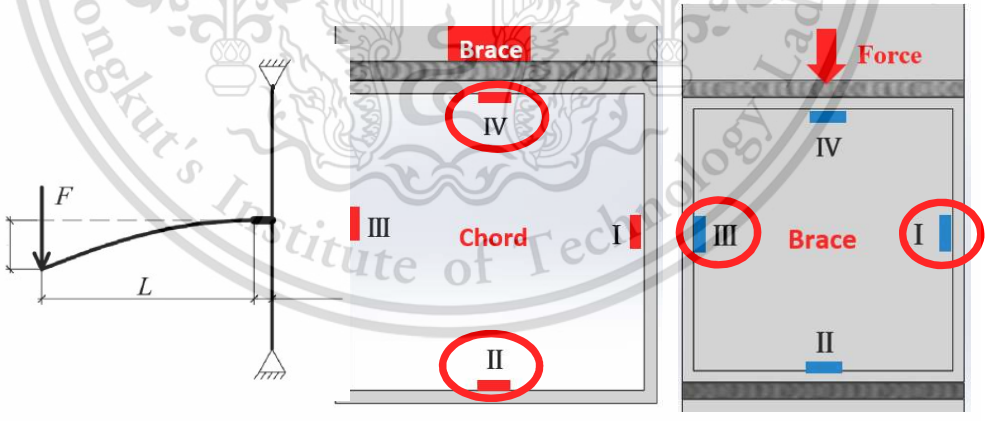

Figure 4.39 Orientation of seam weld for chord and brace (Bending on brace)

For Buckling deformation on the Chord component, the orientation that affected this behavior was I, III position of the chord and II, IV position of the brace as shown in figure 4.40.

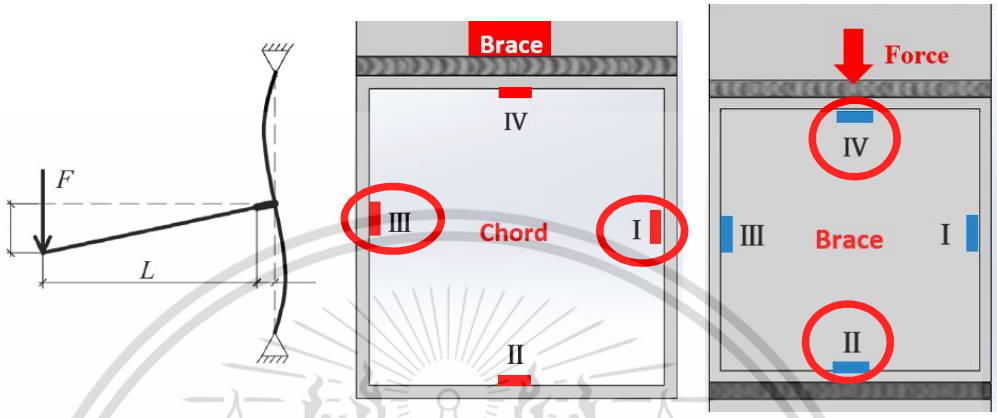

Figure 4.40 Orientation of seam weld for chord and brace (Buckling on chord)

For Tearing deformation of joint, the orientation that affected this behavior was II, IV position of the chord and II, IV position of the brace as shown in figure 4.41.

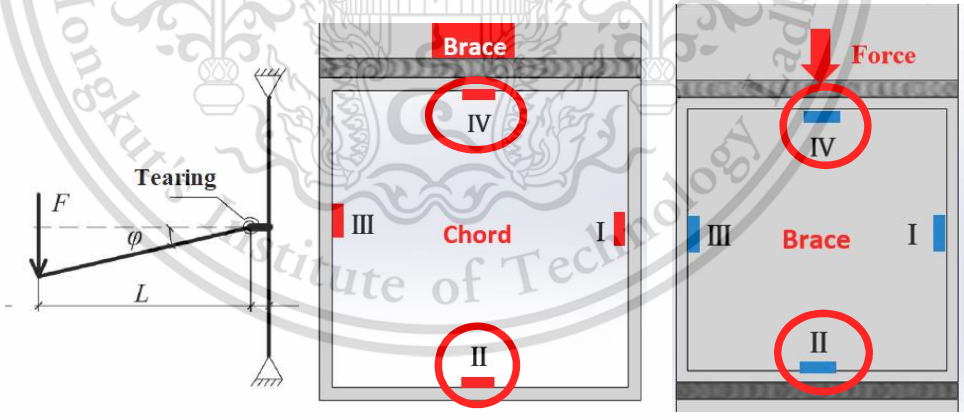

Figure 4.41 Orientation of seam weld for chord and brace (Tearing deformation)

The relation between failure modes and orientation of seam weld was shown in table 4.14

Table 4.14 Correlation between failure mode and orientation

Type		Group	Strength	Seam position	
				chord	brace
Around Weld		Bending on brace	High	II ,IV	I ,III
		Buckling on chord	Low	I ,III	II ,IV
2Sided Weld		Tearing at chord	Medium	I ,III	II ,IV
		Buckling on chord	Low	II ,IV	II ,IV
Corner weld	small	Tearing at weld	Low	I , II , IV	II , III, IV
	Large	Bending on brace	High	II ,IV	I ,III
		Buckling on chord	Low	I ,III	II ,IV

From the table 3, Bending on brace deformation was the greatest type followed by buckling chord and tearing respectively. The specimens with seam welded position II and IV on chord were stronger than others, which IV position is the strongest as shown in figure 4.42 (a-d)

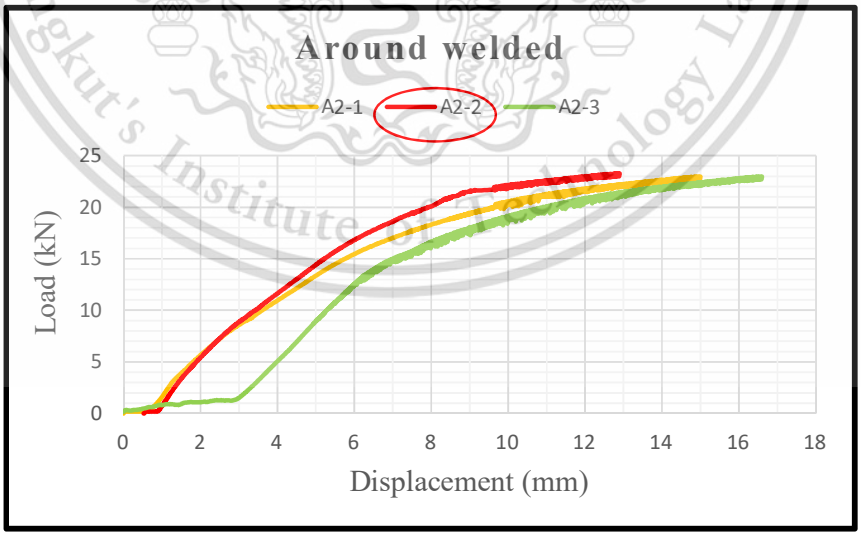

a.) around weld

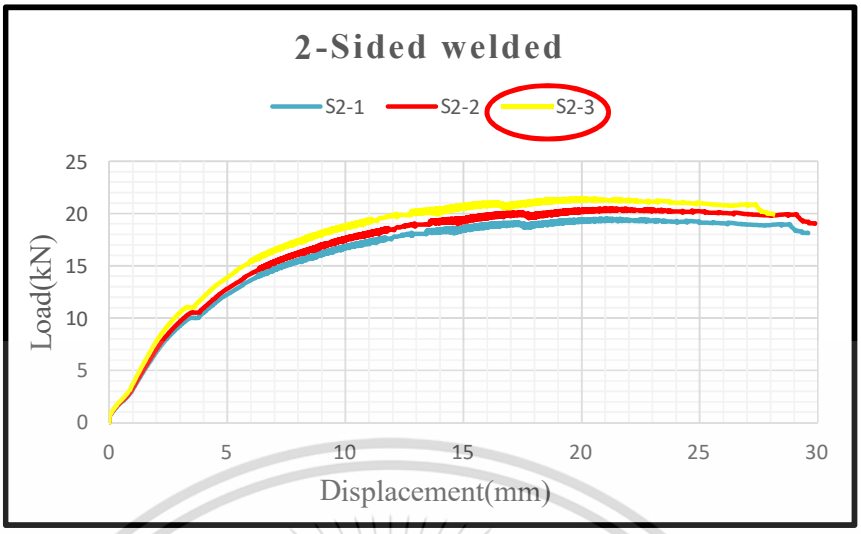

b.) 2-sided weld

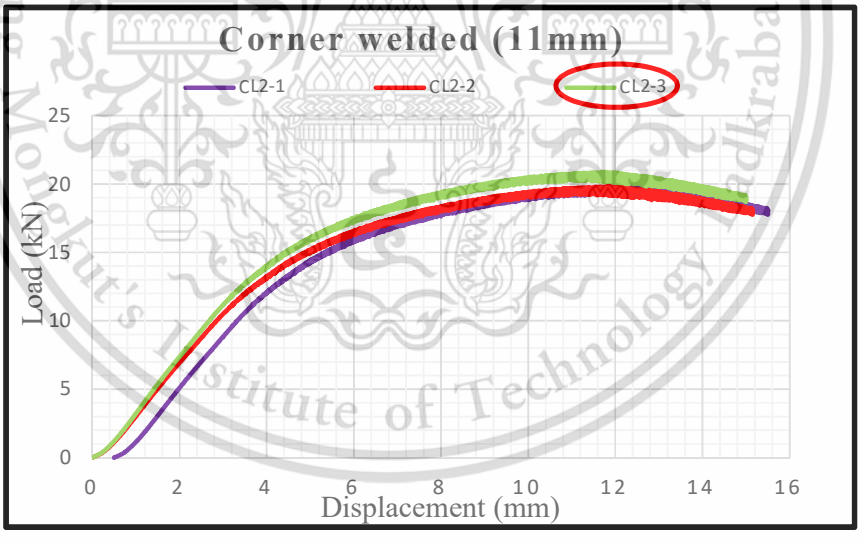

c.) corner welded (Large :11mm)

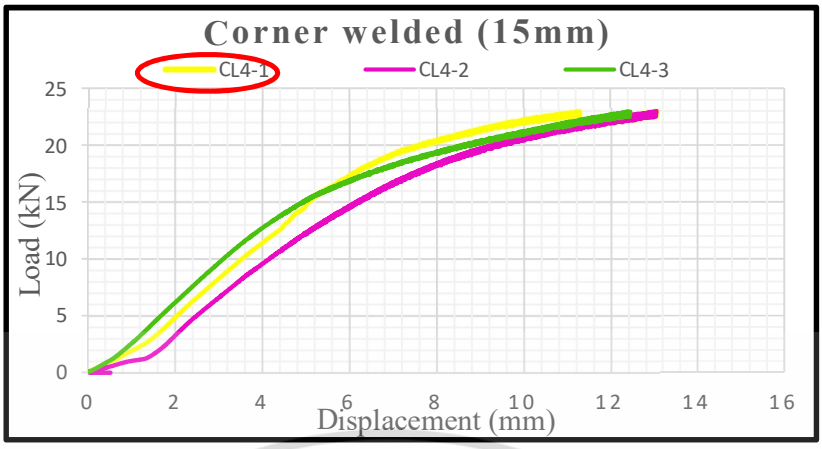

d.) corner welded (Large :15 mm)

Figure 4.42 The strongest specimens on bending deformation on each type

For corner welding (small size), it cannot be concluded with the orientation of the seam weld because the result does not match any pattern. It can be concluded on the next topic

From these 2 factors, it can be concluded that brace deformation is the strongest followed by tearing deformation and chord deformation respectively.

In term of bending on brace deformation, corner weld was stronger than around weld as shown in figure 4.43

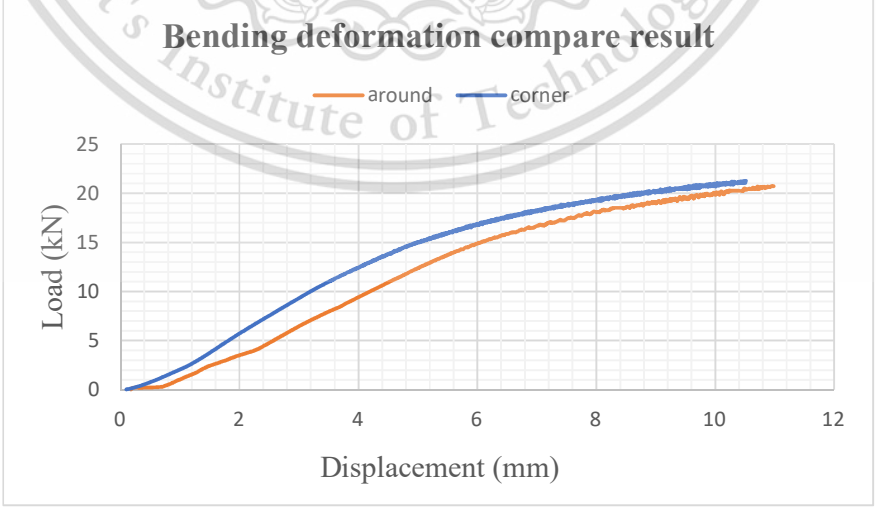

Figure 4.43 Compare result for bending deformation on each group

4.4.1.2 Weld Length on specimens

According to the corner welded (small size) , the deformation behavior cannot be concluded by orientation of seam weld inside hollow tube. So, the length of the weld is an important parameter for of welds small group was 5 ,7 mm and the large group was 11 ,15 mm, which can be seen that the second group was high strength. The first group did not find any buckling or tearing deformation on chord tube. For this experiment, if determine the variable size which can find the length that is appropriate for the applied workload. the example deformation behavior that depends on variable size shown in figure 4.44

Based on the results of this corner welding experiment, it is found that if specimen used the weld size to more than 22 percent, the width of the steel will increase the strength equivalent to the full weld which can reduce the volume of welding materials up to 40-55%.

Figure 4.44 Deformation under welded length condition

4.4.1.3 Auxiliary factor

Resulting in residual stress also weakening in the structure of the material and crack on weld position (Wolfgang Fricke , 2012)Their results showed that the heat in the welding process is one of the parameters that affect the specimens. In addition to causing the residual stress in the specimens, the macrostructure of the specimens will be changed as well. Residual stress was decreased strength of structure and increase risk rate of crack on weld material. Jarmo Havula (2018) studied moment-rotation behavior of welded tubular high strength steel T-joint. they investigate heat effect on base metal by variable heat on the joint and crate sample bending model

Effect of the welding on tensile load test (Cheng chen,2016). They investigate effect of welding on tensile load test. By comparing the load-displacement curves, it is found that the behavior of these two materials have the same pattern. Equations has been used to predict the first yield is conservatively but seem to overestimate at the end of result. The deduction was verified by finite element analysis. It is concluded that welding has significant impact on the strength of high strength. Without considering this impact would lead to overestimation on the load carrying capacity and may be unsafe. According to my specimens, their deformation was governed by bending failure as shown in Figure 4.45a, chord walls buckling was observed as a minor failure mode in all specimens (figure4.45b). Strain hardening and the membrane effect allowed the considerable post-yielding behavior of the joints. Finally cracking in Heat Affected Zone (HAZ) led the specimens to tearing shear failure, as shown in figure 4.45c.

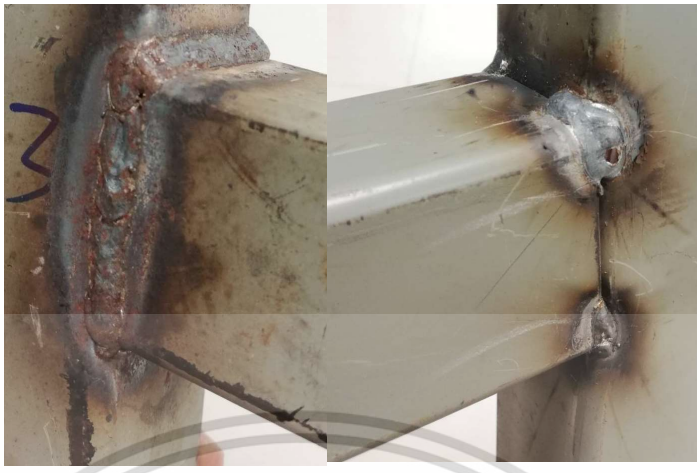

(a) Bending on brace

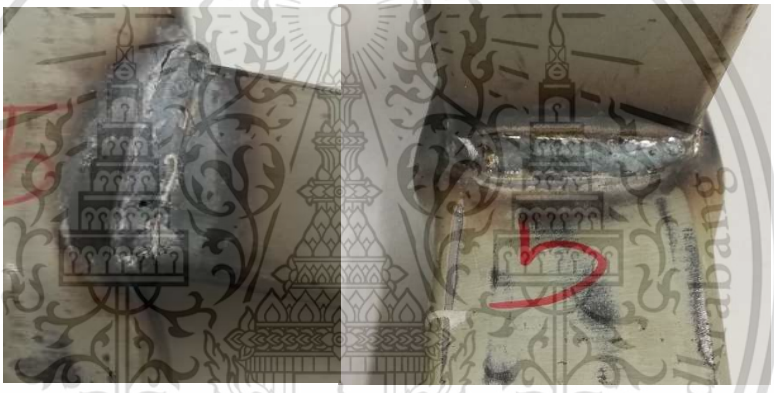

(b) Buckling on chord

(c) Tearing shear

Figure 4.45 Observed failure modes

4.4.2 Rivet joint design validation

According to manual calculation the maximum shear stress on rivet system. The maximum shear stress was same as simulation. Comparing of the two design methods, it was found that the position of the rivet was damaged in the same position as shown in figure4.46 and 4.47.

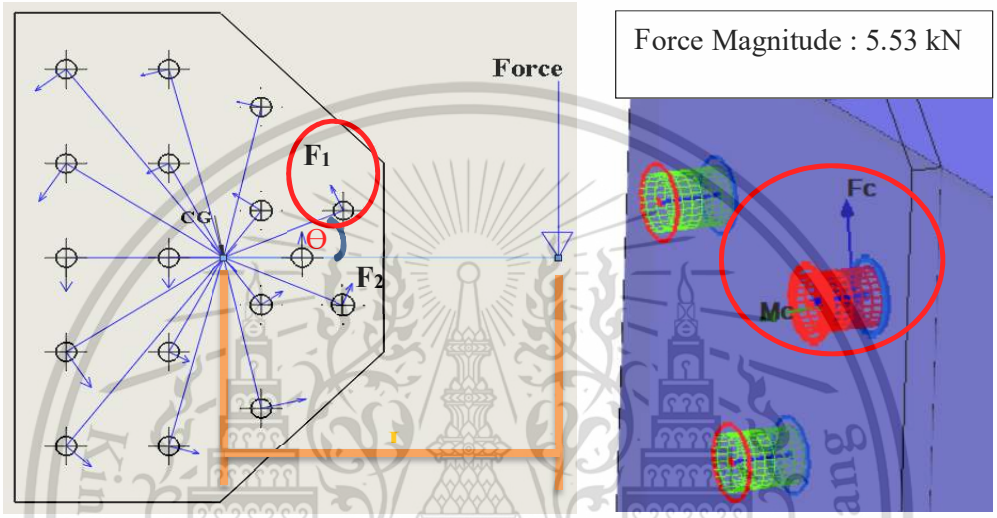

Figure 4.46 Rivet joint failure calculation

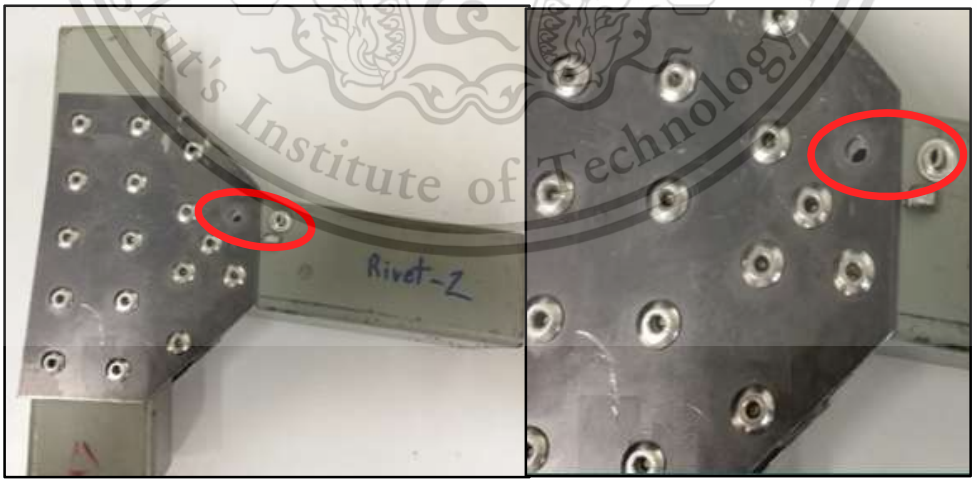

Figure 4.47 Failure position of rivet system

Bracket 1 was proof by Simulation data proof that obtained with shear load and sufficient for this design. Bracket 2 was proof by Simulation data proof that obtained with tensile load and sufficient for this design. Both simulation data were shown in figure 4.48.

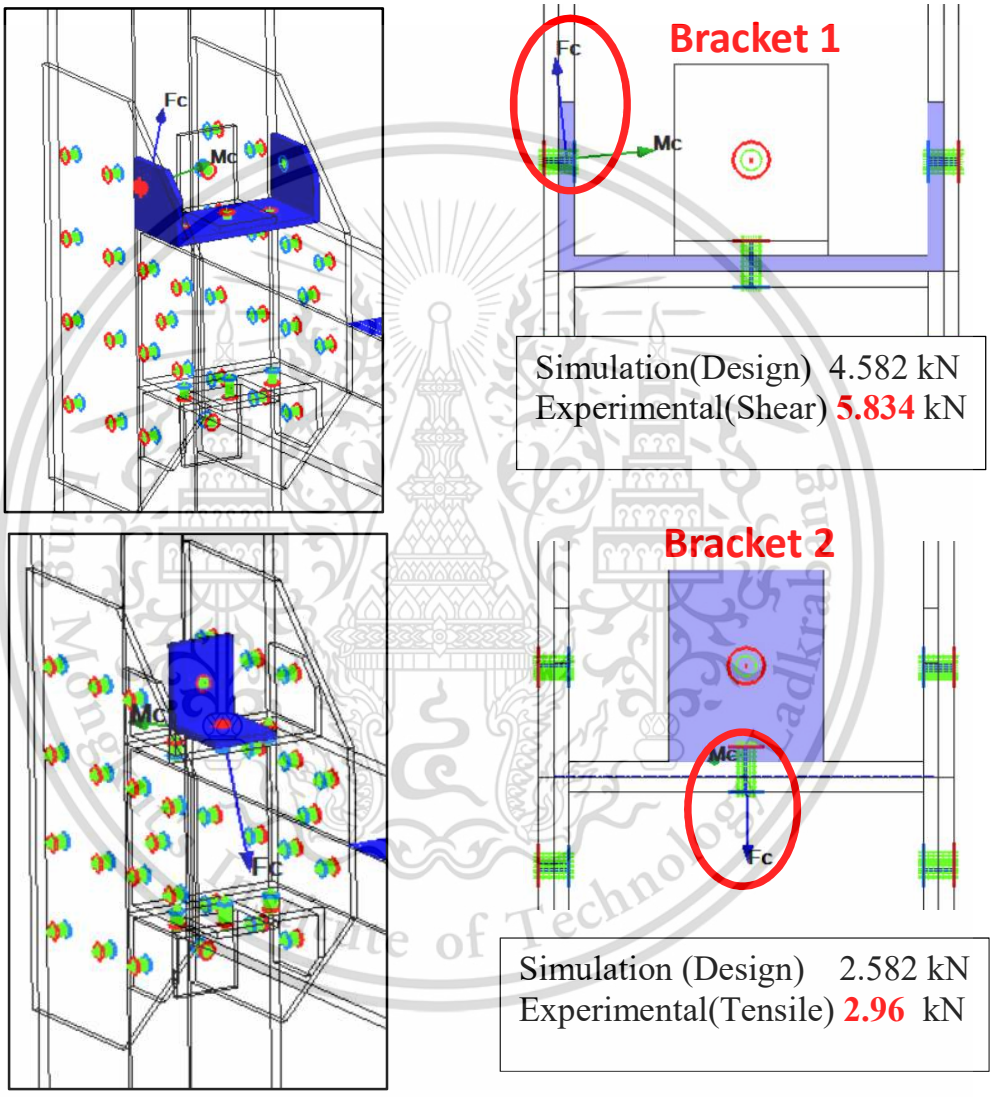

Figure 4.48 Simulation results of bracket 1 and bracket 2

4.5 Advantage and disadvantage of all specimens

From all test results, Application of each type can be summarized as a table 4.15. This table has been rated by the author. For each detail, the best score is 3 points, a good score is 2 points and a bad score is 1 point. From the scores shown in the table, it is found that Rivet joint was the best score. because it was easy to use, high strength as other types, and was no impacted by the orientation of seam welds. the working speed was too slow but must be improved by automatic tools.

Table 4.15 Summarize application and factor on each type

Types / Details	Around welded (Score)	2-Sided welded (Score)	Corner welded (Score)	Rivet joint (Score)
Usable	Easy (3)	Easy (3)	Specific area (2)	Easy (3)
Strength	High (3)	Medium (2)	High (3)	High (3)
Orientation of seam weld affect	High (1)	Medium (2)	Medium (2)	No (3)
Deformation	• Buckling on Chord side • Bending on brace (2)	• Buckling on Chord side • Tearing on chord (2)	• Buckling on Chord(Large Size) • Tearing on chord (Small Size) (3)	• Tearing on rivet (3)
Practically used	Quite Simple (3)	Quite Simple (3)	Need experience (1)	Simple (2)
Cost	High (1)	Medium (2)	Medium (2)	High (1)
Time (s)	60 (2)	35 (1)	85 (2)	600 (1)
Total Score	15	15	15	**16**

CHAPTER 5

CONCLUSIONS AND RECOMMENDATIONS

5.1 Conclusions

This experiment of bending test using designed and developed test rig on 4 different welded types were carried out. The same welding machine and welding parameters were used for all the joints. The specimens were test under vertical loading using a 25kN Universal tensile test machine. The load is applied stroke control at a 1mm/min up to failure. The result can be applied to another section on bus structure. like roof or floor structure.

5.1.1 Deformation parameter

- Bending on brace deformation was the greatest type followed by buckling chord and tearing respectively.
- The specimens with seam welded position II and IV on chord were stronger than others, which IV position is the strongest
- Around weld has the greatest impact from orientation of seam weld inside hollow tube generated from the manufacturing process, which can be seen from the standard deviation higher than others.
- Weld length of specimen will affect the strength of specimens. if specimen used the weld size to more than 22 percent, the width of the steel will increase the strength equivalent to the full weld.
- Heat Affected zone and residual stress would be affect the strength of the specimens. This parameter needs to proof by hardness test.

5.1.2 T-joint comparison

Table 5.1 Summarize application and factor on each type

Types / Details	Around welded (Score)	2-Sided welded (Score)	Corner welded (Score)	Rivet joint (Score)
Usable	Easy (3)	Easy (3)	Specific area (2)	Easy (3)
Strength	High (3)	Medium (2)	High (3)	High (3)
Orientation of seam weld affect	High (1)	Medium (2)	Medium (2)	No (3)
Deformation	• Buckling on Chord side • Bending on brace (2)	• Buckling on Chord side • Tearing on chord (2)	• Buckling on Chord (Large Size) • Tearing on chord (Small Size) (3)	• Tearing on rivet (3)
Practically used	Quite Simple (3)	Quite Simple (3)	Need experience (1)	Simple (2)
Cost	High (1)	Medium (2)	Medium (2)	High (1)
Time (s)	60 (2)	35 (1)	85 (2)	600 (1)
Total Score	15	15	15	**16**

The result and evaluation for this paper was summarize as shown in table 5.1 Yield load has been created to determine the strength of specimens for each type.

- Around welded welding was easy to use, strong and convenient.
- 2-Sided welding was weaker than others. but used for tasks that require speed and not necessary to be strong.
- Corner welding was a strong welding type as compared with others. Because this welding method carried the biaxial load. By comparing the volume of welding material with an existing type (around welds) which can reduce the volume of welding materials saving 40-55%.
- Rivet joint can be replaced to other weld joint depends on the application. This type was reduced the buckling deformation. The strength of rivet joint as strong as the welded joint.

- From the score of the joints, it was suggested that I propose to use the new joints.

5.2 Suggestion for further research

- According to Heat Affected Zone on welding area, preheat treatment process will solve this problem. C.K.Lee (2013). It is found that preheating is beneficial and can effectively reduce the magnitude of residual stress. The heat-affected zone and residual stress are not a concern in this research. It can be proved with a hardness test on each zone in specimens as shown in figure 5.1

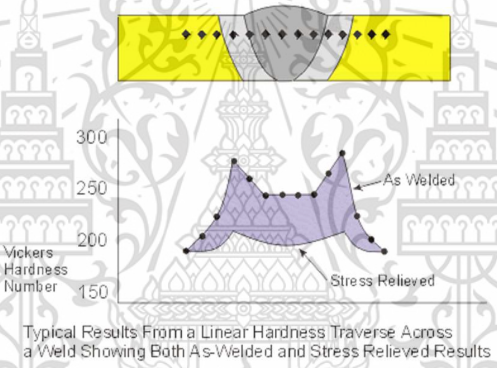

Figure 5.1 example of hardness test on welded area

(Source: http://sumitwaghmare.blogspot.com/2012/10/testing-of-weldments.html)

- For Rivet joint, reinforcement bracket will be developed to a compatible version as shown on figure 5.2

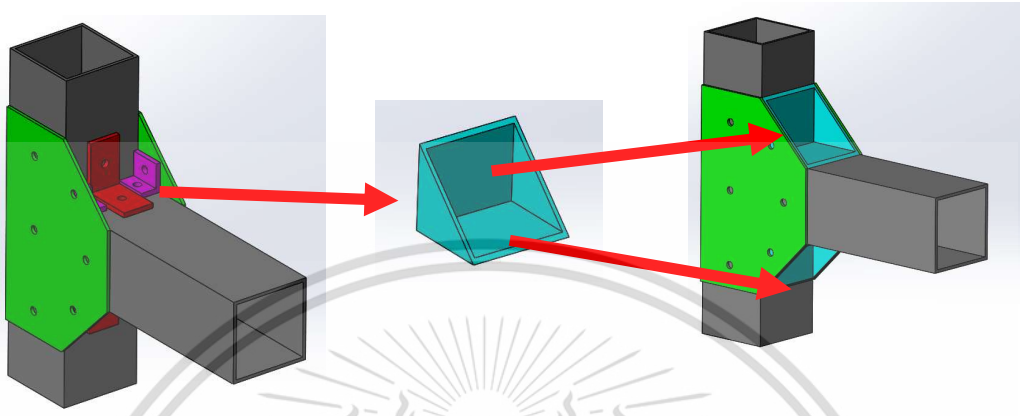

Figure 5.2 Reinforcement bracket compatible version

- Experimental result could be applied to others structure such as roof.

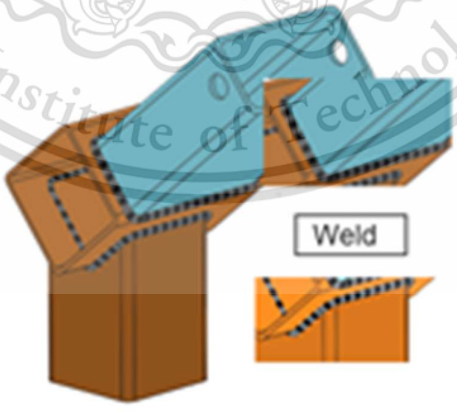

Figure 5.3 Example of another structure

REFERENCES

A. Chattopadhyay, G. Glinka, M. El-Zein, J. Qian and R. Formas, Stress Analysis and fatigue of welded structures, Doc. IIW-2201, recommended for publication by Commission XIII “Fatigue of Welded Components and Structure.”,2011

A. Barroso, Prediction of welding residual stresses and displacements by simplified models. Experimental validation, Materials and Design, 2009

Arunkumar.A, Theoetical and experimental analysis of T-joint in TIG welding process, International Journal of Scientific Engineering and Applied Science,2016

Anandkumar. M. Padashetti, Roof crush simulation of passenger car for improving occupant safety in cabin , International Research Journal of Engineering and Technology,2016

Banleng K. , Design and Analysis of Bus Body Structure (Standard No.1),King Mongkut’s University of Technology North Bangkok ,2010

Baumeister Joachim, Methods for Filling Hollow Structures with Aluminium Foam, Materials Science Forum, 2010

Ben Young, Stainless Steel Tubular Joints - Tests and Design of X- and K-joints in Square Hollow Sections, International Specialty Conference on Cold-Formed Steel Structures ,1994

Bin Chenga, Behaviors of partially concrete-filled welded integral T-joints in steel truss bridges, Engineering Structures, 2018

Cheng Chen, Xiaozhao Zhang, Effects of Welding on the Tensile Performance of High Strength SteelT-stub Joints, Institution of Structural Engineers ,2017

Cho-Chung Liang , Giang-Nam Le,Bus rollover crashworthiness under European standard: an optimal analysis of superstructure strength using successive response surface method

C.-C. LIANG, Optimization of bus rollover strength by consideration of the energy absorption ability, International Journal of Automotive Technology,2010

C.K. Lee S.P. Chiew, Jin Jiang , Residual stress of high strength steel box T-joints Part 1: Experimental study , Journal of Constructional Steel Research 93 ,2013

Djan eirik djavit and erik strande, Fatigue analysis of fillet welded joints used in offshorestructures, Department of shipping and marine technology,2013

E. Ranjbarnodeh, Effect of welding parameters on residual stresses in dissimilar joint of stainless steel to carbon steel, Department of Materials Science and Engineering,Sharif University of Technology, Tehran, Iran,2010

Farah Kamil Abid Muslim, Computer aided design of rivets for steam boiler shell, Al-Qadisiya Journal For Engineering Sciences,2012

Feng Pan, Design optimisation of vehicle roof structures: benefits of using multiple surrogates, International Journal of Crashworthiness,2014

GC Li, P Xue, Shear behavior and failure analysis of a composite T-joint with a cutout, Journal of Composite Materials,2014

Hensham, K., 2009, Design Optimization of Vehicle structures for Crashworthiness Improvement, dissertation, Concordia /university, pp. 7-9.

Marsel Garifullin, Initial in-plane rotational stiffness of welded RHS T joints with axial force in main member, Journal of Constructional Steel Research,2017

Milad Moradi, Hartmut Pasternak, A Study on the Influence of Various Welding Sequence Schemes on the Gain in Strength of Square Hollow Section Steel T-Joint, Journal of Welding and Joining, Vol.35 No.4(2017)

M.S. Zhao, Tensile behavior of high-performance structural steel T-stub joints, Journal of Constructional Steel Research,2015

Jacek mucha, Waldemar Witkowski, Mechanical behavior and failure of riveted joints in tensile and shear tests, Strength of Materials, Vol. 47, No. 5, September, 2015

Jacek mucha, the structure of strength of riveted joints determined in the lap joint tensile shear test, acta mechanica et automatica, 2015

Jarmo Havulaa, Marsel Garifullinb, Markku Heinisuob, Kristo Melab, Sami Pajunenb,Moment-rotation behavior of welded tubular high strength steel T joint, Engineering Structures 172 (2018) 523–537 , 2018

J.A. Packer., J.Wardenier, Y.Kurobane, D. Dutta, N. Yeomans, Design Guide For Rectangular Hollow Section(RHS) Joints Under Predominatly Static Loading ,CIDECT ,Germany, 1992

Jerzy Kaniowski, Comparison of selected rivet and riveting instructions, Fatigue of Aircraft Structures,2014

K. Podaný “Mechanics of Square tubes bending and cross section distorsion” Brno University of Technology, Faculty of Mechanical Engineering,2010

L.S. Sutherland, Statistical experimental design techniques to investigate the strength of adhesively bonded T-joints, Composite Structures,2017

Miguel Lozano, The Influence of the Heat-Affected Zone Mechanical Properties on the Behaviour of the Welding in Transverse Plate-to-Tube Joints, MDPI,2018

M. Garifullin, M.K. Branzova, M.Heinisuo, Cold]-formed RHS T-joints with initial geometrical imperections, Tampere University of Technology, Finland,2018

M Mao, Reinforcement of vehicle roof structure system against rollover occupant injuries, International Journal of Crashworthiness, 2014

M. Skorupa, Observations and analyses of secondary bending for riveted lap joints, International Journal of Fatigue,2015

N. Kosteski, J.A. Packer, R.S.Puthli, A finite element method based yield load determination procedure for hollow structural section connection, University of Toronto ,Canada,2003

Peter Pastucha, Vladimir Ondek, Filip Murgas, Jan Rehor, StanislavHosnedl, Shape Fastener of the Bus Skeleton Testing, International Conference on Electromechanical Control Technology and Transportation (ICECTT 2015)

Pedro Galvez, Study of the behaviour of adhesive joints of steel with CFRP for its application in bus structures, Composites Part B, 2017

Prof. SR. Satish Kumar and Prof. A.R. Santha Kumar, Design of steel structure ,Indian Institute of Technology Madras, 2010

R. Jain, Optimization methodology for beam gauges of the bus body for weight reduction, Applied and Computational Mechanics, 2014

R. Moazed, The Influence of Mechanical and Laser Cutting on the Fatigue Strengths of Square Hollow-Section Welded T-Joints, Journal of Offshore Mechanics and Arctic Engineering,2012

R.M.M.P. de Matos, Resistance and elastic stiffness of RHS “T” joints: part I - axial brace loading, Solids and structures, 2014

S. Butdee, TRIZ method for light weight bus body structure design, journal of Achievements in Materials and Manufacturing Engineering, 2017

S.M.R. Khalili, Effect of Joint Geometry on the Behavior and Failure Modes of Sandwich T-Joints Under Transverse Static and Dynamic Loads, The Journal of Adhesion, 2015

S.M.R. Khalili, Behavior and Failure Modes of Sandwich T-Joint Using Cohesive Zone Material Model and Contact Elements, Applied Composite Material,2012

Sameer Gupta, Using CAE to evaluate a structural foam design for increasing roof strength, LS-DYNA Users Conference, 2011

Sing-Ping Chiew, Fatigue behaviors of square-to-square hollow section T-joint with corner crack. I: Experimental studies, Engineering Fracture Mechanics 74,2007

Chi-King Lee, Fatigue behaviors of square-to-square hollow section T-joint with corner crack. II: Numerical modeling, Engineering Fracture Mechanics 74,2007

Umesh A. Khilare, Investigation of Residual Stresses in Welding and its Effect on Mechanical Behavior of Stainless Steel310, Department of mechanical,2016

U. V. R. S. Turaga, Failure Modes and Load Transfer in Sandwich T-Joints, Journal of Sandwich Structures and Materials,2000

Wolfgang Fricke "IIW Guideline for the Assessment of Weld Root Fatigue" Hamburg University of Technology (TUHH) Ship Structural Design and Analysis,2012

Yu Chen, Investigation of grouted stainless steel SHS tubular X- and T-joints subjected to axial compression, Engineering Structures,2017

Z.M. Yang, Fatigue crack growth analysis of a square hollow section T-joint, Journal of Constructional Steel Research 63 ,2006

Zhao, Xiao-Ling, Static design procedure for welded hollow joints, International Institute of welding, Department of civil Engineering, Monash ,2013

Zhao, Xiao-Ling, T-joints in Rectangular Hollow Sections Subject to combined actions, Department of civil Engineering, Monash ,1991

APPENDIX A

PUBLICATION

The JSAE Annual Spring Congress, 22-24 May 2019 .Yokohama, Japan

講演番号 232

文献番号 20195232

Experimental Bending Tests for Design Improvement of Substructure with Joints in Bus Body

Sarinyavajn S.[1] Benyajati C.[2] Kansuwan P.[3] Okuma M.[4]

1) International College , King Mongkut's Institute of Technology Ladkrabang. Chalongkrung Road, LadKrabang, Bangkok 10520 Thailand. (E-mail: 57610025@kmitl.ac.th)
2) National Metal and Materials Technology Center (MTEC) . (E-mail: chinab@mtec.or.th) 114 Thailand Science Park (TSP), Phahonyothin Rd., KhlongNueng, KhlongLuang, PathumThani 12120 Thailand
3.) Department of Mechanical Engineering, Faculty of Engineering King Mongkut's Institute of Technology Ladkrabang. Chalongkrung Road, LadKrabang, Bangkok 10520 Thailand
4.) Department of Mechanical Engineering Tokyo Institute of Technology , Japan

ABSTRACT: This study will focus on a substructure of a bus body with a significance to a rollover test. Experimental specimens,consisting with T-joint,L-joint configurations and one actual-sized roof corner structural bay of a commercial bus, were obtained from actual bus assembler in Thailand and were subjected to a bending load from two in-house test rigs.The objective was to improve a current structural joint configuration employed by a local assembler, in terms of weight and strength. The results from joint specimens with different joining techniques and designs would be initially used as a guideline prior to a substructure test for further validation.

KEY WORDS: **T-Joint configuration, Joint modelling, Bus structures, Structural Improvement**

1. INTRODUCTION

Buses are one of the main vehicles for public transportation in many countries. The size of buses usually vary between 8-12m in length . Due to transport regulation bus manufactures have to concern about the safety of passengers . Therefore , the strength of bus structure is an important factor for the bus structure design and production process. Various type of beam steels are normally used in a bus structure. Different joints are designed to assemble these steels together. Welding is a joining technique widely used in a bus structure fabrication. Although the welding process is properly controlled , the strength of the bus structure at welded joint areas are decreased because of peculiarities such as inhomogeneous material, welding residual stress and weld geometry[1]. These peculiarities cause difficulty in stress evaluation at welded joints. Moreover, most bus structures in Thailand are designed based on past experiences of engineers in a company but those experiences might not be enough for passenger safety. Computer Aided Design (CAD) and Computer Aided Engineering (CAE) are tools to evaluate the stress on the bus structure under many loading conditions . S. Manokruang[2] presented the bus structure design using Computer Aided Design (CAD) for analysis It was found that a wireframe structure as shown in Fig 1. could be analyzed using beam elements. Furthermore , many studies found that maximum stress normally occurred at welded joints.Useful recommendations of welded structure are also given guideline , e.g. International Institute of welded (IIW)[3], Eurocode[4]. These recommendations are assigned to thick structure with thickness higher than 5mm. However , the bus structure is usually composited of thin steel beams. G. Savaidis and A. Fekikidis [5],[6] studied various welded joints from bus structure . In addition, S.T. Lie[7] studied stress concentration factor and Reduction Factor (FAR) of welded square hollow section T-joint under axial and pure bending .The close form solutions with weld geometry are presented using T-joint model .

Fig. 1 Bus Structure wireframe

2019 JSAE Annual Congress (Spring) May 22 to 24, 2019
Issued on May 17, 2019

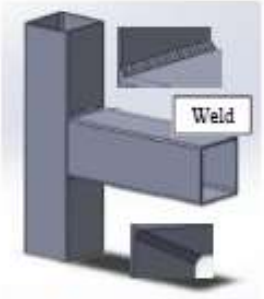

Fig. 2 Welded T-joint

The stiffness of joints could be increased by reinforcements. Many joints in structures are normally reinforced by the plate steel . The square hollow steel (SHS) are applied to prepare welded T-joint specimens a shown in Fig 2. The scope of this study was to investigate different welding configurations , welding sequence on T-joint of thin steel beams with thickness less than 5 mm which are commonly used in a bus structure under static in-plane bending.

2. METHODOLOGY

This section explains the reviewing work process methodology of this study shown as a diagram in Fig 3. After reviewing joints in the bus structure , different types of welding position in the welded joint were to be studied .

Fig. 3 Work process

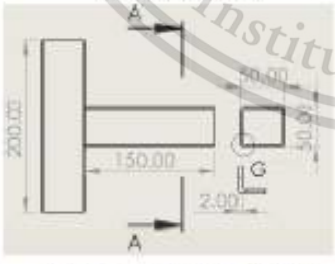

Fig.4 Dimension of T-joint (mm)

Square hollow beam steels with the geometry dimension shown in Fig 4 were used to make test specimens .

A test rig has been designed to be used with an uniaxial compression test machine as shown in Fig 5. The test rig was also developed with a view of accommodating various size of T-joint specimens

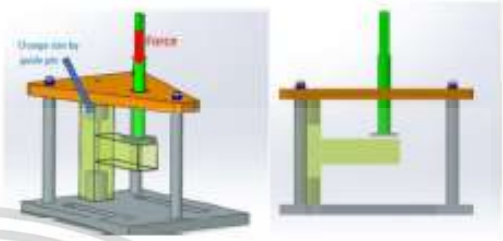

Fig. 5 Test rig for T-joints bending test

2.1 Experimental tools

The experiments were carried out using Uniaxial tensile machine (UTM). this machine will be applied force on specimens joint (Fig.6) and collect corresponding graph between force and displacement. Universal Video Extensometer will be applied to this machine as shown in Fig 7

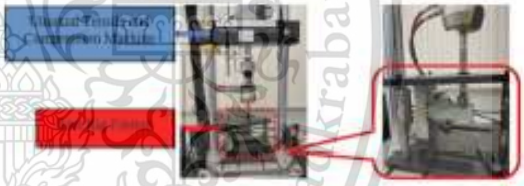

Fig. 6 Test Rig on Uniaxial Tensile Machine

Fig.7 Univeral Video Extensometer with UTM

2.2 Materials properties test

Uniaxial Tensile Machine was also used for investigation of material properties. The dimension of specimens and equipment set up are shown in Fig 8. Resulting graph between stress and strain was show in results.

Fig. 8 Specimens dimension and Equipment set up

2.3 T-Joint test

Three Specimen types were provide in this study as shown in Fig 9(a-c). The specimens were fabricated using square hollow section steel. The weld profile and the specimen preparation were carried out in accordance with the International Institute of welded (IIW) specification[3]

2.3.1 Around Welded joint

Around weld joint was a perfect joint which is obtained by the fusion around of the edges of the two to be joined together. This is the most common connection of bus structures. This specimen was studied deformation behavior.

Fig. 9 a Welded Around Joint

2.3.2 2-Side Welded joint

2-side welded was a permanent joint which is obtained by fusion 2 sides of both edges joint. This type was created to study the deformation behavior and find ways to reduce the cost of welds.

Fig. 9b 2-Side Welded Joint

2.3.3 Welded Corner joint

This type was combined from around welded and 2-side welded to study Deformation behavior, improve and develop a new welding method that was stronger or equal to other types.

Fig. 9c Corner Welded Joint

3. EXPERIMENTAL RESULTS

3.1 Material Properties test

The obtained stress and strain of all specimens are plotted in Fig10. All specimens showed similar value as summarized in Table 1. Images of tested specimens with resulting deformation and fracture damage are shown in Fig 11

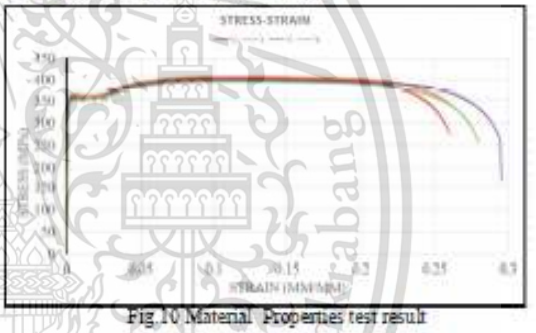

Fig.10 Material Properties test result

Table 1 Dogbone Experimental result

Specimen	Tensile Strength (Mpa)	Young Modulus (Gpa)
1	400	440
2	396	474
3	404	504
4	406	452

Fig. 11 Experimental specimens before and after the test

3.2 T-joint configuration results

3.2.1 Around Welded Joint

The vertical load versus displacement curves of all around-welded-joint specimens are plotted in Fig 12. Due to the deformation behavior and load results of specimen type. The results could be divided into 2 groups. The first group is C1-1, C1-2, C1-3 and the second group is C2-1, C2-2, C2-3.

It can be seen that the first group was able to receive smaller load than the second group due to the effects of heat that has been obtained from the welding process, resulting in residual stress also weakening in the structure of the material and crack on weld position[12] shown in Fig 13 and 14. Furthermore, according to 1st group, the position of seam weld inside the tube has also seem to affected the strength of the joint specimens[9] shown in Fig 15.

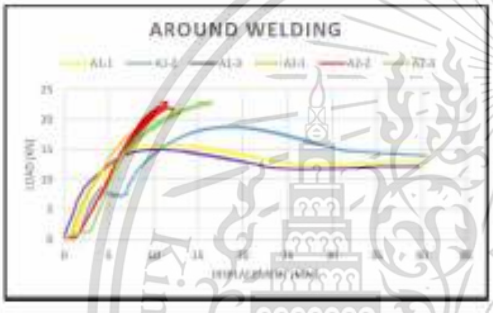

Fig. 12 Around welded test result

Fig. 13 Deformation Bahavior for Around welded group 1

Fig. 14 Deformation Behavior for Around Welded group2

Fig. 15 Different seam welded positions on an internal surface of vertical structural steel member in T-joint specimens

3.2.2 Corner Welded Joint

The veritical load versus displacement curves of all corner-welded-joint specimens are plotted in Fig 16. Due to this specimen type, specify the size of the welding. The results could be divided into 2 groups. The first group, which has an average weld size of 4.95 mm, is C1-1, C1-2, C1-3 and the second group ,which has an average weld size of 13.5 mm, is C2-1, C2-2, C2-3

it could be seen that the first group was able to receive much smaller load than the second group. The size of the weld of 2nd group was larger as shown in Fig 17 and 18, making it possible to receive a significant higher load. The heat of welding process also affects the microstructure of specimens.

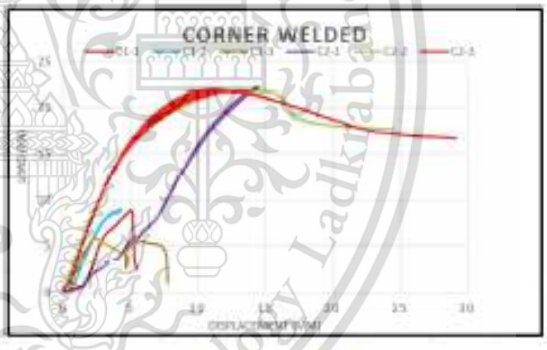

Fig. 16 Corner welded result

Fig. 17 Deformation Bahavior for Corner welded group 1

Fig. 18 Deformation Bahavior for Corner welded group 2

3.2.3 2-Side Welded Joint

The vertical load versus displacement curves of all 2Side welded specimens are plotted in Fig19. Due to the deformation behavior and load results of specimen type. The results showed that specimens could be divided into 2 groups. the first group is S1-1,S1-2,S1-3 and second group is S2-1, S2-2,S2-3.

It could be seen that the specimen group 1 is stronger than group 2 because the second group is affected by the heat that generates from the welding process as shown in Fig 20 and 21.

Fig. 19 2-Side welded result

Fig. 20 Deformation Bahavior for 2-Side welded group 1

Fig. 21 Deformation Bahavior for 2-Side welded group 2

When comparing between Around Welded and 2-Side welded, it can be seen that there were differences around the weld area where 2-Side Welded case would tear the specimens wall. On the other hand, Around welded will had a deformation of the specimens instead as shown in Fig 22.

Fig. 22 Deformation comparison between Around welded and 2-Side Welded

According to experimental data result that not affected by heat, namely around weld group 2, Corner weld group 2 and 2-side welded group 2 as shown in Table.2. Load (kN) and Displacement (mm) chart shown in Fig 23. , Around Welded specimens exhibited the highest strength followed by 2Side Welded and Corner Welded respectively.

Table 2. Experimental Results

Specimen	Averaged Maximum Compressive Load (kN)	Averaged Compressive Strength (kgf/cm²)
2-Side	17.67	363.323
Corner	16.34	320.41
Around	18.19	371.02

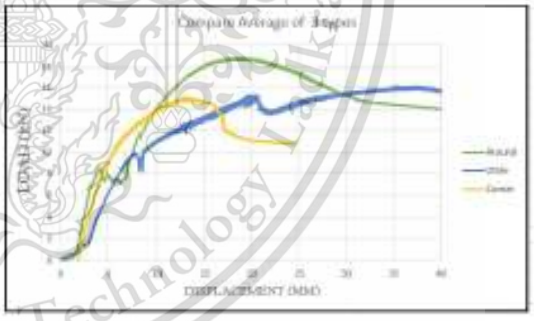

Fig. 23 Load and Displacement comparison between each welding type

4. DISSCUSSION

According to experimental results , 3 parameters that was believed to significantly affect the strength of T-joint specimens were the Heat Affected Zone , position of seam weld line inside the steel tube member and welding size .

4.1 Deformation Parameter

4.1.1 Heat Affected Zone

The results showed that the heat in the welding process is one of the parameters that affect the specimens. In addition to causing the residual stress in the specimens[10], the microstructure of the specimens will be changed as well[11]. Heat affected zone was decreased strength of structure and increase risk rate of crack on weld material[12]. All specimen types will affect this parameter as shown in fig 24 ,25 and 26. It is unavoidable factor in the welded joints, while evaluating the performance of welded joint it is important to consider the influence of residual stress[9].

Fig. 24 Compare Deformation of Heat Affect and Non-heat Affect for Around Welded

Fig. 25 Compare Deformation of Heat Affect and Non-heat Affect for 2-Side Welded

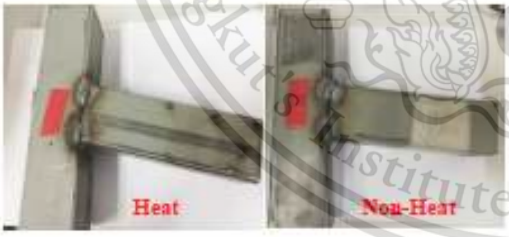

Fig. 26 Compare Deformation of Heat Affectand Non-heat Affect for Corner Welded

4.1.2 Position of Seam welded on Square Hollow box

Post-test examination showed that the position of seam weld inside the tube considerably affected the oversall strength of specimen[8]. TheA2-1 specimen of Around weld was the strongest . Because Seam weld on the same side of the force are applied the position IV in Fig. 27 and Table 3 .the rest specimens wall were not affected by the force.

Fig 27. Seam Weld Position

Table 3. Position of seam welded

Type		Seam Weld Position			
		I	II	III	IV
Around Weld	1-1	✓			
	1-2				✓
	1-3			✓	
	2-1		✓		
	2-2				✓
	2-3	✓			
2-Side Weld	1-1	✓			
	1-2				✓
	1-3			✓	
	2-1			✓	
	2-2			✓	
	2-3				✓
Corner Weld	1-1		✓		
	1-2				✓
	1-3		✓		
	2-1				✓
	2-2	✓			
	2-3			✓	

4.1.3 Welded size on specimens

Corner welding, the length of the weld is an important parameter for the strength of specimens. For this experiment, the average length of welds first group was 4.95 mm and the second group was 13.5 mm, which can be seen that the second group was high strength. For this experiment, if determine the variable size which can find the length that is appropriate for the applied workload. the example deformation behavior that depends on variable size shown in fig 28

Fig. 28 Deformation behavior under welded size condition

4.2 Advantage and disadvantage for each type

4.2.1 Around Welded

Advantage : quite simple , aesthetically appealing , High-strength

Disadvantage : High affect by heat generate on welding process

4.2.2 2-Side Welded

Advantage : Less affect by heat generate on welding process , High Strength

Disadvantage : Tear on specimen wall

4.2.3 Corner Welded

Advantage : Less affect by heat generate on welding process , High Strength

Disadvantage : Need experience in determining the appropriate length , difficult to use in practically

5. CONCLUSION

This experiments of bending test using designed and developed test rig on 3 different welded types were carried out . The test rig was operated with 20kN Universal tensile test machine. The result can be applied to other buses structures like roof structures. In the future, the design of the Rig test will be applied to a larger scale of specimens.

- The result and evaluation for this paper. Each type of welding is suitable for different tasks.

- Heat Affected zone and residual stress will affect the strength of the specimens. The specimen was weak and deform when received too much heat on the welding process.

- The Position of the seam welded wall on square hollow box can be applied to all specimens types.

- Around welded welding is easy to use and strong, but this type must be consider the heat afftect from welding because it can deform the specimens. Therefore, this welding method can be use with the work pieces that needs fast and convenient.

- 2-Side welding that can reduce the risk caused by the impact of heat generated by the welding process, tear on the wall of the specimen, but can be solved by increasing the thickness of the specimen to help can reduce tearing problems for work that requires reducing the risk of deformation of the workpieces due to heat accumulation.

- Corner welding is the welding applied between the around weld and 2-Side Weld. Because this welding method will reduce both the risk caused by heat and reduce the risk of tearing on the wall of the workpieces as well. But this type must investigate the appropriate weld size and various welding sequence scenario which in the future experiment.

- For future work, there will be other mounting tests that can be used to replace welding to avoid the effects that will occur and apply to other types of joints as well.

REFERENCES

(1) D. Radaj, "Review of fatigue strength assessment of non welded and welded structures based on local parameter ,"*Int. J. Fatigue*., vol. 18, no. 3, pp. 153–170, Apr. 1996.

(2) S. Manokruang, "Design and Analysis of bus body structure for high decker bus (Standard No.1)," Master Thesis

(3) A. Hobbacher, "Recommendations for fatigue design of welded joints an components," IIW doc XIII-2151r4-07/XV-1254r4-07., Int Inst Welding, Dec 2008.

(4) European Committee for Standardization, "Eurocode 3," Design of steel structures. Part 1-1: General rules for buildings., ENV, 1993

(5) G. Savaidis, M. Vormwald, "Hot-spot evaluation of fatigue in welded structural connections supported by finite element analysis," *Int. J. Fatigue*., vol. 22, no. 2, pp. 85–91, Feb. 2000.

(6) A. Fokilidis, G. Savaidis, "Experimental investigation of fatigue of thin-walled welded structures of commercial vehicle frames," *Int. Conf. Diagnosis and Prediction in Mechanical Engineering Systems*., vol 2, pp. 34–38, Oct. 2007.

(7) F.P. Brennan, P. Peleties, A.K. Hellier, "Predicting weld toe stress concentration factors for T and skewed T-joint plate connections," *Int. J.Fatigue*., vol. 22, no. 7, pp. 85–91, Aug. 2000.

(8) K. Podany "Mechanics of Square tubes bending and cross section distortion" Brno University of Technology, Faculty of Mechanical Engineering,2010

(9) Milad Moradi, "A Study on the Influence of Various Welding Sequence Schemes on the Gain in Strength of Square Hollow Section Steel T-Joint" Institute of Steel and Timber Structure ,2017

(10) C.K. Lee , S.P. Chiew, Jin Jiang "Residual stress of high strength steel box T-joints Part 1: Experimental study" School of Civil Environmental Engineering, Nanyang Technological University, 2013

(11)E. Ranjbarnodeh , S. Serajzadeh ,A. H. Kokabi ,A.Fischer "Effect of welding parameters on residual stresses in dissimilar joint of stainless steel to carbon steel" Department of Materials Science and Engineering, Sharif University of Technology, Iran,2010

(12) Wolfgang Fricke "IIW Guideline for the Assessment of Weld Root Fatigue" Hamburg University of Technology (TUHH) Ship Structural Design and Analysis,2012

AUTHOR BIOGRAPHY

Author:	Mr. Sagpichest Sarinyavajn
Degree:	Master of Engineering
Date of Graduation:	24th July 2019
Date of Birth:	11th 1991
Place of Birth:	Bangkok, Thailand

Undergraduate and Graduate Education:

Master of Engineering in Automotive Engineering,
King Mongkut's Institute of Technology Ladkrabang, Bangkok, 2018

Bachelor degree in Mechanical Engineering ,
Kasetsart University , 2012

Major: Automotive Engineering

Presentations and Publications:

[1] Sagpichest Sarinyavajn, Chi-na Benyajati, Panya Kansuwan, And Masaaki Okuma, "Experimental Bending Tests for Design Improvement of Substructure with Joints in Bus Body", Technical Paper, 2019 JSAE Annual Spring Congress, 22-24 May 2019, Yokohama Japan.